Sequential Extraction of Trace Metals as Geochemical Indicators of Land Use Near Ancient Metallurgical Sites in Faynan, Jordan

by

Sarah Turner

A thesis
presented to the University of Waterloo
in fulfillment of the
thesis requirement for the degree of
Master of Science
in
Earth Sciences

Waterloo, Ontario, Canada, 2023

Author's Declaration

I hereby declare that I am the sole author of this thesis. This is a true copy of the thesis, including any required final revisions, as accepted by my examiners.

I understand that my thesis may be made electronically available to the public.

Abstract

Civilizations are tied to soils through a reliance on agriculture. In the Faynan Valley, southern Jordan, both the individuals who tend to the soils and the soils themselves have evolved through a series of environmental changes and adaptations in land use over the course of millennia. The desert sediments in the Faynan Valley hold a rich archaeological history that detail the millennia of metallurgy for which the region is known. The accumulation of metals through mining wastes in the sediments in Faynan pose a known danger that has afflicted the residents of Faynan since the Early Bronze Age when the production of copper moved out of the mines and into the wadis and agricultural fields. Metal residua from the processing and smelting of Cu and Mn ores remains in the sediment until physically broken down or removed. This research presents a new perspective on the extent and nature of the pollution in the hyper-arid sediments of Faynan, going beyond the known zones of high contamination in the immediate vicinity of archaeometallurgical sites and provding the missing link between metal concentrations in the sediments and the local flora and fauna.

Sediment samples were collected from two contemporaneous archaeological sites in the desert environment of Faynan; the alluvial Wadi 100 site with evidence of historical and modern agriculture and the aeolian Barqa el-Hetiye site near the base of a smelting ridge. Metals associated with mining (Cu, Mn, Pb) and elements associated with known archaeological features (Mg, P, Sr, Cd, Ni, Cr, Zn) were extracted in four operationally defined sediment fractions, including exchangeable, reducible, oxidizable, and residual fractions. The fractional distributions of these elements were measured and used to assess both the potential anthropogenic and natural sources of these elements in the Faynan Valley, and the potential risk to the biogeochemical environment associated with labile elements.

More than 50% of the total concentration of Mg, Mn, Sr, and Cd were recovered from the exchangeable fraction at both sites indicating that these elements are the most labile in the sediments analyzed. The largest proportion (> 40%) of Cr, Ni, Zn, Cu, and Pb were extracted from the residual fraction at both sites suggesting that these metals are the least mobile and not easily accessible to local biota. The sediments sampled from the Wadi 100 site have been altered by modern agriculture and irrigation, as evidenced by Cd, P, Mg, and Zn concentrations. The samples from the Barqa el-Hetiye site likely reflect element concentrations from a minimum of two stratigraphic layers, with at least one layer reflecting the local background concentrations and the redistribution of metals from more highly contaminated areas through aeolian and fluvial processes, and another layer indicative of archaeometallurgical contamination. These results show how the mobility of heavy metals associated with archaeometallurgical activity in Faynan is dependent on soil properties and how variations in land-use, both historic and modern, can alter soil properties and thus the mobility and bioavailability of these metals.

Acknowledgements

As I think back on these past few years of research, I find a strange kind of comfort in their culmination. Though I have found this research to be very rewarding, these past few years have also been challenging. Since starting my graduate studies in 2019, I have lost four grandparents. Ensuing pandemic restrictions and the distances between us meant it was not possible for me to attend their funerals and acknowledge the impact they each had on my life. To my grandparents, Pake Jan, Pappy, Pake Ype, and Nanny, whose love and support crossed continents, thank you. To the many people who have supported me in various ways throughout the course of my research, thank you for reminding me that asking for help is not giving up, it is refusing to give up.

There are many people without whom this thesis would have been even more delayed. I would like to acknowledge you all but coming up with the order in which to do so has proven to be an unexpected challenge. Channelling the wise words of my father (and Julie Andrews), I've decided to 'start at the very beginning, a very good place to start'.

To my family who have supported me since day one, thank you for encouraging me and for showing interest every time I came to you with a new-and-improved, long-winded, and confoundingly convoluted elevator pitch. To my favourite(s), who know(s) who they are even when left unnamed, thank you for always offering an ear, shoulder, and your words (both when I knew I needed them and when I didn't). Thank you for encouraging me to celebrate the many small milestones that have brought me to where I am today.

To one to my first friends at the University of Waterloo and co-Prime Minister of Watrox, Carson Kinney, who first told me about a possible MSc project involving sand and archaeology in Turkey, thank you. Though your recollection of the location of the project was slightly off, your confidence in my interest for the project was not.

After learning about this MSc project, I spent the next eight months working with my undergraduate thesis supervisor and MSc committee member, Dr. John Johnston, who taught me how to use what I *do* know to form logical connections that help me answer my own questions. John, the critical thinking skills I learned through working with you have been invaluable throughout the course of this project, thank you.

Within weeks of completing my BSc, I was on my way to Jordan where I met the other students and staff involved with the Barqa Landscape Project (BLP); a multi-disciplined research group focused on exploring the archaeometallurgical history in Faynan. It was during the BLP's 2019 field season that I was able to collect the sediment samples discussed in this thesis and build personal and professional relationships with many of the students and professionals affiliated with the project.

When I arrived in Faynan, I was immediately taken aback by its barrenness and spent my first week waffling and unsure about the direction of my research. Any desolate feelings were short-lived, as they were quickly alleviated upon the arrival of Dr. John Grattan and Keith Haylock, whose enthusiasm and regional knowledge had me quickly rethinking my initial impressions of Faynan. John and Keith, I learned more from one hour in the field with you than I had in the entire week that I spent alone.

I would also like to thank Alan Weston (British Columbia Institute of Technology) for surveying my collection sites, teaching me about total stations, and leaving behind trails of eggshells for me to follow in case we got separated in the field. Thank you for the maps you created of my study sites; they are superior to my fieldnote sketches in every way.

Upon returning to Waterloo and starting my graduate studies, I quickly learned how little I knew about soil science. Thankfully, Dr Maren Oelbermann was offering a course on soil dynamics, and much to my delight, her three-hour-long morning lectures never challenged my attendance. Thank you, Maren, for helping me understand how deeply interconnected soil is with the environment and opening my eyes to a new application of my earth science knowledge.

Thank you to Dr. Brian Kendall for your assistance in the University of Waterloo's MIG lab, to Sarah McCaugherty for teaching me how to practice safe chemistry, and to Ivan and Chris for helping me that one time I sneezed in the lab.

To my committee members, Dr. John Johnston and Dr. Maren Oelbermann, thank you for continuing to encourage me and my interests in sedimentary geology and soil science.

To my honorary committee member, Dr. John Grattan (University of Aberystwyth, Wales), thank you for continuously offering your support and insight and showing a sincere interest in my research. Your detailed works on the sediments in Faynan have proven to be an invaluable resource throughout the course of my research. Having you in my corner has made this experience far more interesting and enjoyable than I could have imagined. The quality of and my confidence in this research has been significantly improved by your contributions.

Finally, to my supervisor, Dr. Chris Yakymchuk, 'thank you' feels insufficient. You are one of few people who know of the many challenges I have faced along this academic journey. Your unwavering support and encouragement have helped me to grow as both a researcher and academic writer, and your patience allowed me to pause my research and invest time in myself when I needed it the most. Though it goes without saying, I now, more than ever, feel it is most important to acknowledge that this endeavour would not have been possible without your guidance and expertise. As always,

Thank you,

All the best,

Sarah

Table of Contents

AUTHOR'S DECLARATION ..... **ii**
ABSTRACT ..... **iii**
ACKNOWLEDGEMENTS ..... **iv**
LIST OF FIGURES ..... **viii**
LIST OF TABLES ..... **iv**
LIST OF ABBREVIATIONS ..... **x**
1.0 INTRODUCTION **1**
2.0 RESEARCH OBJECTIVES **3**
3.0 BACKGROUND **4**
3.1 Regional Geology 4
3.2 Local Geology 5
3.3 Study Site 9
3.3.1 Surficial Wadi Deposits *9*
3.3.2 Soil Classification *10*
3.3.3 Climate and Precipitation *11*
3.3.4 Vegetation *12*
3.3.5 Groundwater *13*
3.3.6 The Wadi 100 site *14*
3.3.7 The Barqa el-Hetiye site *15*
3.4 Previous Work 16
4.0 METHODS **17**
4.1 Sample Collection 18
4.1.1 Wadi 100 Samples *18*
4.1.2 Barqa el-Hetiye Samples *20*
4.2 Sample Preparation 22
4.2.1 Physical Sample Preparation *23*
4.2.2 Chemical Sample Preparation *23*
4.2.3 Exchangeable Fraction Extraction *24*
4.2.4 Reducible Fraction Extraction *25*
4.2.5 Oxidizable Fraction Extraction *25*
4.2.6 Residual Fraction Extraction *26*
4.2.7 Preparing Samples for Analysis *26*
4.3 Sample Analysis (QQQ-ICP-MS) 27
4.4 Quality Assurance 28
4.5 Statistical Analysis 30
5.0 RESULTS **31**
5.1 Major Element Concentrations 32
5.1.1 Magnesium *33*
5.1.2 Aluminum *34*
5.1.3 Phosphorus *35*
5.1.4 Manganese *36*
5.1.5 Iron *37*
5.1.6 Strontium *38*
5.1.7 Major Element Summary *39*
5.2 Trace Element Concentrations 39
5.2.1 Copper *40*

5.2.2 Chromium ... *41*
5.2.3 Nickel ... *42*
5.2.4 Zinc ... *43*
5.2.5 Cadmium ... *44*
5.2.6 Lead ... *45*
5.2.7 Trace Element Summary ... *46*
5.3 Fractional Distrubution Summary ... 46
5.3.1 Exchangeable Fraction Summary ... *46*
5.3.2 Reducible Fraction Summary ... *46*
5.3.3 Oxidizable Fraction Summary ... *46*
5.3.4 Residual Fraction Summary ... *46*
5.4 Statistical Analysis ... 46
5.4.1 Recovery Rates ... *48*
5.4.2 t-test Results ... *48*
6.0 DISCUSSION ... 50
6.1 Total Element Concentrations ... 50
6.2 Fractional Element Distribution ... 51
6.2.1 Exchangeable Fraction ... *52*
6.2.2 Reducible Fraction ... *52*
6.2.3 Oxidizable Fraction ... *53*
6.2.4 Residual Fraction ... *53*
6.3 Elements of Concern ... 54
6.3.1 High-risk Elements ... *54*
Magnesium ... *54*
Strontium ... *54*
Phosphorus ... *54*
6.3.2 Metals Associated with Metallurgy ... *60*
Manganese ... *54*
Cadmium ... *54*
Copper ... *54*
Lead ... *54*
Zinc ... *54*
7.0 CONCLUSIONS ... **70**
7.1 Future Work ... 73
REFERENCES ... **75**
APPENDICES ... **86**
APPENDIX A: WADI 100 SEQUENTIAL EXTRACTION DATA ... **86**
APPENDIX B: BARQA EL-HETIYE SEQUENTIAL EXTRACTION DATA ... **88**
APPENDIX C: SUPPLEMENTAL ELEMENT STATISTICS FOR ALL SAMPLES ... **90**

List of Figures

Figure 3.1: A map of Jordan with the locations of major geographic features relative to Faynan **4**

Figure 3.2: A topographic profile across the Wadi 'Araba Valley at Faynan **5**

Figure 3.3: A stratigraphic chart with the dominant lithological sequence in the Wadi ‘Araba escarpment near Faynan. **6**

Figure 3.4: A hand sample of local ore collected from the Barqa el-Hetiye site **7**

Figure 3.5: A drawn map of the study area relative to the Wadi 100 and Barqa el-Hetiye sites **8**

Figure 3.6: The relationship between vegetation, precipitation, and elveation along a SW-NE transect through Faynan **12**

Figure 4.1: A satellite image of Faynan with the locations of the study sites. **17**

Figure 4.2: A field photo taken at the Wadi 100 site. **18**

Figure 4.3: esri imagery of the Wadi 100 site and surrounding Wadi Faynan field system **19**

Figure 4.4: A map of the Wadi 100 site and the location of samling transects. **20**

Figure 4.5: A field photo taken at the Barqa el-Hetiye site. **21**

Figure 4.6: esri imagery of the Barqa el-Hetiye site and surrounding area. **21**

Figure 4.7: A map of the Barqa el-Hetiye site and the locations of collected samples. **22**

Figure 5.1: A box and whisker plot showing the ranges in the total concentrations of major elements **32**

Figure 5.2: Distribution of Mg concentrations across all sediment fractions **33**

Figure 5.3: Distribution of Al concentrations across all sediment fractions **34**

Figure 5.4: Distribution of P concentrations across all sediment fractions **35**

Figure 5.5: Distribution of Mn concentrations across all sediment fractions **36**

Figure 5.6: Distribution of Fe concentrations across all sediment fractions **37**

Figure 5.7: Distribution of Sr concentrations across all sediment fractions **38**

Figure 5.8: A bar graph showing the distribution of average major element concentrations across all sediment fractions **39**

Figure 5.9: A box and whisker plot showing the range in the total concentrations of trace elements **39**

Figure 5.10: Distribution of Cu concentrations across all sediment fractions **40**

Figure 5.11: Distribution of Cr concentrations across all sediment fractions **41**

Figure 5.12: Distribution of Ni concentrations across all sediment fractions **42**

Figure 5.13: Distribution of Zn concentrations across all sediment fractions **43**

Figure 5.14: Distribution of Cd concentrations across all sediment fractions **44**

Figure 5.15: Distribution of Pb concentrations across all sediment fractions **45**

Figure 5.16: A bar graph showing the distribution of average trace element concentrations across all sediment fractions **46**

Figure 6.1: The general trend of metal lability based on the operation form of the metal in sediment **52**

List of Tables

Table 1.1: A simplified chronology of the Periods of occupation present in Faynan **1**

Table 4.1: Examples of archaeological features and associated geochemical indicators **22**

Table 4.2: An outline of the four-step sequential extraction scheme used in the analysis of all samples in this thesis **23**

Table 5.1: A summary of the proportional distribution of each element across all fractions **31**

Table 5.2: A summary of the geochemistry results for major elements **31**

Table 5.3: A summary of the geochemistry results for trace elements **32**

Table 5.4: A summary of *p* values for element concentrations in Wadi 100 and Barqa el-Hetiye samples **47**

Table 6.1: The minimum, maximum, and mean concentrations of Cd, Cu, Pb, and Zn in sediments from this study compared to CSQG maximum values **60**

Table A1: All sequential extraction concentrations from Wadi 100 Samples **85**

Table A2: All sequential extraction concentrations from Barqa el-Hetiye samples **87**

Table A3: A statistical overview of the mean total element concentrations in Wadi 100 samples **88**

Table A4: A statistical overview of the mean total element concentrations in Barqa el-Hetiye samples **88**

Table A5: A summary of the fractional distribution of each element for the Wadi 100 samples **89**

Table A6: A summary of the fractional distribution of each element for the Barqa el-Hetiye samples **89**

List of Abbreviations

BLP …… Barqa Landscape Project

CH_3COOH…… glacial acetic acid

CH_3COONH_4……ammonium acetate

CSQG…… Canadian Soil Quality Guidelines

DF…….. dilution factor

EBA……..Early Bronze Age

HF……. hydrofluoric acid

H_2O……water

H_2O_2……..hydrogen peroxide

HCl……..hydrochloric acid

HNO_3……. nitric acid

IAG …..…… International Association of Geoanalysts

LDPE……..Low-Density Polyethylene

LOD……..limit of detection

M……. molarity

Ma……. million years ago

MIG Lab…….. Metal Isotopes Geochemistry Laboratory

n ……..…… number of samples

$NH_2OH•HCL$ ……..……. hydroxylammonium chloride

NH_4OH ……..……..... ammonium hydroxide

OM……..…….. organic matter

QQQ-ICP-MS…..…..……. Triple-Quadrupole Inductively Coupled Mass Spectrometer

rpm ..……..……..…… ..... revolutions per minute

RSD ..……..……..…….. relative standard deviation

SD ..……..……..……. standard deviation

TWF ..……..……..…… Tell Wadi Faynan (archaeological site)

ug/g..……..……..……. micrograms per gram (equivalent to ppm)

v/v..……..…….. ‘volume for volume (i.e., water content: 10 mL/L or 1% (v/v))

WF1 ..……..……..……. Khirbat Faynan (archaeological site)

WF100 ……Wadi Faynan 100 (site name for the Wadi 100 archaeological excavations)

wt. %..……..…..……..……..…… weight percent (grams per 100 gram)

w/w..……. ‘weight for weight’ (i.e., water content: 10g/kg or 1% (w/w))

1.0 Introduction

Environmental pollution and contamination as a by-product of metallurgical activity is not simply a complication associated with the rise of modern industry, but one that has been impeding on the success of global environments for millennia. Civilizations in the Near East have been refining ores into metals to produce tradable commodities since the Chalcolithic Period (Table 1.1), leaving behind toxic metals that persist in the sediments to this day (Barker 2007, Hauptmann 2007). Some of the earliest evidence of copper production remains preserved in the desert of southern Jordan where the region's mineral wealth was exploited throughout the span of human occupation in the southern Levant, modern day Jordan-Israel-Palestine; from the Neolithic Period, *c.* 7000 years ago, into the Medieval Ages with only a short hiatus during the Middle and Late Bronze Ages (Levy et al. 1999, Grattan et al. 2007, Hauptmann 2007).

Situated in the Wadi 'Araba Valley, the Roman city of Phaeno now lies as ruins in the Faynan Valley where it once served as a major centre for copper production for the ancient world (Grattan et al. 2002, 2003a; Hauptmann 2007). Evidence of the extensive mining operations that once dominated the region such as pottery shards and stone tools lay uncovered across wadi floors, though not all the evidence of cultural activity in Faynan is visible. Mixed into the sediment are metals that have accumulated over the millennia; a relic of the metallurgical activity that still dominates the landscape. Much like the stone tools and pottery, these metals remain in the environment until they are physically removed or broken down.

Table 1.1: A simplified chronology of the periods of occupation present in Faynan with corresponding dates in Common Era (CE) notation and in years Before Present (BP), where events are dated relative to the year 1950 CE. (Modified from Hauptmann 2007).

Period	Date	Years BP
Neolithic	8500 BCE – 4500 BCE	10,450 – 6450
Chalcolithic	4500 BCE – 3500 BCE	6450 – 5450
Early Bronze Age	3500 BCE – 2300 BCE	5450 – 4250
Iron Age	1250 BCE – 587 CE	3200 – 2537
Roman Age	40 CE – 350 CE	1990 – 1600
Byzantine	350 CE – 640 CE	1600 – 1310

The sediments in Faynan are known to host elevated concentrations of Cu, Mn, and Pb that continue to contaminate the landscape through various biological pathways (Pyatt et al. 2000, Grattan et al. 2007). The mobility and bioavailability of these metals can be highly variable and is dependent on the nature and composition of the host sediment (McBride 1981, Alloway 2013).

The formation and composition of sediment is dictated by five principal factors: parent material, climate, biota, topography, and time (Weil and Brady 2019). Though these five factors are consistent across much of the Faynan Valley, modern depositional processes and land use practices vary from the alluvial and colluvial wadi deposits used for the cultivation of tomato plants at the Wadi 100 site to the aeolian deposits at the Barqa el-Hetiye site. Evaluating the concentrations of metals Mg, Sr, Cr, Mn, Fe, Ni, Cu, Zn, Al, Pb, and the reactive nonmetal P at these two contemporaneous archaeological sites will make use of this natural laboratory and offer a better understanding of the impacts of modern agriculture pertaining to the behaviour metals in regions of historical mining and smelting.

2.0 Research Objectives

Faynan is known as an important center for copper production in the ancient world and for the highly contaminated sediments resultant of this long history of metallurgy. Many earlier studies have focused on the historical context of known metallurgical sites in Faynan (e.g., Hauptmann 2007, Levy et al. 2012), and encouraged geochemical studies focused on sites near areas of known mining, smelting, and ore-processing that report very high concentrations of metals (e.g., Grattan et al. 2007; 2014). When interpreting land use in a region as full of archaeology as Faynan, the absence of metals is just as informative as an abundance of metals. More recent studies have adopted similar concerns, prompting further investigations of sediment geochemistry across the landscape in Faynan as defined by total element concentrations determined through total digestion or by X-ray fluorescence (e.g., Grattan et al. 2007; 2013; 2016, Knabb et al. 2016; 2019).

The primary objective of this research is to further the understanding of trace element behaviour in the sediments of Faynan. This objective will be achieved by quantifying the total and fractional concentrations of a series of elements in the sediments from the Wadi 100 and Barqa el-Hetiye sites in Faynan to fulfill the following subobjectives:

1. Compare and evaluate any differences in the fractional distribution of Mg, Al, P, Cr, Fe, Ni, Cu, Zn, Sr, Cd, and Pb at both the Wadi 100 and Barqa el-Hetiye sites.
2. Evaluate if near surface major and trace element concentrations in the sediment samples collected from the Wadi 100 site are statistically different from those measured in the samples collected from the Barqa el-Hetiye site.
3. Evaluate the potential environmental consequences of labile elements.
4. Identify possible geogenic and anthropogenic sources for elements with significant concentrations and determine if these sources contributed to the reduction or accretion of localized trace elements.

3.0 Background

3.1 Regional Geology

The Hashemite Kingdom of Jordan is located in the northwestern part of the Arabian Peninsula along the Dead Sea Transform, an active passive margin that separates the Arabian Plate from the Palestine-Sinai Subplate (Niemi et al. 2001, Haberland et al. 2007, Förster et al. 2010). The Wadi 'Araba Valley occupies the southern portion of the Dead Sea Transform margin, connecting the Dead Sea in the north to the Red Sea in the south. Along the eastern side of the Wadi 'Araba Valley is a narrow mountain chain, historically known as the Mountains of Edom, comprising the southern portion of the Wadi 'Araba Escarpment (Figure 3.1) (Bender 1974, Hauptmann 2007).

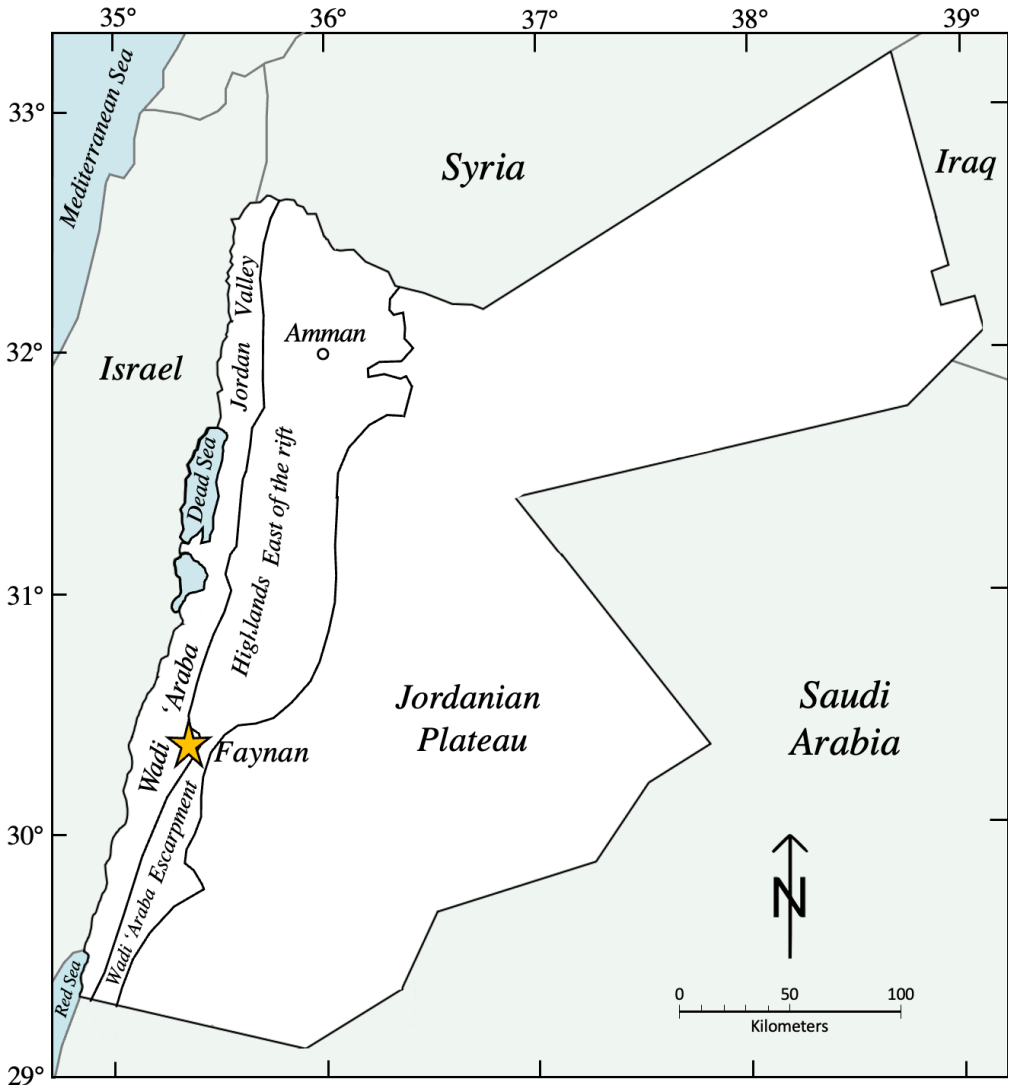

Figure 3.1: A map of Jordan with the locations of major geographic features relative to Faynan. The location of the study sites in Faynan are identified by a yellow star (☆). Modified from Bender (1974).

The Wadi ʻAraba Escarpment is part of the Transjordanian Mountain Block, a hanging wall that is regionally tilted towards the northwest from its footwall, the Jordanian Plateau in the east (Figure 3.2) (Bender 1974, Wdowinski & Zilberman 1997). In Israel, the western rim of the Transjordanian Block is heavily arched and down-flexed and most of the subsequent rock record is buried (Wdowinski & Zilberman 1997). In Jordan, the eastern margin has been uplifted, exposing all sedimentary sequences down to the basement rock along the face of the escarpment including the blue-green copper-bearing strata (Bender 1974, Wdowinski & Zilberman 1997).

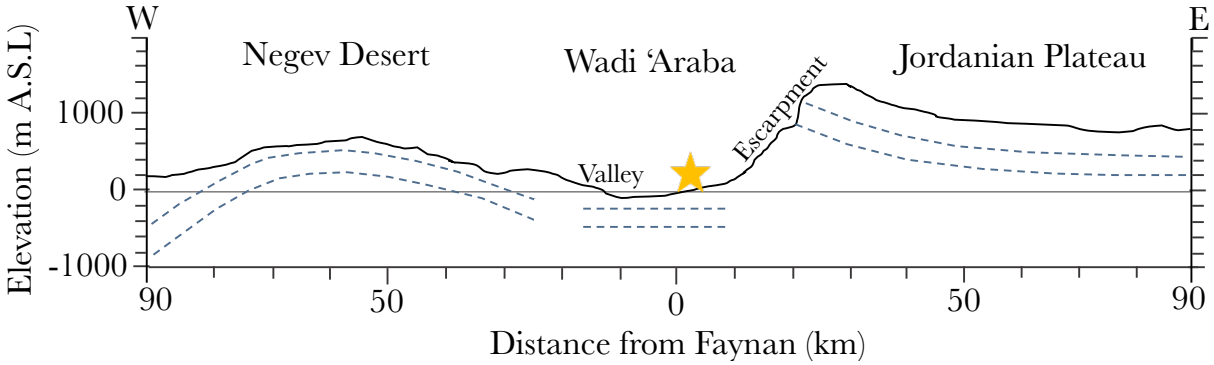

Figure 3.2: A topographic profile across the Wadi ʻAraba Valley at Faynan. This cross-section (from west to east) through Faynan shows the heavily eroded and gradual rise to the Negev Desert west of Faynan and the steep change in elevation up the Wadi ʻAraba Escarpment onto the Jordanian Plateau to the east of Faynan. The broken lines show the general trends in bedding; the western side of the rift is flexed down (antiform) towards the Wadi ʻAraba axis; the eastern side of the rift is flexed up (synform) towards the Wadi ʻAraba axis. The unconsolidated sediments in the Wadi ʻAraba Valley are deposited horizontally. Elevation given in meters Above Sea Level (A.S.L). Modified after Wdowinski & Zilberman (1997).

3.2 Local Geology

The granitic rocks of the ʻAraba basement complex outcrop along the Wadi ʻAraba Valley and in the Faynan Valley (Bender 1974, Rabb'a 1994). The Finān Granite suite (550 – 540 Ma) is the youngest phase of the ʻAraba basement complex that underlies the Phanerozoic stable shelf sedimentary rocks that cover most of southern Jordan (Figure 3.3) (Rabb'a 1994). The Finān Granite is the dominant basement rock in Faynan and forms the Jabal Hamrat Fidān, a prominent granitic ridge *c.* 8 km in length and 200 m high. In Faynan, the Finān Granite is cross-cut by Late Proterozoic and Early Cambrian rhyolitic basalt dikes that contain cupriferous minerals and represent several phases of volcanic activity (Bender 1974, Barjous 1992, Rabb'a 1994, Förster et al. 2010). The formation of the Wadi ʻAraba Valley triggered the dissolution and remobilization of primary Cu-Fe sulphide minerals in the Precambrian igneous rocks and the subsequent erosion of these rocks formed stratiform syn-sedimentary Cu and Mn deposits (Hauptmann 2007, Palmer et al. 2007).

Unconformably overlying the Finān Granite is a series of Palaeozoic braided river deposits that comprise the Ram Sandstone Group (Rabb'a 1994). Within the Ram Sandstone Group, the Umm 'Ishrīn Sandstone, Numayrī Dolostone, and Salib Sandstone Members contain local Cu, Pb, and Mn deposits, though only the Umm 'Ishrīn Sandstone and Numayrī Dolostone have evidence of mining near Faynan (Barjous 1992, Rabb'a 1994, Palmer et al. 2007). The Umm 'Ishrīn Sandstone at the top of the Ram Sandstone Group contains mineralized Cu and Mn in fillings and fractures (Rabb'a 1994, Palmer et al. 2007). Unconformably overlying the Ram Sandstone group is the Early Cretaceous Kurnub Sandstone Group and the Middle Cretaceous Aljun Group (Barjous 1992, Rabb'a 1994). The braided river deposits of the Kurnub Sandstone Group and the shallow marine deposits of the Ajlun Group near Faynan do not contain any Cu, Pb, or Mn deposits or notable mineralization (Barjous 1992, Rabb'a 1994, Barker et al. 2007).

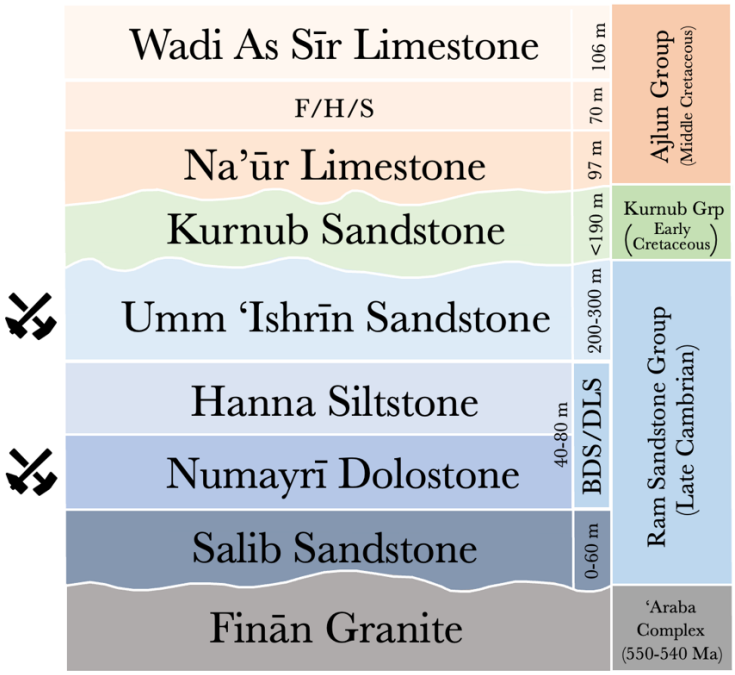

Figure 3.3: A stratigraphic chart with the dominant lithological sequence in the Wadi 'Araba Escarpment at Faynan. Lithologies from the Late Cretaceous to modern Holocene deposits are not included. For a more comprehensive description of all geologic units in Faynan see Barjous (1992), Rabb'a (1994), and Palmer et al. (2007) (Modified from Barjous 1992, Rabb'a 1994).

More than 250 mines and shafts have been identified in the Faynan Orefield and more than half of them are in the Numayrī Dolostone (Hauptmann et al. 1992, Pyatt et al. 2000, Barker et al. 2007). Cu, Pb, and Mn mineralization occur in pockets and veins throughout the Numayrī Dolostone; a large shale unit in the upper section of the dolostone contains the most substantial Cu, Pb, and Mn mineralization (Bender 1975) as well as nodules and layers of phosphorite and

barite (Hauptmann 2007). Copper mineralization in the Numayrī Dolostone member occurs primarily as chrysocolla (Figure 3.4) and malachite with phosphates in a clay and sand matrix supporting quartz and feldspar grains up to 2 mm in diameter (Hauptmann et al. 1992). Other copper-bearing minerals in this member include cuprite and azurite (Rabb'a 1994, Hauptmann 2007). Previous geochemical analyses of the mineralised strata in these sedimentary rocks yield Cu values between 0.41 and 5.9 wt. % in low-grade ores while high-grade ores can contain more than 45 wt. % Cu (Rabb'a 1994, El-Hasan et al. 2001). Mn values range from 3.4 to 7.2 wt. % in the ores found in the wadis to the east of Faynan, and up to 27 wt. % in the ores found in the wadis north of Faynan (El-Hasan et al. 2001). Pb content in the Numayrī Dolostone can exceed 6 wt. % Pb, while Pb in the Umm 'Ishrīn Sandstone is only present in trace amounts (Hauptmann 2007).

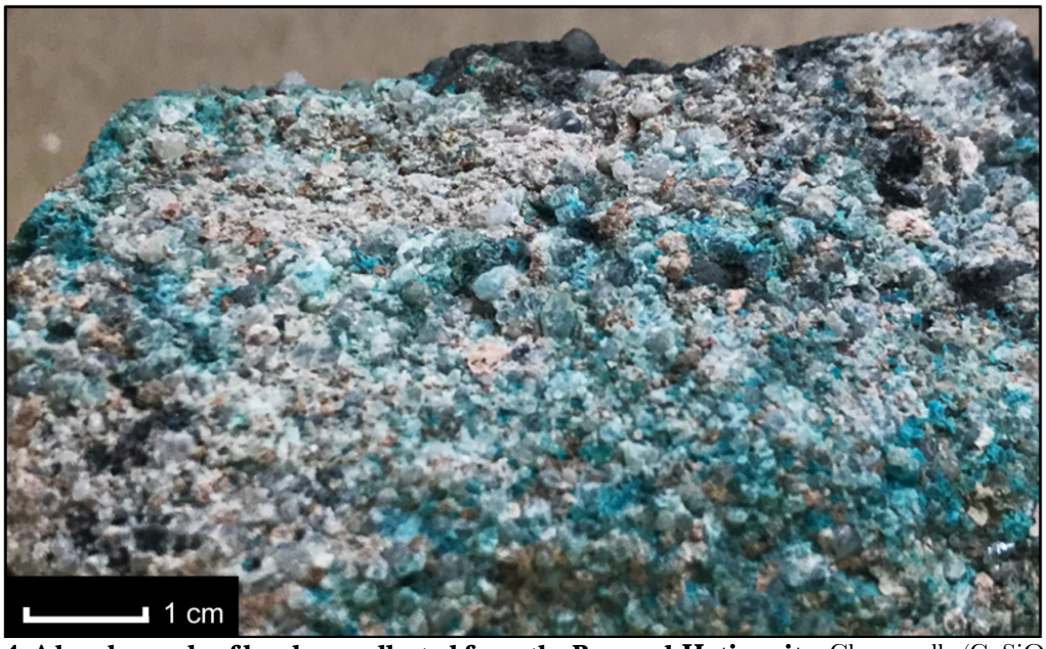

Figure 3.4: A hand sample of local ore collected from the Barqa el-Hetiye site. Chrysocolla ($CuSiO_3 \cdot 2H_2O$) (blue/green) and pyrolusite (MnO_2) (black), with quartz and feldspar are held loosely in a sand and clay matrix.

Mn mineralization is also present in the Numayrī Dolostone in the form of cavity infills predominantly as pyrolusite (MnO_2) (Rabb'a 1994). Measured concentrations of Mn (>5000 μg/g) and Cu (*c.* 5000 μg/g) are also present in the basal conglomerate unit of the arkosic Salib Sandstone Formation, along with high amounts of Pb (*c.* 10,000 μg/g) (Rabb'a 1994). Mine tailings sampled near the largest Roman Age smelter at the well documented Khirbat Faynan site (WF1; Figure 3.5) contain substantial and dangerous concentrations of Cu, Pb, and Tl with values often exceeding 16,000 μg/g, 40,000 μg/g, and 90 μg/g, respectively (Grattan et al. 2007).

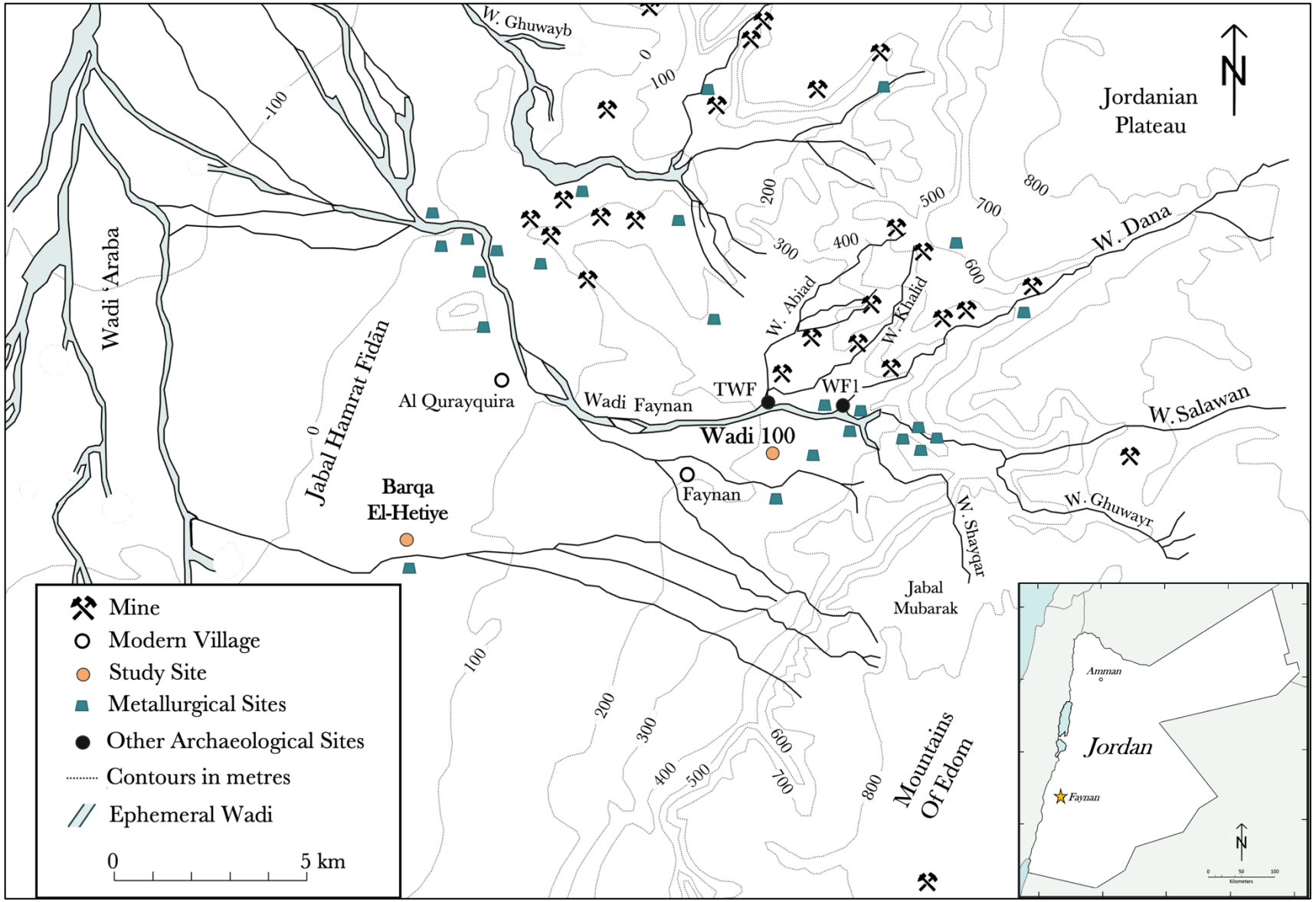

Figure 3.5: A drawn map of the study area relative to the Wadi 100 and Barqa el-Hetiye sites. Other archaeological sites mentioned in this text (Khirbat Faynan (WF1); Tell Wadi Faynan (TWF)), and mines, relative to the main wadi channels and topography. Modified from Grattan et al. (2016).

3.3 Study Site

The studied area is located near the modern villages of Al Qurayqira and Faynan (Figure 3.5), commonly referred to as the region of Faynan or Faynan Valley, 150 km south of Jordan's capital city, Amman. The site can only be accessed via an unnamed road connected to the Jordan Valley Highway, making it relatively secluded from the rest of Jordan due to its isolating geomorphology. Faynan is bordered in the west by the Jabal Hamrat Fidān (Figure 3.5), a NNE–SSW trending granitic ridge of raised basement rocks. The Wadi 'Araba is flanked in the east by the Wadi 'Araba Escarpment that ascends onto the Jordanian Plateau, and in the west by a steep rise that plateaus onto the Negev Desert in Israel (Figure 3.2) (Hauptmann 2007). Faynan is located at the base of the Wadi 'Araba Escarpment and is believed to have been a resting point and corridor for early groups travelling between the Wadi 'Araba and the Jordanian Plateau (Barker et al. 2007). The bedrock underlying the surficial deposits between the escarpment and Jabal Hamrat Fidān gently slopes down towards the north-west, draining rainwater out of the smaller wadis (Wadis Dana, Ghuwayr, and Khalid) through the Wadi Faynan and into the larger Wadi 'Araba (Rabb'a 1994, Al-Bakri 2008).

3.3.1 Surficial Wadi Deposits

The recent Quaternary deposits in the Wadi 'Araba are generally quite thin due to the relatively low sedimentation rates that are common in rifting basins (Sawkins 1984). The Wadi 'Araba sediments are derived from the weathering of the exposed Phanerozoic shelf rocks that comprise the Wadi 'Araba Escarpment and Jordanian Plateau. Flood waters transport sediments from the east through the Wadi Faynan and into the Wadi 'Araba (Pyatt et al. 1999, Hauptmann 2007). Katabatic winds and water deposit sediment at the base of the escarpment as colluvium then further across the wadi as alluvium or dispersed by the wind as aeolian sediment into the area known locally as the sand sea (Pyatt et al. 1999, Al-Qudah 2001, Al-Bakri 2008). Prevailing winds from the northwest redisperse and introduce aeolian sediment from the Wadi 'Araba into the sand sea and Wadi Faynan (Hauptmann 2007, Palmer et al. 2007). The redistribution of aeolian sediments has been documented in the Hisma Basin, 65 km south of Faynan, where the addition of aeolian Wadi 'Araba sediment have reportedly introduced foreign minerals (K-feldspar, plagioclase feldspar, gypsum) to the arid sediments (Ugolini et al. 2008).

The Wadi 'Araba has been defined as a limestone desert because the primary source of the wadi sediment is clastic calcareous material derived from limestone and sandstone parent material

(Bender 1974, Hauptmann 2007). The Wadi 'Araba is also considered a mixed desert (Bender 1974) as there is both alluvium and aeolian sediment (Grattan et al. 2003b, Al-Bakri 2008). In addition to the natural weathering of the surrounding bedrock, mining and smelting operations have contributed to the anthropogenic weathering of copper-rich strata which has been redistributed by both aeolian and fluvial processes (Grattan et al. 2003b).

Near the base of the Wadi 'Araba Escarpment, the Wadi Faynan is flanked by Pleistocene gravel terraces to the north and south (Rabb'a 1994). The alluvial sediment along the Wadi Faynan fines upward in sequences from gravel to sand with a small surficial clay fraction and some larger cobbles and boulders of both sedimentary and igneous origins (Rabb'a 1994). Bimodal sediments, wherein sand and gravel dominate, commonly develop from gravel river beds when an external source of sand is introduced (Smith et al. 1997); an ongoing process in Faynan. Erosion occurs rapidly in the characteristically organic-poor and vegetation-free sediments of the Faynan Valley (Pyatt et al. 2002, Palmer et al. 2007). Evidence of erosion and the reworking of sediments by wind and water is apparent along the Wadi Faynan floodplain, both preserved in the stratigraphy (Hunt et al. 2007) and on the modern wadi floor (Palmer et al. 2007).

Further south and beyond the floodplains of the wadis, sediment in the sand sea is moderately well sorted and dominated by frosted fine-grained quartz and feldspar with a clay mineral fraction (<10%) and occasional coarse to angular mineral grains settling in the low areas between the sand dunes. This sediment has been oxidized and has a reddish hue. The sand dunes are stratified with layers between 0.2 cm to 1 cm in thickness. The dunes trend east to west, are up to 50 m wide, and over 5 m in height (Palmer et al. 2007). Between the dunes is a desert pavement, composed of fluviatile sediments (Rabb'a 1994).

3.3.2 Soil Classification

Wadi 'Araba soils can be classified under the hyperthermic temperature regime and the aridic moisture regime (Al-Qudah 2001, Al-Bakri 2008). Soils in this region typically have a granular structure, are coarse-grained, contain small lithic clasts and calcareous nodules, and often have a weakly developed calcic horizon as the result of the accumulation of secondary carbonates (Al-Bakri 2008). The soils in Faynan have been characterized by very low levels of organic matter (OM), a very restricted water supply, and high alkalinity (Palmer et al. 2007, Al-Bakri 2008).

The yellow steppic soils of Faynan can be sorted into either the Camorthid Great Group or the Calciorthid Great Group of the Aridisol Taxonomic Order (Al-Qudah 2001). A typical

horizon sequences of these soils starts with desert pavement crust, the result of a high silt content which limits soil formation and makes germination difficult, leading to soils with very low levels of OM (Weil and Brady 2019). These soils are typically characterized by a thin ochric epipedon that overlays a weak calcic horizon in Calciorthid soil, and a weak cambic horizon in Camorthid soils (Al Qudah, 2001), though these soil horizons are too weak to identify in the sediments in Faynan. The weak development of or lack of soil horizons are typical of younger sediment profiles or those that have not been greatly affected by soil forming processes (Weil and Brady 2019).

3.3.3 Climate and Precipitation

The climate in Faynan is primarily influenced by the Saharo-Arabian desert belt in the southern and eastern parts of Jordan (Barker et al. 2007). January is the coldest month with temperatures rarely dropping below 12°C, while summers are very hot and dry, with temperatures often exceeding 40°C (Barker et al. 2007, Freiwan and Kadioğlu 2008). Erosion occurs rapidly in this arid desert environment as there is very little vegetation or moisture to hold the sediment in place, allowing the prevailing winds to redistribute sediment and metalliferous dusts, causing widespread deflation (Grattan et al. 2003a, Hunt et al. 2007, Barker et al. 2007).

Annual precipitation in Faynan is strongly influenced by topography and increases with increasing elevation, ranging from 1 to 15 mm/year in the sand sea, up to 50 mm/year near the base of the escarpment (Pyatt et al. 2000). Precipitation rates at the top of the escarpment can exceed 250 mm/year (Hunt et al. 2004, Wade et al. 2011). The rainy season in Faynan falls between October and March and seasonal flooding occurs when rain falls along the escarpment or atop plateau to the east (Hunt et al. 2007, Barker et al. 2007).

The rainfall over the desert pavement is ineffective as it is limited to only 15 mm over a 6-month rainy season, which would typically make sediments more likely to be highly leached (Weil and Brady 2019). In Faynan, most moisture evaporates before it can percolate through the hard desert crust which inhibits chemical weathering processes (Crook 2009). Consequently, it seems that metal contaminants are less likely to be chemically leached from a soil that would otherwise have a high affinity for leaching due to the high permeability of sand. Therefore, the slowed rates of chemical weathering resulting from the high temperatures and low precipitation rates (Weil and Brady 2019), have resulted in a shallow bedrock that has a strong control over the surface topography in Faynan (Rabb'a 1994).

3.3.4 Vegetation

The distribution and variety of vegetation in modern Faynan is directly related to the precipitation rates that vary significantly with elevation (Palmer et al. 2007). In the 'Araba Valley, where precipitation is less than 10 mm/year and land elevation is below sea level, there is very limited shrub vegetation, while atop the escarpment (>1000 m A.S.L) precipitation can exceed 250 mm/year and vegetation is diverse (Figure 3.6) (Hunt et al. 2004; 2007, Palmer et al. 2007).

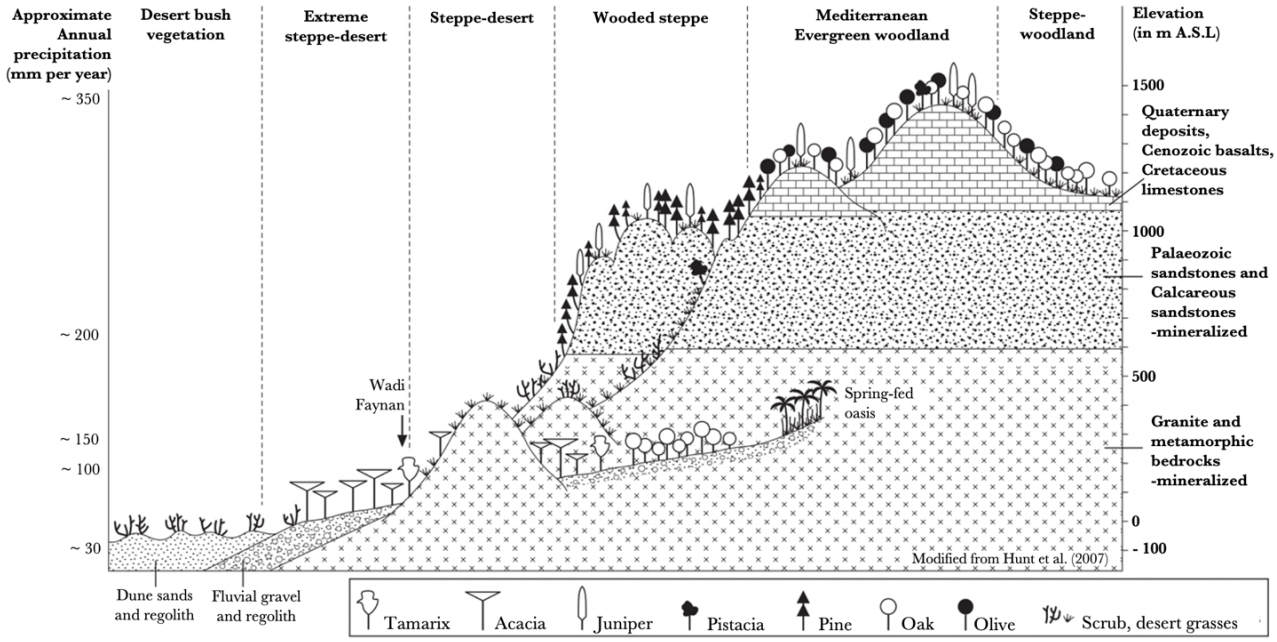

Figure 3.6: **The relationship between vegetation, precipitation, and elevation along a SW-NE transect through Faynan,** from the Wadi 'Araba Valley to the Wadi 'Araba Escarpment. (Illustration: David Gilbertson, Ian Gulley, and Antony Smith, after Baierle et al. 1989; Mohamed 1999.) Modified from Hunt et al. (2007).

The earlier classification of Faynan as an extreme desert based on annual precipitation rates is a relatively recent change in the local environment that was significantly affected by global environmental changes throughout the Holocene (Baruch and Bottema, 1991, Issar 1998, McLaren et al. 2004, Roberts et al. 2004, Hunt et al, 2004; 2007). The type and distribution of vegetation in Faynan has changed substantially in the 7000 years since it was first inhabited.

In the Chalcolithic Period (*c.* 6500 years BP) (Table 1.1) the environment in Faynan was more typical of a steppic environment with a few limited tree species (Hunt et al. 2007). The Chalcolithic sediments in the Faynan Valley have lower levels of tree pollen, show fewer sings of disturbance, and have more evidence of drought than the older stratigraphy, suggesting that overgrazing from Neolithic and Chalcolithic herds could have prevented the regeneration of trees and initiated the persistent erosion of sediment in the Faynan Valley that exists today (Hunt et al.

2007). The results of a biochar analysis found and that fuel sources at Early Bronze Age, Iron Age, and Roman Age smelting sites varied considerably, suggesting that the availability of these resources in the local wadis and up into the escarpment also changed (Engel and Frey 1996). By the Roman Age, much of the vegetation (e.g., oak and olive trees) that was an abundant resource for the Early Bronze Age miners and used to start smelting fires was no longer available below the Wadi 'Araba Escarpment (Engel and Frey 1996). The vegetation that was available to miners in the Roman Age would have been similar to the modern vegetation in Faynan (Figure 3.6) (Engle and Frey 1996, Hunt et al. 2007).

3.3.5 Groundwater

There are three main sources for groundwater in Faynan that provide water for the nearby villages of Faynan and Al Qurayqira: the Wadi Ghuwayr, Wadi Dana, and the headworks of a Roman Age/Byzantine conduit system in the Fidān Spring (Figure 3.5) (Crook 2009). The source of the groundwater is in the alkaline Palaeozoic sandstone in the Wadi 'Araba Escarpment and the Jordanian Plateau (Rabb'a 1994, Crook 2009). Consequently, groundwater sampled from natural springs in the Wadi Dana, the Wadi Ghuwayr, and the Fidān Spring, is alkaline and have pH values of 8.70, 8.89, and 9.11, respectively (Crook 2009).

Al Qurayqira sits directly on the Finān Member granitic bedrock (Rabb'a 1994). While stratigraphic data from boreholes drilled near Al Qurayqira indicate that the water table is more than 200 m below the surface (Crook 2009), the surrounding Holocene alluvium and sand in the Wadi Faynan forms a continuous aquifer with Palaeozoic sandstone (Rabb'a 1994). In some areas of the Wadi Faynan, the water table is within a few metres of the ground surface and large holes have been dug to access groundwater which is then pumped through hose pipes across the floor of the wadi and used to irrigate crops (J.P. Grattan, personal communication, 2022).

Hauptmann (2007) indicated that most of the land farmed by the modern Bedouin via hose-pipe irrigation was organized through the 'Jordan Valley Authority' and located closer to the modern village of Al Qurayquira (Figure 3.5). At the time, the Wadi Faynan field system and single agricultural fields in the Wadi Ghuwayr were operational (Hauptmann 2007), but the small-scale cultivation of tomato crops at the Wadi 100 site (observed in 2019) was not mentioned. Satellite images from Google Earth, published in May 2011, show no evidence of agriculture in the Wadi 100 fields, while images published in 2019 show the land being used for cultivation. This suggests that the use of the Wadi 100 fields for modern agriculture is a recent change in land-use.

3.3.6 The Wadi 100 site

The Wadi 100 site sampled in this study is part of an Early Bronze Age (EBA) archaeological site that was excavated by Wright et al. (1998), originally called Wadi Faynan 100 (WF100), was named for its location 500 m south of the main channel of the Wadi Faynan. The WF100 site, and thus the Wadi 100 site, is 11 hectares in size and the largest known EBA site in the Faynan Valley (Wright et al. 1998). This site is situated on a colluvial gravel terrace that rises 2 m above the main bed of the Wadi Faynan and runs east-west along the southern edge of the channel (Rabb'a 1994, Wright et al. 1998). The WF100 site is enclosed on four sides by a series of discontinuous EBA stone walls and has internal field walls that were built later in the Early Bronze Age (Wright et al. 1998).

The WF100 site is a part of the larger Wadi Faynan Field System, where agricultural and metallurgical activity occurred in tandem from the EBA into the Roman Period and modern Bedouin farmers continue to cultivate tomatoes in the soils within the EBA stone walls (Wright et al. 1998, Hauptmann 2007). Agricultural practices such as tilling, ploughing, and water divergence have continued to alter the Wadi 100 site, convoluting the depositional history (Wright et al. 1998). The Wadi Faynan experiences seasonal flooding which is known to wash away finer sediment particles, deflating the landscape, and depositing colluvium and alluvium, all of which have affected the sediments in the EBA Wadi 100 site post-occupation (Wright et al. 1998, Palmer et al. 2007, Hunt et al. 2007).

In a report on the first excavations of the WF100 site, Wright et al. (1998) noted that the EBA occupational layer was buried at a depth of 70 cm. At the time of sampling for this thesis, the test excavations dug in 1997 had not been filled in and the occupational surface was still visible. A field analysis of the surficial sediment on this occupational layer was conducted using a portable XRF (X-Ray fluorescence) machine that measured Cu and Pb at concentrations over 1000 μg/g (Grattan 2019, unpublished). These concentrations of Cu and Pb are much higher than any concentrations measured in the sediments sampled from the Wadi 100 site in this thesis (Table 5.2 and Table 5.3). Because the samples collected in this thesis were sampled at a depth of 30 cm and the data from these samples show much lower concentration of Cu and Pb, it is inferred that they were sampled from more recent sediments and do not reflect the Cu and Pb concentration in the EBA sediments, but more likely reflect the redistribution of metals from more highly contaminated areas (e.g., TWF and WF1 sites. Figure 3.5) through aeolian and fluvial processes.

3.3.7 The Barqa el-Hetiye site

The Barqa el-Hetiye site is in an area known locally as the sand sea, 5 km south and west of the Wadi Faynan along the northern base of a limestone ridge and 12 km west of the WF1 site (Figure 3.5). The site is situated more than twice the distance from the mines than any other site in Faynan and is believed to have been selected to make use of the limestone ridge; prevailing winds from the north provide optimal conditions for smelting at the top of this ridge (Fritz 1994, Hauptmann 2007). Barqa el-Hetiye is an EBA settlement site where ore was crushed, smelted, and processed into rod-shaped ingots (Fritz 1994, Hauptmann 2007). Many Iron Age and Roman Age artifacts can be found together with EBA artifacts on the deflated land surface. Though there is archaeological evidence of agriculture at the Barqa el-Hetiye site, no evidence of historical farming has been uncovered near the sampling location for the sediments analyzed in this thesis. At the time of sample collection, during the 2019 field school with the BLP, modern Bedouin farmers were growing melons in fields approximately 1 km to the east of the sampling area and a large hole over 10 m wide and 3 m deep had been dug to access ground water approximately 100 m to the northwest of the sampling area. No other instances of modern agriculture near the Barqa el-Hetiye site are known.

There are many stone structures throughout the Barqa el-Hetiye site, including EBA and Iron Age constructions and Roman Age watch towers (Fritz 1994, Hauptmann 2007). Evidence of mining has been found in the cultural strata outside of these stone structures, many of which have been identified as EBA and Iron Age dwellings and indicate that many of the people whole lived and worked in the mining community had no reprieve from the metals, dusts, and smoke associated with metallurgical processes (Fritz 1994). The construction of these stone buildings as dwellings for the workers presupposes an urban centre built around the mining operation as early as the EBA (Fritz 1994).

The Barqa el-Hetiye site is believed to have been one of the largest centres of ore production during the EBA and Iron Age (Hauptmann 2007). Although the Khirbet Faynan site in the Wadi Faynan (Figure 3.5, WF1) quickly became the epicentre of ore refining by the Roman Age, the limestone ridge at the Barqa el-Hetiye site was still seen as favourable and remained in use by the Romans who built watch towers to fortify the site and guard the enslaved workers (Fritz 1994, Hauptmann 2007).

3.4 Previous Work

Previous studies detailing the pollution in both the modern and ancient environments of Faynan have been conducted by various authors in collaboration with the Barqa Landscape Project (BPL), establishing Faynan as the oldest and longest sustained copper producing site in history. Earlier studies have revealed that elevated levels of heavy metal concentrations exist in various sedimentary deposits (Grattan et al. 2007; 2013; 2016) across Faynan. Species known to be afflicted by the bioaccumulation of these metals include the ancient inhabitants (Grattan et al. 2002; 2005, Pyatt et al. 2005, Perry et al. 2009; 2011, Beherec et al. 2016), the modern Bedouin population (Grattan et al. 2003b, Pyatt et al. 2005), and the goat and sheep that they herd (Pyatt et al. 2000). Today, the primary pathways for the bioaccumulation of these metals starts with the local vegetation (Pyatt et al. 2000) and invertebrate species (Pyatt et al. 2002, Grattan et al. 2003a). These previous geochemical studies demonstrate the ability of local sediments and biological remains to retain metal contaminants for extended periods of time and have established the modern metal concentrations in the local sediments, flora, and fauna. What is not yet known, is the percentage of these reported sediment metal concentrations that is easily accessible to these plants and organisms.

4.0 Methods

During the 2019 field season of the Barqa Landscape Project (BLP), 102 samples were collected from two known archaeological sites in the Faynan Valley in southern Jordan: 61 from the Wadi 100 site, 41 from the Barqa el-Hetiye site (Figure 4.1). The 2019 sampling strategy was designed to assist the BLP in the planning of future archaeological excavations. Samples were collected with the intention of performing a single step total digestion by aqua regia. The project later shifted to focus on the mobility and availability of various elements in four operationally defined sediment fractions through sequential digestion analysis. All samples from the Wadi 100 and Barqa el-Hetiye sites were prepared for analysis and analyzed in the Metal Isotope Geochemistry Laboratory (MIG Lab) at the University of Waterloo, Ontario. A small subset of 16 samples from the Wadi 100 and Barqa el-Hetiye sites were sent to Activation Laboratories (Actlabs; Ancaster, Ontario) for total analysis by aqua regia.

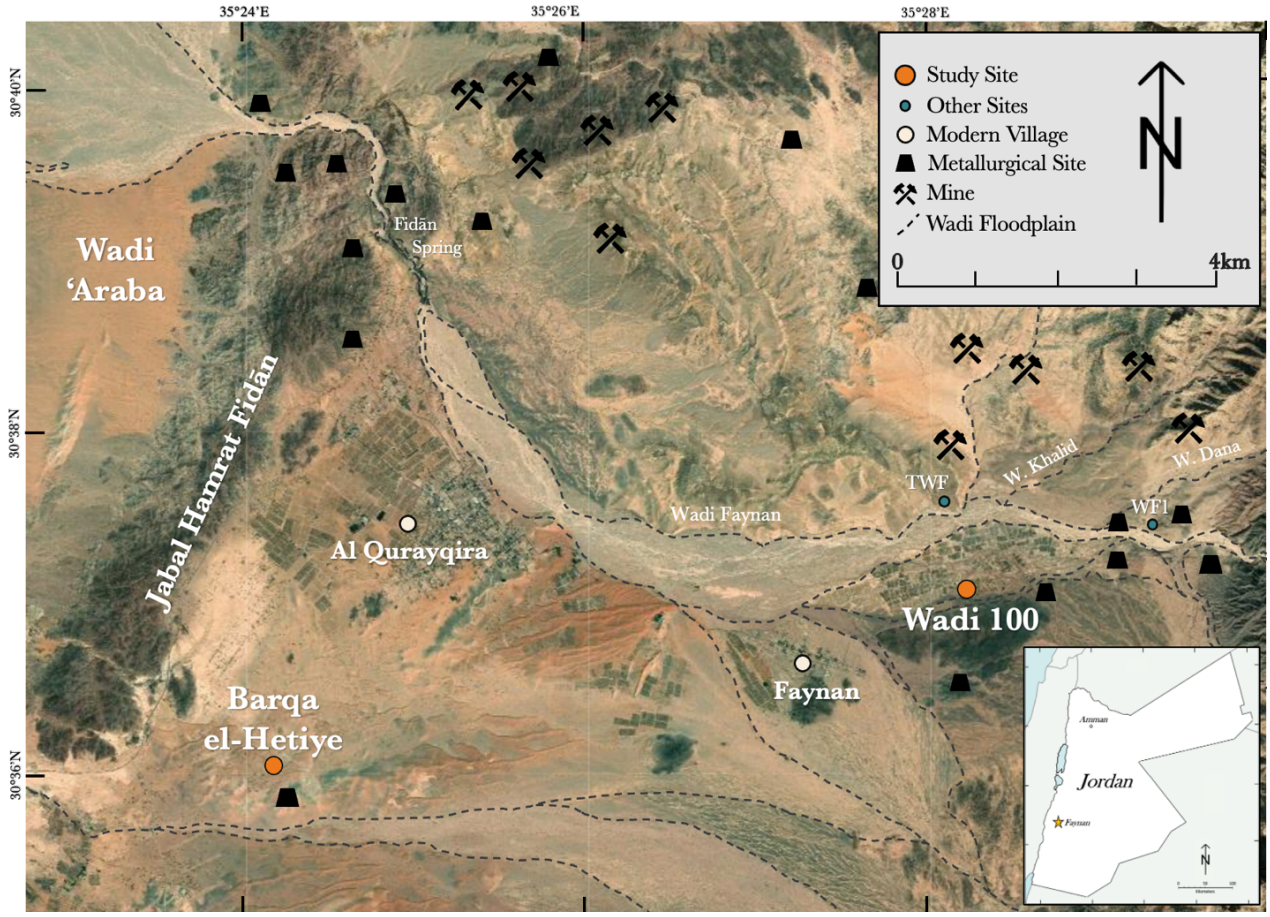

Figure 4.1: A satellite image of Faynan with the locations of the study sites (Wadi 100 and Barqa el-Hetiye) relative to other known archaeological sites, metallurgical sites, mines, and the modern villages of Al Qurayqira and Faynan. Modified from Hauptmann (2007) and esri Earthstar Geographics (2021).

4.1 Sample Collection

The sampling sites of Wadi 100 and Barqa el-Hetiye were surveyed by Alan Weston from the British Columbia Institute of Technology on behalf of the BLP. The locations of the sampling sites were digitized by Weston (2019) using a geographic information system (GIS) to produce accurate site maps for spatial analysis. Samples were collected using a stainless-steel soil auger and transported in plastic zip bags to the field lab in Al Qurayqira (Figure 3.5) where 10g of each air-dried sample was transferred into smaller sample bags and shipped to the MIG Lab at the University of Waterloo. The remainder of the original samples are stored at the American Centre for Oriental Research in Amman, Jordan.

4.1.1 Wadi 100 Samples

West of Khirbet Faynan (WF1, Figure 3.5) is an extensive system of fields separated by a series of stone walls. The Wadi 100 site is located along the southern edge of this ancient field system, 500 m south of the main Wadi Finān channel (Figure 4.1). Previous archaeological excavations at this site identify Wadi 100 as an occupational site dating to the EBA *c.* 3500 BCE (Barker et al. 1997, Hauptmann 2007). External stone walls built during the EBA separate this site from the rest of the field system and internal stone walls subdivide the site into 5 sections that are visible both in the field (Figure 4.2) and by satellite (Figure 4.3).

Figure 4.2: A field photo taken at the Wadi 100 site (2019). Photo taken while standing in the middle of the Wadi 100 site looking north towards the main wadi channel. Two stone walls are visible in the middle ground and separate the cultivated land north of the first wall from the uncultivated land south of the wall.

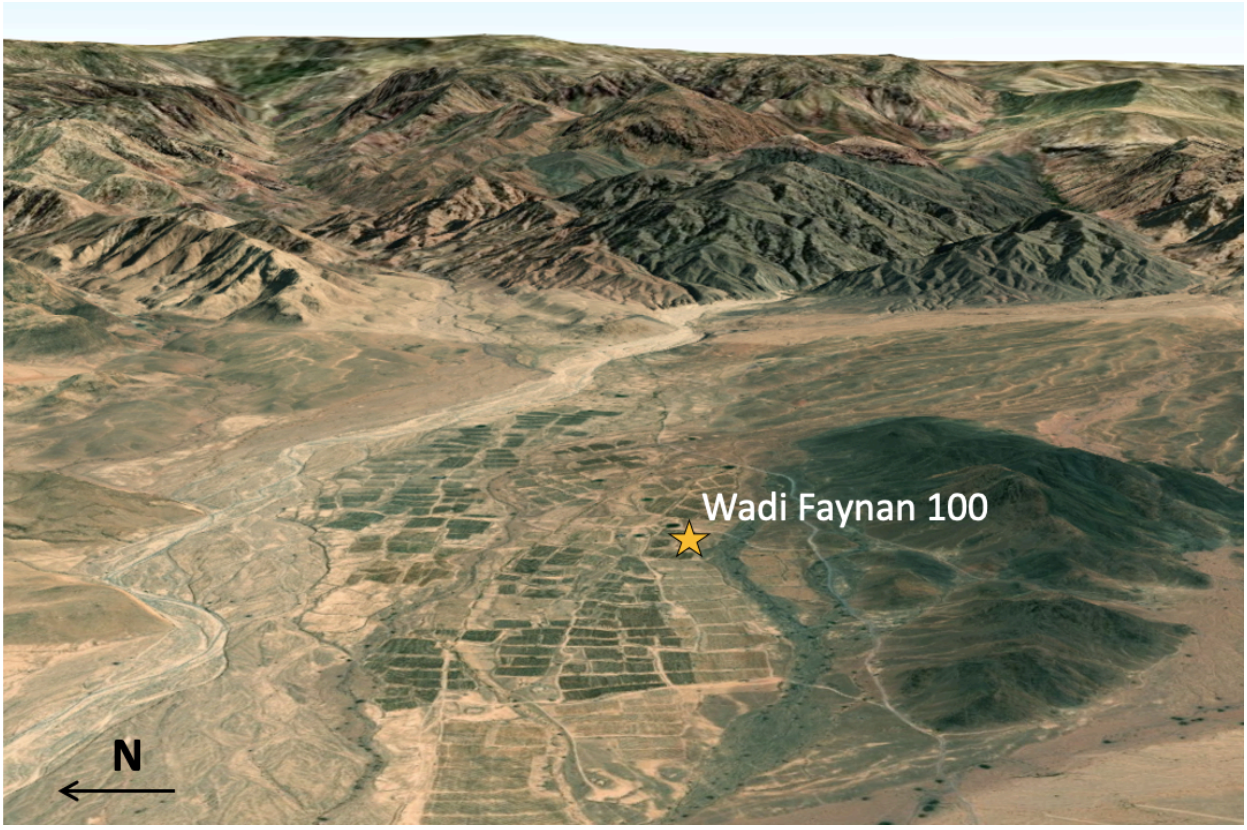

Figure 4.3: esri imagery of the Wadi 100 site and surrounding Wadi Faynan field system. The location of the Wadi 100 site (marked by a yellow star) is situated 500 m south of the main wadi channel. The stone walls used by modern Bedouin farmers to separate crops and are visible in this satellite imagery. Modified from Esri (2020).

The sampling strategy at the Wadi 100 site was influenced by pre-existing site conditions. Modern Bedouin farmers were cultivating tomatoes in the three of the five internal fields along the northern edge of the site. Sampling at the Wadi 100 site was conducted to establish the distribution of metal concentrations across this part of the Wadi Faynan floodplain and to determine the archaeological potential of the WF100 site. Diagonal transects through fields A, B, C, and D, used for modern agriculture were sampled in the northern and western portions of this site (Figure 4.4). These fields were in active use for crop production and the uppermost portion of sediment was disturbed. This sediment was sampled at an arbitrary depth of 30 cm. Field E in the southeastern portion of the Wadi 100 site, did not have evidence of modern agricultural activity (Figure 3.4). Field E samples were collected along an X-transect at a depth of 15 cm because sampling beyond this depth was restricted by large boulders and shards of pottery encountered 15 to 20 cm below the surface.

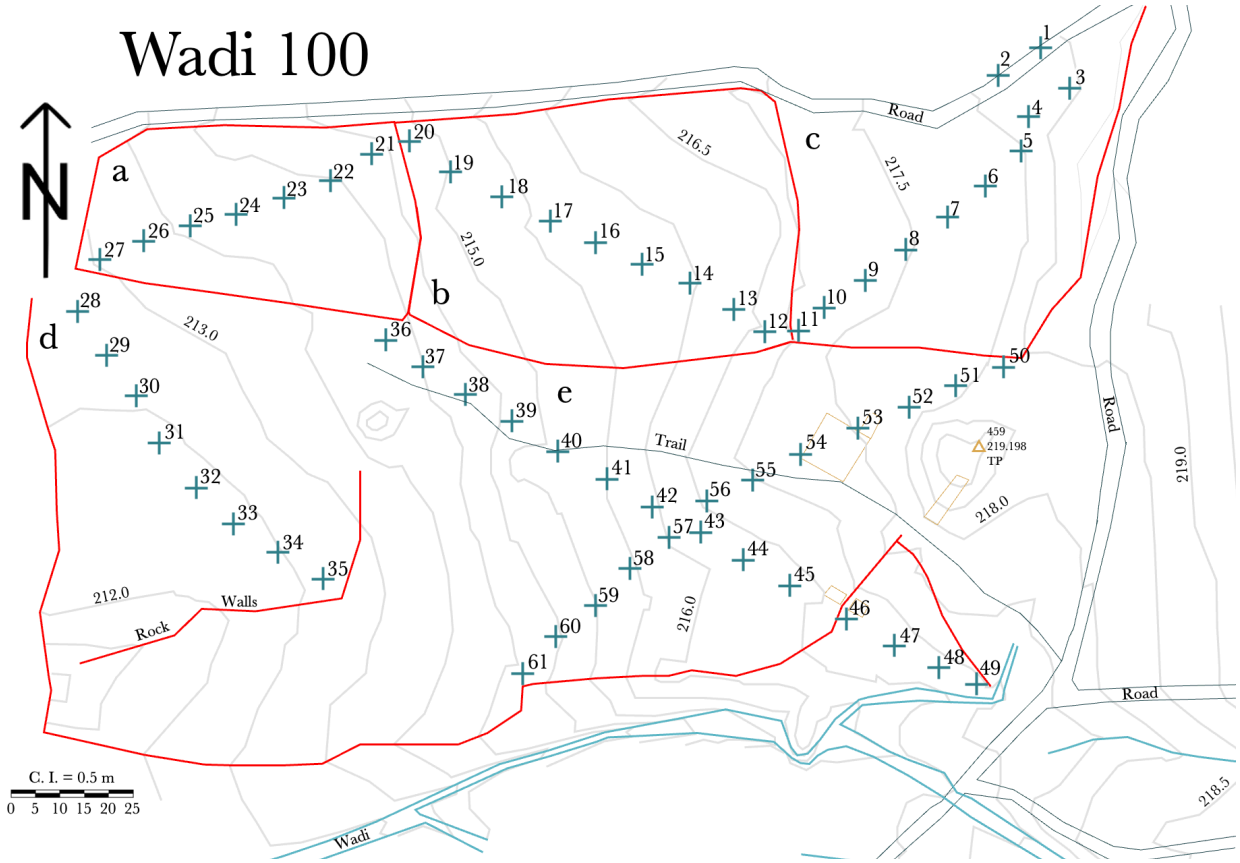

Figure 4.4: A map of the Wadi 100 site and the location of sampling transects (Weston 2019b). The location of each sample is denoted by a blue cross (+). Fields a, b, and c had signs of tilling and were actively used to grow tomato plants. Field d had evidence of tilling but no active crops. Field c sediments had no evidence of disturbance but an abundance of surficial EBA and Roman Age cultural material associated with earlier archaeological excavations, outlined in yellow.

4.1.2 Barqa el-Hetiye Samples

A few kilometers south of Al Qurayqira (Figure 3.5) in the sand sea, nearly 8 km from the next nearest known archaeological site, are the Barqa el-Hetiye sites; a small cluster of EBA dwellings and Roman watch towers at the base of a limestone ridge used for smelting (Figure 4.5). Sampling at Barqa el-Hetiye was conducted along a T-section in exposed EBA sediment between two sand dunes (Figures 4.6). Sediment was sampled at a depth of 30 cm at 23 locations along 2 transects (Figure 4.7). Fifteen samples were collected 10 m apart along the first transect, following the east-west trend of the sand dunes for 140 m. This first transect bypassed 4 previously excavated archaeological sites including a cluster of 3 burials south of the transect and a larger excavation north of the transect. A further 8 samples were collected 10 m apart along a second transect connecting the southern dune to the northern dune. Copper prills and pottery shards from various time periods could be seen along the deflated surface of the sampling area.

Figure 4.5: A field photo taken at the Barqa el-Hetiye site, looking south at the limestone ridge. The large dark area at the top of the ridge is the remnants of a slag heap from the furnaces used to smelt ore during the EBA and Roman Age.

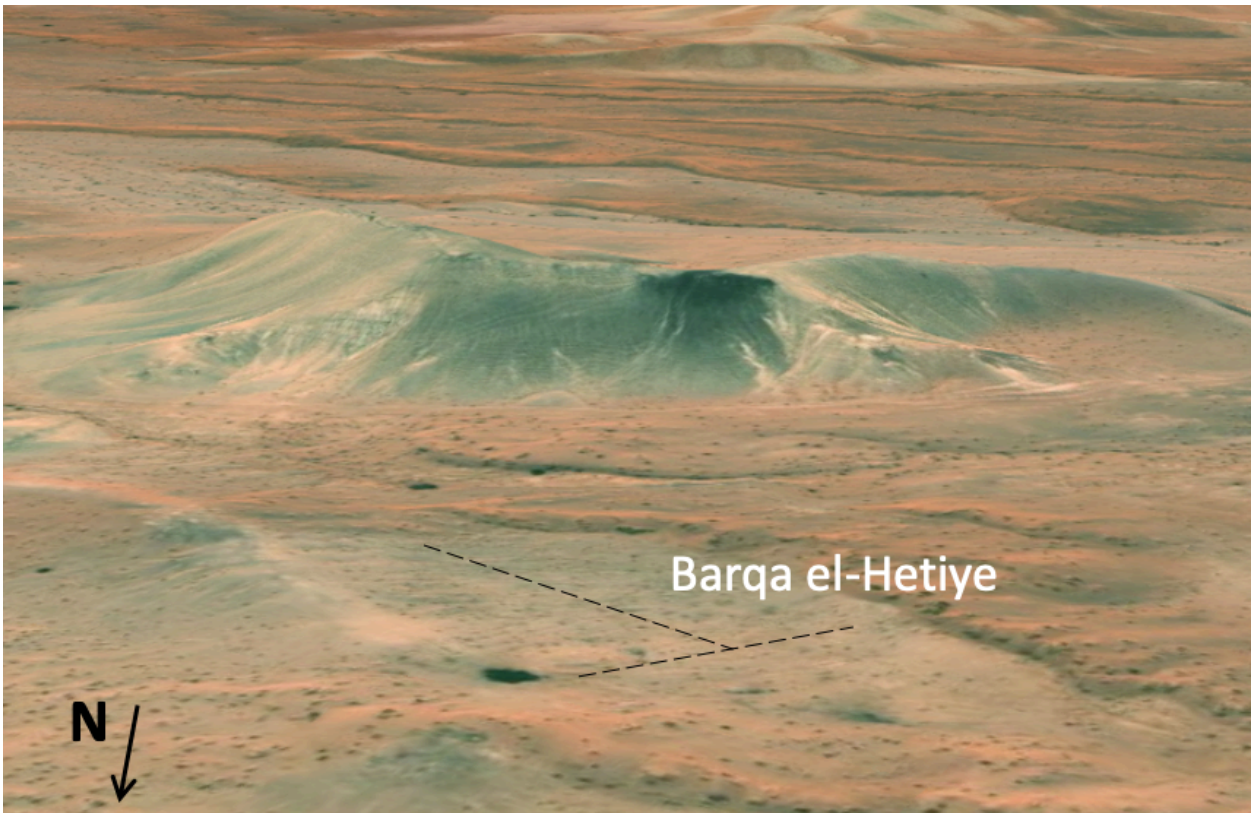

Figure 4.6: esri imagery of the Barqa el-Hetiye site and surrounding area. The dashed lines show the location of the T-section from which the sediment samples were collected. This T-section is situated along the desert pavement between two sand dunes, 230 m north of the limestone ridge and smelting site. Modified from esri (2020).

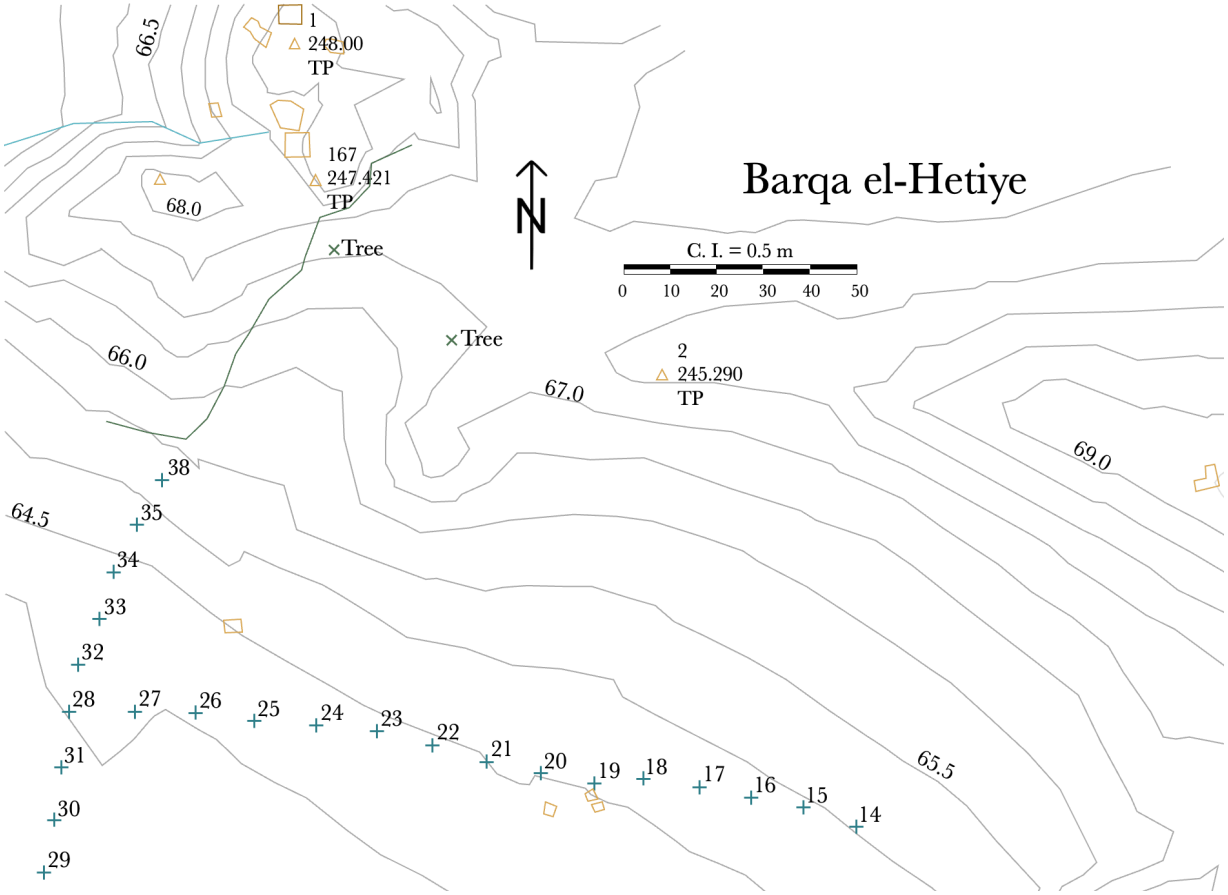

Figure 4.7: A map of the Barqa el-Hetiye site and the locations of collected samples, denoted by a blue cross (+). Known archaeological excavations are outlined in yellow and include 3 burials near sample 19, and a larger excavation north of sample 26 (Weston 2019a).

4.2 Sample Preparation

The elements selected for analysis are divided into two subgroups based on total element concentration; major elements Mg, Al, P, Mn, Fe, and Sr have mean total concentrations >150 μg/g; trace elements Cu, Cr, Ni, Zn, Cd, and Pb have mean total concentrations < 150 μg/g. Mn, Cu, and Pb were selected for analysis based on known associations with archaeometallurgy in Faynan. All other elements were selected for analysis based on other known geoarchaeological applications and use as geochemical indicators of archaeological features (Table 4.1).

Table 4.1: Examples of archaeological features and associated geochemical indicators. Modified from Oonk et al (2009) and Holliday and Gartner (2007) to include elements specific to archaeometallurgical sites in Faynan (*).

Archaeological Feature	Element
Burials and graves	P, Cu, Mn
Hearths	P, K, Mg
Middens	P, K
Farmhouses	P, Mg, Fe, Th, Rb, Pb, Zn, Sr
Mining, smelting, and ore-handling sites	Cu, Mn, Pb, Tl*, Cd*, Zn*, Cr*, As*
General archaeological sites	Cu, Mg, Mn, Ni, P, K, Zn

4.2.1 Physical Sample Preparation

The physical preparation of all samples collected during the BLP's 2019 field season was completed at the University of Waterloo. Air-dried samples were passed through a 2 mm sieve to remove pebbles and pottery shards before weighing the samples. To maintain balance while milling the samples in the ball mill, samples that were to be processed together weighed within 0.1 g of each other. On average, 5 g of each sample were milled using the Retsch PM200 Planetary Ball Mill in agate grinding jars with 3 agate balls. The ball-mill was run at 550 rpm for 20 minutes, pausing for 30 seconds every 5 minutes, not changing rotation. Samples were transferred from the agate grinding jars into labelled 20 mL glass vials for storage. Agate balls and grinding jars were rinsed with water and ethanol and milled with metal-free silica sand for 5 minutes between each sample run to minimize cross-contamination between samples.

In a pressurized balance room, 50 mL centrifuge tubes were labelled and weighed ($m_{50mL\ tube}$), and 0.2 g from each powdered sample was added ($m_{sample\ +50mL\ tube}$). The mass of the sediment sample (m_{sed}) analyzed was calculated using **Equation 1**.

(**1**) $$m_{sed} = m_{sample\ +50mL\ tube} - m_{50mL\ tube}$$

4.2.2 Chemical Sample Preparation

All samples from the Wadi 100 and Barqa el-Hetiye sites were chemically prepared for analysis at the University of Waterloo's MIG Lab following the sequential acid digestion outlined by the Standards Measuring and Testing program (SM&T, formerly BCR) of the European Union, in a class 10,000 metal-free cleanroom. This sequential digestion was designed to separate metals into four operationally defined fractions (Table 4.2). Sequentially digested material was dissolved and diluted in HNO_3 10% (w/w) and measured using an Agilent 8800 triple-quadrupole inductively coupled plasma mass spectrometer (QQQ-ICP-MS) in the MIG Lab.

Table 4.2: The four-step sequential extraction scheme used in the analysis of all samples in this thesis. Modified from the SM&T (formerly BCR) three-step sequential extraction scheme to include a 4th step (*) for analysis of the residual fraction (Davidson et al. 1998)

Fraction	Reagents	Targeted metals
Exchangeable	0.11 M, pH 3, CH_3COOH	Soil solution, exchangeable metals, and metals bonded to carbonates.
Reducible	0.1 M, pH 2, $NH_2OH{\cdot}HCl$	Metals bonded to Fe and Mn oxides.
Oxidizable	30% H_2O_2, and 1.0 M, pH 2, CH_3COONH_4	Metals bonded to organic matter and sulphides.
Residual*	aqua regia	Metals fixed in crystal lattices.

Fisher Scientific TraceMetal™ Grade hydrochloric acid (HCl) 35% (w/w), hydrofluoric acid (HF) 50% (w/w), and nitric acid (HNO_3) 70% (w/w), were used to transfer, stabilize, and analyze the digested samples respectively. All other chemicals used in the preparation of extraction solutions were of analytical-reagent grade purity or higher: glacial acetic acid (CH_3COOH) 99.7% (w/w); hydroxylammonium chloride ($NH_2OH \cdot HCl$) 99% (w/w); hydrogen peroxide (H_2O_2) 30% (w/w); ammonium hydroxide (NH_4OH) 28% (w/w). Deionized water from a Milli-Q® Advantage A10 Water Purification System was used throughout the procedure and is simply referred to as H_2O for the remainder of this section unless stated otherwise.

4.2.3 Exchangeable Fraction Extraction

In the cleanroom in the University of Waterloo's MIG Lab, a 0.1M acetic acid solution was prepared by mixing 2.87 mL of CH_3COOH and 497 mL of H_2O. Twenty mL of this solution were added to each labelled 50 mL centrifuge tube containing a 0.2 g sediment sample. Prepared samples were loaded onto a VWR Signature™ Rocking Platform Shaker and shaken for 16 hours. Shaken samples were transferred to a Thermo Scientific™ Sorvall™ ST 8 Small Benchtop Centrifuge and centrifuged at 4500 rpm for 5 minutes to allow sediments to settle. The decanted supernatant was poured into labelled 20 mL Teflon beakers and placed on a hotplate set to 110˚C to evaporate the solution. The test tube samples were rinsed a total of three times, each time with 5 mL of H_2O and centrifuged again for 5 minutes at 4500 rpm. The decanted rinse solution was added to the Teflon beakers and evaporated. The supernatant from the third rinse was poured off and discarded as waste.

Samples remained on the hotplate until the solution was evaporated. The remaining material was dissolved in 2 mL of 6M HCl and transferred into weighed and labelled 7 mL low-density polyethylene (LDPE) vials ($m_{LDPEvial}$). The Teflon beakers were rinsed with 2 mL of 6M HCl two more times. In total, 6 mL of 6M HCl were used to transfer each sample from the Teflon beakers to the LDPE vials and 2 drops of 0.5% (v/v) HF were added to the stock solutions before they were weighed ($m_{LDPEvial+sample}$) and stored under the fume hood. The mass of the stock solution (m_{stock}) stored in the LDPE vials was calculated using **Equation 2**.

$$m_{stock} = m_{LDPEvial+sample} - m_{LDPEvial} \quad (2)$$

4.2.4 Reducible Fraction Extraction

After the extraction of elements bonded in the exchangeable fraction, the remaining sediments in the sample tubes were rinsed and a 0.5 M hydroxylammonium chloride solution was prepared by combining 17.34 g of $NH_2OH \cdot HCl$ (salt) and 500 mL of H_2O. Twenty mL of the hydroxylammonium chloride solution were pipetted into each sample tube. Prepared samples were loaded onto the VWR Signature™ Rocking Platform Shaker and shaken for 16 hours. After shaking, the samples were transferred to the Thermo Scientific™ Sorvall™ ST 8 Small Benchtop Centrifuge and centrifuged at 4500 rpm for 5 minutes. The supernatant was poured into cleaned and labelled 20 mL Teflon beakers and placed on a hotplate at 110°C to evaporate the solution. The samples were rinsed three times with 5 mL of H_2O and centrifuged for 5 minutes at 4500 rpm. The decanted rinse solutions from the first and second rise were added to the Teflon beakers and evaporated. The supernatant from the third rinse was discarded as waste. The sample was transferred into 7 mL LDPE vials using 6 mL of 6M HCl. Two drops of 0.5% (v/v) HF were added to the LDPE vials and the samples were stored under the fume hood. The mass of the reducible fraction stock solution was calculated using Equation 2.

4.2.5 Oxidizable Fraction Extraction

The third digestion in this sequential extraction required an additional step, wherein 25 mL of hydrogen peroxide (H_2O_2) were added to the sediment samples and the samples were left uncovered under the fume hood for 1 hour to release any organic gasses. The samples were placed in a water bath and heated until the H_2O_2 had evaporated.

A 1M ammonium acetate (CH_3COONH_4) solution was prepared by combining 28.7 mL of CH_3COOH and 34.5 mL of NH_4OH in 437 mL of H_2O. Twenty-five mL of the solution were added to the samples in the 50 mL centrifuge tubes and the samples were loaded on to the VWR Signature™ Rocking Platform Shaker and shaken for 16 hours. The samples were centrifuged at 4500 rpm for 5 minutes and the supernatant was poured into 20 mL Teflon beakers and placed on a hotplate to evaporate. The samples were rinsed three times with H_2O; the supernatants from the first and second rinse were added to the Teflon beakers and evaporated; the supernatant from the third rinse was discarded as waste. Samples were transferred to 7 mL LDPE vials using 6 mL of 6M HCl. Two drops of 0.5% (v/v) HF were added before the stock solutions were weighed and stored under the fume hood. The stock solution masses were calculated using Equation 2.

4.2.6 Residual Fraction Extraction

After the extraction of the first three fractions, the residual samples were dried on a hotplate set to 70˚C and weighed in their original 50 mL centrifuge tubes to obtain the mass of the remaining sediment. The dried sediment was transferred to 20 mL Teflon beakers with 3 mL of HCl and 1 mL of HNO_3. The empty 50 mL centrifuges tubes were dried and weighed again to obtain the mass of any residual sample that was not transferred ($m_{50mLtube2}$). The Teflon lids were secured tightly, and the samples were placed on a hotplate set to 110˚C for 48 hours. The samples were removed from the hotplate and brought down to room temperature before the lids were removed and the samples were returned the hotplate for 2 to 3 hours, or until the extractant solution was evaporated. During this time the samples were monitored closely to ensure they were taken off the hotplate as soon as they were dry to limit the exposure of the metals to the oxygen in the air.

Once dry, 2 mL of HCl were added, the Teflon lids were secured tightly, and the samples were placed on the hotplate at 110˚C for a further 24 hours. The samples were then removed from the heat and allowed to cool down completely. Once cooled the Teflon lids were removed and the samples were placed back on the hotplate until the HCl was evaporated. Once dried, 2 mL of 6M HCl were added and the samples were left for 2 hours, away from the hotplate, to allow the HCl time to dissolve any extracted trace elements and to allow the remaining silicates time to settle out of solution. A pipette was used to transfer the supernatant from the Teflon beakers into 7 mL LDPE vials. The samples were rinsed two more times with 2 mL of 6M HCl and transferred to the LDPE vials. Two drops of 0.5% (v/v) HF were added and the stock solutions were weighed and stored under the fume hood. The mass of each stock solution was calculated using Equation 2.

4.2.7 Preparing Samples for Analysis

All samples were prepared for analysis in the same way. The predicted aliquot volumes were calculated using **Equation 3**:

$$\textbf{(3)} \qquad Predicted\ Aliquot\ Volume\ (mL) = \frac{(m_s \times 10\ \text{mL} \times 0.85\ \text{mL})}{m_{sed} \times DF}$$

Wherein 10 mL is the target final volume of the analyte solution, 0.85 mL is the volume of analyte used for ICP-MS analysis, and DF is the target dilution factor. The predicted aliquot volumes were pipetted into weighed 7 mL Teflon beakers ($m_{empty\ teflon}$) and weighed ($m_{teflon+aliquot}$). The mass of the aliquot (m_a) was calculated using **Equation 4**.

(4) $$m_a = m_{teflon+aliquot} - m_{empty\ teflon}$$

Weighed samples were placed on a hotplate set to 110˚C until evaporated. The precipitates were transferred to weighed 15 mL centrifuge tubes (m_{tub}) using 10 mL of 2% (v/v) HNO_3 and 2 drops of 0.5% (v/v) HF. Each centrifuge tube with analyte solutions was weighed ($m_{tube+sample}$) and recorded. The mass of the total sample diluted for analysis (m_{sa}) was determined using **Equation 5**.

(5) $$m_{sa} = m_{tube+sample} - m_{tube}$$

The true dilution factor (DF_t) of each analyte sample was calculated using **Equation 6**.

(6) $$DF_t = \frac{m_s}{m_{sed}} \times \frac{m_{sa}}{m_a}$$

4.3 Sample Analysis (QQQ-ICP-MS)

Major and trace element concentrations for diluted samples were measured using an Agilent 8000 triple-quadrupole inductively coupled plasma mass spectrometer (QQQ-ICP-MS) instrument in the University of Waterloo's MIG Lab. The analyte solutions from the exchangeable, reducible, and oxidizable fractions (DF = 500) were analyzed in with samples from the same site to minimize contamination between fractions. The residual fraction (DF = 5000) was analyzed independently to avoid element build up and minimize error margins in the QQQ-ICP-MS instrument. The result of each QQQ-ICP-MS run was recorded using the Agilent MassHunter software and transferred to Excel for data analysis. Measured element concentrations (C_m) were given in parts-per-billion (ng/g) and converted to parts-per-million (µg/g) to calculate the true element concentration (C_t) using **Equation 7**:

(7) $$C_t = \frac{C_m \times DF_t}{1000}$$

The total concentration of each element (X_t) was calculated as the sum of the measured concentrations of from each of the four analyzed fractions using **Equation 8**:

(8) $$X_t = X_{org} + X_{carb} + X_{ox} + X_{res}$$

4.4 Quality Assurance

External reference material from the International Association of Geoanalysts (IAG) for selective extraction by aqua regia (SdAR-H1, SdAR-M2, SdAR-L2; IAG 2020) was used to assess the quality of and confidence in the clean lab work and sample preparation. These IAG standards were acquired when the focus of this project was to determine metal concentrations in a single step aqua regia digestion. The specific use of these standards for extraction by aqua regia went unnoticed until the sequential extraction of the first three fractions was completed, at which point, lab time was severely restricted due to COVID-19 safety protocols. Two sets of IAG standards were analyzed with Wadi 100 and Barqa el-Hetiye samples and prepared for analysis in the same way as the sediment samples. A third set of IAG standard was analyzed with a small subset of samples using a single aqua regia digestion. The total element concentrations obtained through total digestion were used to determine the percent recovery of each element.

The total element concentrations of the IAG standards were measured as a four-part sum of the element concentrations determined through sequential extraction. A consequence of this four-part extraction is an increased risk in contamination and sample-loss through sample transfer that was not a factor in the reported concentrations of the IAG reference standards. For the SdAR-H1 IAG standards analyzed through sequential analysis, the total concentrations of Cr, Ni, Cu, Cd, and Pb were within 10% of the expected concentrations, Zn and Sr were within 20%, and As, Rb, Zr, Mo, Tl, and Th were less than 30% of their expected values and had at least one value below the LOD. For the SdAR-M2 standards analyzed by sequential extraction, the concentrations of Cr, Ni, Sr, Cd, Pb, and Th were all within 10% of their expected values, while the concentrations of Cu and Zn were within 20% of the expected values. The total measurable concentrations of As, Rb, Zr, Mo, and Tl were all less than 30% of their expected SdAR-M2 values and each of these elements had at least one fractional concentration below the LOD. The total concentrations of As and Tl from the sequential analysis of the SdAR-L2 standards were more than 50% higher than their expected values, while the total concentrations of Rb and Mo were less 50% of their expected values. The total concentrations of Cr, Zn, Sr, Cd, and Pb were within 10% and Ni, Cu, and Th were within 20% of their expected SdAR-L2 values.

Comparatively, the element concentrations measured though total digestion are as follows: Ni, As, Cd, Pb, Th within 10%, Cr, Cu, Mo, Tl within 20%, Zn, Sr within 30%, Rb and Zr over 200% for SdAR-H1. For the SdAR-M2 standard; Ni, Cu, Zn, As, Pb within 10%, Cr, Rb, Sr, Th

within 20%, Mo, Cd, and Tl within 40%, and Zr was over 300% of their expected values. For the SdAR-L2 standards; Cr, Ni, Cu, Zn, Sr, Tl, and Pb within 10%, Rb, As, and Tl within 15%, and Mo within 20% of their expected values.

All three of the IAG standards were prepared for aqua regia analysis using the same dilution factor as the sediment samples digested with the standards (DF = 500). The total concentrations of the elements in the samples collected from the Wadi 100 and Barqa el-Hetiye sites in this study are of the same magnitude as the expected concentrations in the SdAR-L2 standard (i.e., the mean concentration of Ni in Wadi 100 sediment is 13 ± 3.8 μg/g, and 12.9 μg/g in SdAR-L2, while SdAR-M2 and SdAR-H1 have 47 μg/g, and 222 μg/g Ni, respectively). Therefore, it is likely that some of the reported element concentrations for the SdAR-M2 and SdAR-H1standards required different dilutions for accurate analysis (i.e., DF > 500).

The measured element concentrations from the total digestion of the SdAR-L2 IAG standard ($X_{SdAR-L2}$) were uses to calculate the recovery rates of Cr, Ni, Cu, Sr, Zr, Cd, and Pb in the sequential extraction digestions using **Equation 9**:

(**9**)
$$\%\ Recovery\ X = \left(\frac{X_{ex}\ X_{red}\ X_{ox}\ X_{res}}{X_{SdAR-L2}}\right)\ x\ 100$$

Where X_{ex}, X_{red}, X_{ox}, and X_{res} are the measured concentrations of element (X measured in μg/g) in the exchangeable, reducible, oxidizable, and residual fractions, respectively.

In addition to the use of the external standards noted above, the United States Geological Survey (USGS) Certified Water Standards (T207, T211, T225, T231) and four internal standard elements (scandium (^{45}Sc), germanium (^{72}Ge), indium (^{115}In), and bismuth (^{209}Bi)) were analyzed between samples to correct for instrument drift. These internal standards are reported with element concentrations and a relative standard deviation (RSD) value which is measured as a percentage. Most individual samples had RSD values < 5% for each analyte. The recorded RSD values for Mo were greater than 10% in each analysed sample. The RSD values for As, Cd, and Tl were above 10% in some samples, though the mean RSD values for these elements were all below 10%. The mean RSD values for all other elements and samples were below 5%. Similarly, most individual total digestion samples had RSD values below 5% for each element analyzed. Of the 16 total digestion samples analyzed, As had 9, Mo had 13, Cd had 16, and Tl had 11 samples with RSD values over 10%.

Furthermore, one duplicate sample was prepared for every 10 samples analyzed: 6 duplicates with the Wadi 100 samples and 4 duplicates with the Barqa el-Hetiye samples. Total procedural blank samples were also prepared and analyzed with each fraction.

Based on the results reported above, the data obtained for Mo, Zr, As, and Tl were deemed unfit for further analysis and are not referenced in future sections. The results for Rb are reported in Section 5, but no further analysis is provided. The measured concentrations of Mg, Al, P, Mn, Fe, Sr, Cu, Cr, Ni, Zn, Cd, and Pb have been deemed fit for further analysis and are reported below in Section 5.

4.5 Statistical Analysis

Unpaired t-tests are used to compare the total element concentrations and the fractional element concentrations from the Wadi 100 and Barqa el-Hetiye sites to test that near-surface trace metal concentrations are not statistically different in sediments from the Wadi 100 floodplain and the aeolian sediments at Barqa el-Hetiye. The significance value for this test is set at .05, assuming a 95% confidence interval. A p value > .05 fails to reject the null hypothesis and indicates that there is no statistical difference in the element concentration at the Wadi 100 site and the concentration of that same element at the Barqa el-Hetiye site. A p value < .05 implies that there is a statistically significant difference in the element concentrations and would reject the null hypothesis.

5.0 Results

The following section is a summary of the geochemistry results from the analysis of the sequential extraction described above. The fractional distribution of each element as a percentage of the total element concentration is summarized in Table 5.1. The mean concentrations of each element in all four sediment fractions are summarized below in Table 5.2 and Table 5.3. Complete data tables for all elements, samples, and sediment fractions are in Appendix A.

Table 5.1: A summary of the proportional distribution of each element across all fractions. Values for each fraction are stated as a percentage (by weight) of the total concentration of each element (i.e., 57% of the total Mg in Wadi 100 sediments is in the exchangeable fraction).

Fraction	Site	Mg	Al	P	Mn	Fe	Sr	Cu	Cr	Ni	Zn	Cd	Pb
Exchangeable	Wadi 100	57	4	8	51	2	85	12	9	17	13	92	2
	Barqa el-Hetiye	50	7	18	47	2	70	27	10	7	13	100	5
Reducible	Wadi 100	6	9	80	26	8	6	28	7	13	19	8	23
	Barqa el-Hetiye	10	8	64	37	8	6	28	10	16	5	0	43
Oxidizable	Wadi 100	9	4	4	3	2	1	17	14	12	3	0	17
	Barqa el-Hetiye	12	5	2	2	1	5	12	9	9	40	0	9
Residual	Wadi 100	28	83	8	20	88	8	43	70	58	65	0	58
	Barqa el-Hetiye	28	80	16	14	89	19	33	71	68	42	0	43

Table 5.2: A summary of the geochemistry results for all major elements. All values are reported as the mean ± 1 SD for major element concentrations in each digested fraction based on 24 samples where *n* is the number of samples with a measurable concentration of each element. Values are reported in μg/g.

Fraction	Site	Mg (μg/g)	Al (μg/g)	P (μg/g)	Mn (μg/g)	Fe (μg/g)	Sr (μg/g)
Exchangeable Fraction	Wadi 100	4820 ± 790 (*n* = 24)	400 ± 96 (*n* = 24)	89 ± 92 (*n* = 24)	141 ± 39 (*n* = 24)	157 ± 41 (*n* = 24)	222 ± 56 (*n* = 24)
	Barqa el-Hetiye	2790 ± 1130 (*n* = 24)	712 ± 290 (*n* = 24)	69 ± 60 (*n* = 20)	174 ± 185 (*n* = 24)	124 ± 61 (*n* = 24)	110 ± 74 (*n* = 24)
Reducible Fraction	Wadi 100	470 ± 81 (*n* = 24)	889 ± 110 (*n* = 24)	914 ± 180 (*n* = 24)	72 ± 14 (*n* = 24)	603 ± 56 (*n* = 24)	16 ± 5.9 (*n* = 24)
	Barqa el-Hetiye	575 ± 310 (*n* = 24)	791 ± 840 (*n* = 24)	207 ± 69 (*n* = 24)	136 ± 194 (*n* = 24)	501 ± 105 (*n* = 24)	8.9 ± 18 (*n* = 24)
Oxidizable Fraction	Wadi 100	768 ± 140 (*n* = 24)	341 ± 140 (*n* = 24)	49 ± 20 (*n* = 23)	8.4 ± 1.8 (*n* = 24)	134 ± 74 (*n* = 24)	1.5 ± 0.4 (*n* = 24)
	Barqa el-Hetiye	642 ± 270 (*n* = 24)	537 ± 220 (*n* = 24)	16 ± 3.9 (*n* = 10)	6.7 ± 3.3 (*n* = 24)	71 ± 54 (*n* = 24)	7.9 ± 4.7 (*n* = 24)
Residual Fraction	Wadi 100	2400 ± 1290 (*n* = 24)	8140 ± 3730 (*n* = 24)	117 ± 73 (*n* = 20)	56 ± 26 (*n* = 24)	7010 ± 3350 (*n* = 24)	21 ± 12 (*n* = 23)
	Barqa el-Hetiye	1570 ± 800 (*n* = 24)	8040 ± 2960 (*n* = 24)	51 ± 19 (*n* = 24)	52 ± 20 (*n* = 24)	5740 ± 1790 (*n* = 24)	31 ± 13 (*n* = 24)
Total*	Wadi 100	8460 ± 1440 (*n* = 24)	9770 ± 3660 (*n* = 24)	1150 ± 220 (*n* = 24)	277 ± 33 (*n* = 24)	7900 ± 3330 (*n* = 24)	260 ± 62 (*n* = 24)
	Barqa el-Hetiye	5570 ± 2340 (*n* = 24)	10100 ± 3150 (*n* = 24)	326 ± 125 (*n* = 24)	369 ± 380 (*n* = 24)	6430 ± 1810 (*n* = 24)	158 ± 84 (*n* = 24)

* The mean total concentration of each element. Reported as the sum of the measured concentrations of each element in the exchangeable, reducible, oxidizable, and residual fractions.

Table 5.3: A summary of the geochemistry results for all trace elements. All values are reported as the mean ± 1 SD for trace element concentrations in each digested fraction based on 24 samples where *n* is the number of samples with a measurable concentration of each element. Values are reported in µg/g.

Fraction	Site	Cu (µg/g)	Cr (µg/g)	Ni (µg/g)	Zn (µg/g)	Cd (µg/g)	Pb (µg/g)
Exchangeable Fraction	Wadi 100	18 ± 17 (*n* = 22)	2.0 ± 0.3 (n = 24)	2.3 ± 0.6 (n = 24)	4.1 ± 1.2 (n = 21)	0.42 ± 0.11 (n = 21)	0.15 ± 0.03 (n = 24)
	Barqa el-Hetiye	34 ± 36 (*n* = 24)	1.3 ± 0.3 (n = 24)	2.4 ± 0.7 (n = 4)	8.9 ± 14 (n = 24)	0.11 ± 0.04 (n = 21)	0.52 ± 0.37 (n =22)
Reducible Fraction	Wadi 100	45 ± 35 (*n* = 23)	1.6 ± 0.2 (n = 24)	1.7 ± 0.2 (n = 24)	5.4 ± 3.2 (n = 24)	0.10 ± 0.02 (n = 7)	1.5 ± 0.3 (n = 24)
	Barqa el-Hetiye	36 ± 34 (*n* = 24)	1.2 ± 0.5 (n = 24)	0.98 ± 0.25 (n = 24)	3.2 ± 2.4 (n = 24)	< LOD	4.1 ± 3.5 (n = 24)
Oxidizable Fraction	Wadi 100	26 ± 31 (*n* = 24)	3.1 ± 0.6 (n = 24)	1.7 ± 0.3 (n = 24)	1.2 ± 0.4 (n = 18)	< LOD	1.1 ± 0.4 (n = 24)
	Barqa el-Hetiye	14 ± 13 (*n* = 24)	1.1 ± 0.3 (n = 24)	0.58 ± 0.18 (n = 21)	27 ± 8.1 (n = 24)	< LOD	0.87 ± 0.51 (n = 24)
Residual Fraction	Wadi 100	65 ± 47 (*n* = 24)	16 ± 7.5 (n = 23)	7.8 ± 3.9 (n = 24)	21 ± 12 (n = 21)	< LOD	3.8 ± 2.2 (n = 24)
	Barqa el-Hetiye	42 ± 33 (*n* = 24)	9.2 ± 3.3 (n = 23)	4.1 ± 1.7 (n = 24)	29 ± 4.1 (n = 24)	< LOD	4.0 ± 1.1 (n = 24)
Total*	Wadi 100	151 ± 76 (*n* = 24)	22 ± 7.9 (n = 24)	13 ± 3.8 (n = 24)	28 ± 13 (n = 24)	0.43 ± 0.14 (n = 22)	6.5 ± 2.3 (n = 24)
	Barqa el-Hetiye	125 ± 105 (*n* = 24)	12 ± 4.0 (n = 24)	5.9 ± 2.4 (n = 24)	69 ± 19 (n = 24)	0.11 ± 0.04 (n = 21)	9.5 ± 4.9 (n = 24)

* The mean total concentration of each element. Reported as the sum of the measured concentrations of each element in the exchangeable, reducible, oxidizable, and residual fractions.
< LOD indicates that no concentration could be measured; concentrations were below the Limit of Detection.

5.1 Major Element Concentrations

The ranges in the total concentrations of Mg, Al, P, Mn, Fe, and Sr at both the Wadi 100 and Barqa el-Hetiye sites are compared in Figure 5.1. The concentrations of each element in the exchangeable, reducible, oxidizable, and residual fractions are detailed below.

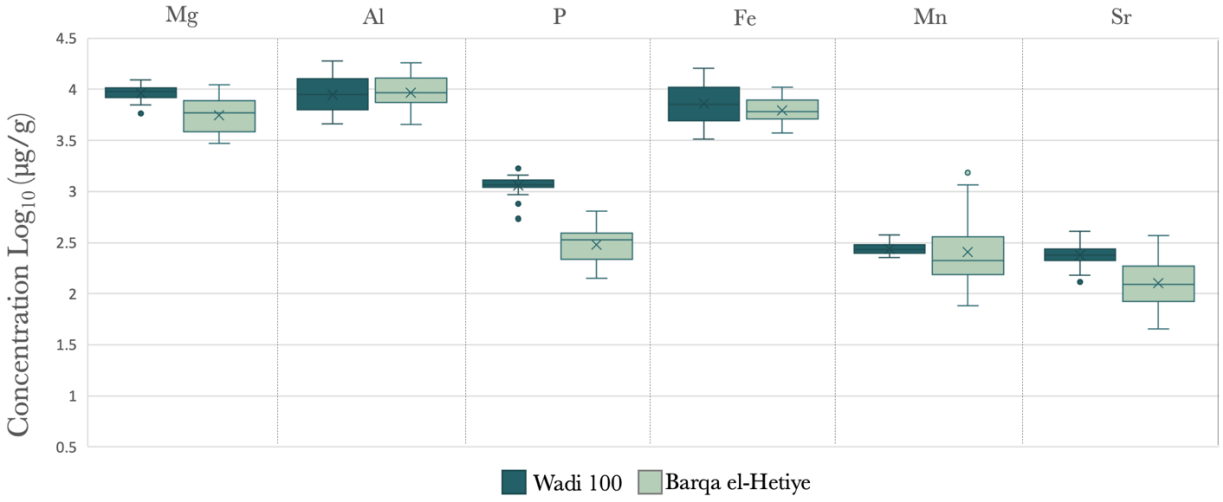

Figure 5.1: A box and whisker plot showing the range in the total concentrations of all elements. Boxes extend to show the interquartile range of each element. The horizontal lines mark the median, the x is the mean, and the whiskers extend to show the maximum and minimum values. Outliers are marked by dots and are in line with the whiskers.

5.1.1 Magnesium

The total Mg concentrations at the Wadi 100 site ranges from 5360 µg/g to 11,300 µg/g and have a mean of 8460 ± 1440 µg/g (n = 24). Sequential extraction data indicate that 57% of the Mg at Wadi 100 is available in the exchangeable fraction, 6% is in the reducible fraction, 9% in the oxidizable fraction, and 28% is locked in the residual fraction (Figure 5.2). Exchangeable Mg concentrations range from 3360 µg/g to 6370 µg/g and have a mean value of 4820 ± 790 µg/g (n = 24). The reducible fraction at Wadi 100 has the lowest amount of Mg and concentrations ranging from 266 to 593 µg/g, with a mean of 470 ± 81 µg/g (n = 24). Mg concentrations are slightly higher in the oxidizable fraction and range from 380 to 974 µg/g with a mean of 768 ± 140 µg/g (n = 24). The residual fraction has the second highest concentration of Mg that ranges from 564 to 5360 µg/g with a mean of 2400 ± 1290 µg/g (n = 24).

The total concentrations of Mg in Barqa el-Hetiye sediments range from 2740 µg/g to 10,100 µg/g and have a mean of 5570 ± 2340 µg/g (n = 24). Exchangeable Mg accounts for 50% of all Mg at the Barqa el-Hetiye site, 10% is reducible Mg, 12% is oxidizable Mg, and 28% is reducible Mg. Exchangeable Mg concentrations range from 5180 µg/g and 1590 µg/g and have a mean value of 2790 57 (n = 24). The reducible fraction has the lowest concentration of Mg, ranging from 190 µg/g to 1210 µg/g, with an average of 575 ± 310 µg/g (n = 24). Mg concentrations in the oxidizable fraction range from a minimum of 256 µg/g to a maximum of 1250 µg/g and have a mean value of 642 ± 270 µg/g (n = 24). Residual Mg concentrations range from 560 to 3170 µg/g and produce a mean concentration of 1570 ± 800 µg/g (n = 24).

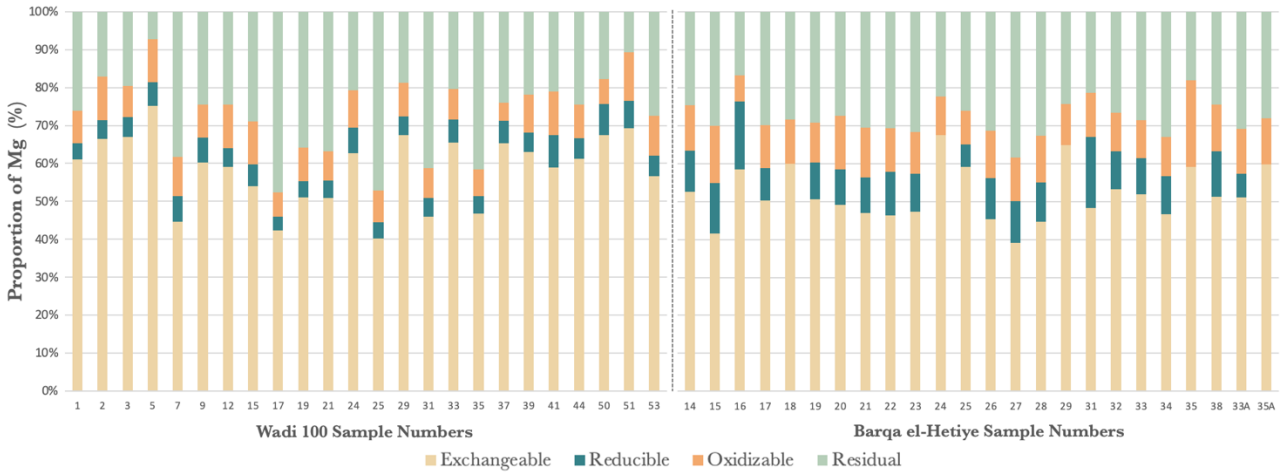

Figure 5.2: Distribution of Mg concentrations across all sediment fractions as a percentage (%) of the total concentration of Mg at Wadi 100 (left) and Barqa el-Hetiye (right).

5.1.2 Aluminum

The total Al concentration at the Wadi 100 site ranges from 4670 to 18,500 μg/g, with a mean of 9770 ± 3660 μg/g (n = 24). The exchangeable fraction at Wadi 100 has an average concentration of 400 ± 96 μg/g (n = 24) and ranges from 209 μg/g to 612 μg/g. Al concentrations in the reducible fraction at Wadi 100 range from 685 to 1100 μg/g and have a mean of 889 ± 110 μg/g (n = 24). Al concentrations are slightly lower in the oxidizable fraction and range from 133 to 740 μg/g, with a mean of 341 ± 140 μg/g (n = 24). The residual fraction has the largest range in Al concentrations from a minimum of 2930 μg/g to a maximum of 16,800 μg/g, and a mean of 8140 ± 3730 μg/g (n = 24). In Wadi 100 sediments, 4% of the Al is exchangeable Al, 9% is reducible Al, 4% is oxidizable Al, and 83% is residual Al (Figure 5.3).

In Barqa el-Hetiye sediments, total concentrations range from 5220 to 17,500 μg/g, with a mean of 10,100 ± 3150 μg/g (n = 24). The exchangeable fraction at Barqa el-Hetiye contains 7% of the total Al, while the reducible fraction has 8%, the oxidizable fraction has 5%, and the residual fraction accounts for 80%. Al concentrations in the exchangeable fraction range from 283 μg/g to 1500 μg/g and have a mean value of 712 ± 290 μg/g (n = 24). Al in the reducible fraction ranges in concentration from 370 to 1050 μg/g and has a mean concentration of 622 ± 108 μg/g (n = 24). Al concentrations are lowest in the oxidizable fraction, ranging from 271 to 1220 μg/g and have a mean of 537 ± 220 μg/g (n = 24). The residual fraction has the largest range of Al concentrations with a minimum of 3840 μg/g and a maximum of 15,000 μg/g. The mean residual Al concentration is 8040 ± 2960 μg/g (n = 24).

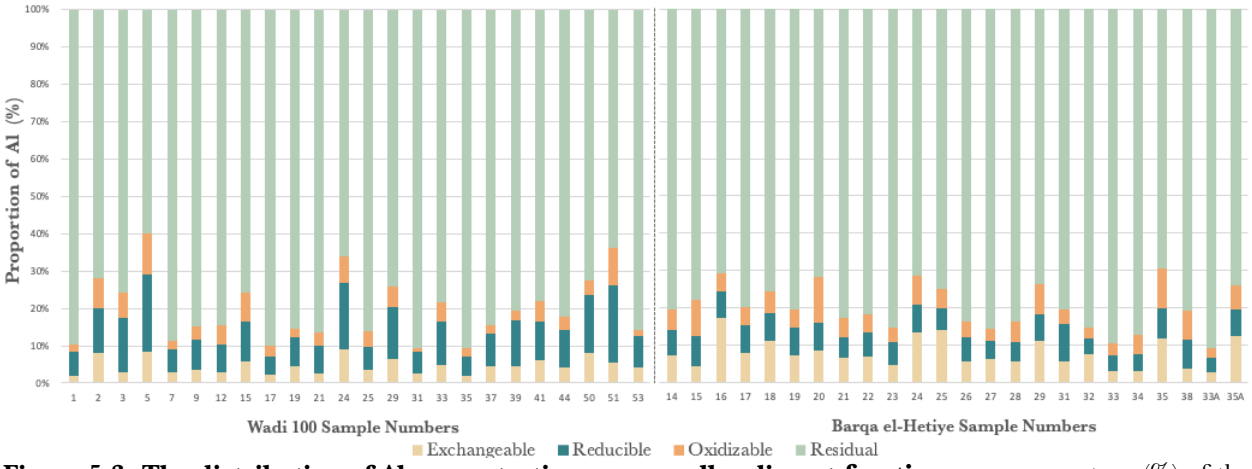

Figure 5.3: The distribution of Al concentrations across all sediment fractions as a percentage (%) of the total concentration of Al at Wadi 100 (left) and Barqa el-Hetiye (right).

5.1.3 Phosphorus

The total P concentrations in Wadi 100 sediments range from 520 to 1660 µg/g and have a mean of 1150 ± 220 µg/g (n = 24). Exchangeable P has a minimum concentration of 31 µg/g and a maximum of 503 µg/g, producing a mean of 89 ± 92 µg/g (n = 24). Reducible P concentrations range from 457 to 1320 µg/g and have a mean of 914 ± 180 µg/g (n = 24). Oxidizable P concentrations range from 22 to 98 µg/g and have a mean of 49 ± 20 µg/g (n = 23). The residual fraction has the second highest P concentration at Wadi 100, with values ranging from 40 to 323 µg/g with a mean of 117 ± 73 µg/g (n = 20). In the Wadi 100 sediments, 8% of the total P is exchangeable, 80% is reducible, 4% is oxidizable, and 8% is residual (Figure 5.4).

The Barqa el-Hetiye sediments have total P concentrations that range from 122 µg/g to 639 µg/g and a mean total concentration of 326 ± 130 µg/g (n = 24). Phosphorous in the exchangeable fraction at Barqa el-Hetiye ranges in concentration from 16 µg/g to 305 µg/g and has a mean value of 69 ± 60 µg/g (n = 21). The highest P concentrations are in the reducible fraction which range from 101 µg/g to 334 µg/g and have a mean concentration of 207 ± 69 µg/g (n = 24). P concentrations are lowest in the oxidizable fraction which has an average concentration of 16 ± 4 µg/g, ranging from 11 µg/g to 23 µg/g (n = 10). Residual P ranges from 21 to 93 µg/g with a mean of 52 ± 20 µg/g (n = 24). In Barqa el-Hetiye sediments, 18% of the total P is available in the exchangeable fraction, 64% is in the residual fraction, 24% in the oxidizable fraction, and 16% is locked in the residual fraction.

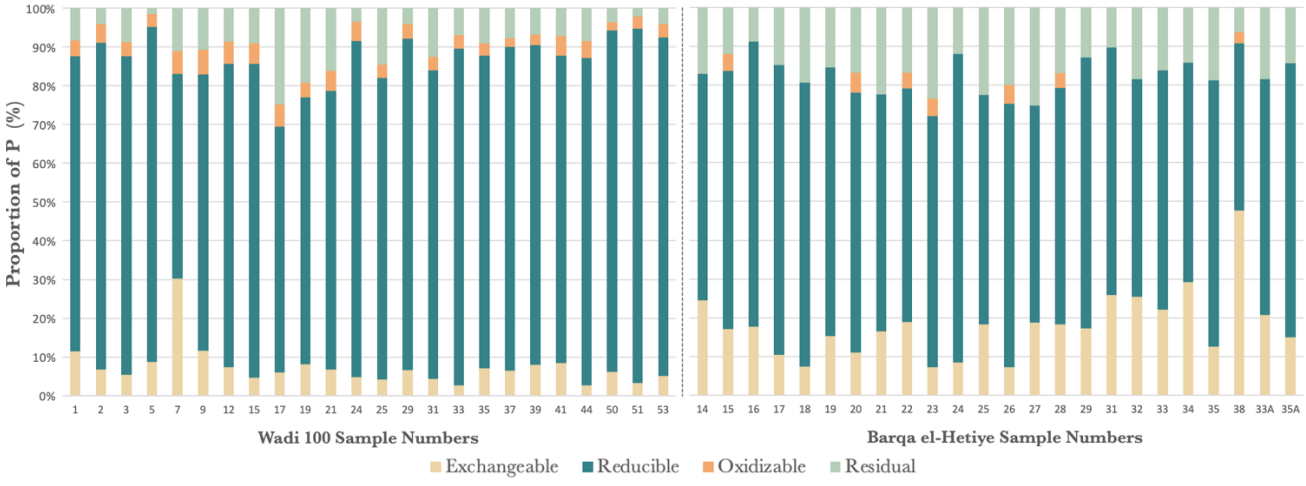

Figure 5.4: The distribution of P concentrations across all sediment fractions as a percentage (%) of the total concentration of P at Wadi 100 (left) and Barqa el-Hetiye (right).

5.1.4 Manganese

The total concentrations of Mn in Wadi 100 sediments range from 229 to 380 µg/g, with a mean of 277 ± 33 µg/g (n = 24). The concentrations of exchangeable Mn range from 83 µg/g to 270 µg/g and have a mean of 141 ± 39 µg/g (n = 24). The reducible Mn concentrations range from 37 to 94 µg/g with a mean of 72 ± 14 µg/g (n = 24). Mn concentrations are lowest in the oxidizable fraction and range from 5.1 to 13 µg/g with a mean of 8.4 ± 1.8 µg/g (n = 24). Mn concentrations in the residual fraction range from 19 µg/g to 119 µg/g and have a mean value of 56 ± 26 µg/g (n = 24). In the sediments collected from the Wadi 100 site, 51% of Mn was available in the exchangeable fraction, 26% was in the reducible fraction, 3% was in the oxidizable fraction, and 20% remained in the residual fraction (Figure 5.5).

In the sediments collected from the Barqa el-Hetiye site, 47% of Mn was extracted from the exchangeable fraction, 37% was recovered from the reducible fraction, 2% was in the oxidizable fraction, and 14% was locked in the residual fraction. Total Mn concentrations range from 78 to 1520 µg/g and have a mean value of 369 ± 380 µg/g (n = 24). Exchangeable Mn concentrations range from 41 to 689 µg/g and have a mean value of 174 ± 185 µg/g (n = 24). The Mn concentrations in the reducible fraction range from 13 to 819 µg/g and have a mean of 136 ± 194 µg/g (n = 24). Mn concentrations are lowest in the oxidizable fraction, ranging from 2.3 to 16 µg/g and have a mean of 6.7 ± 3.3 µg/g (n = 24). Residual Mn concentrations at Barqa el-Hetiye range from a minimum of 19.8 µg/g to a maximum of 93.4 µg/g and have a mean of 52 ± 19 µg/g (n = 24).

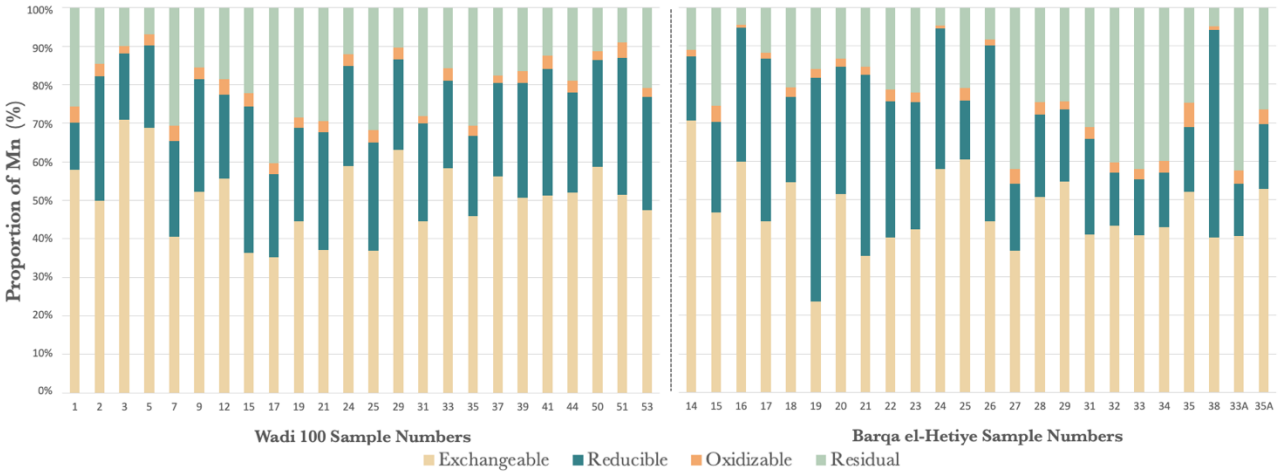

Figure 5.5: The distribution of Mn concentrations across all sediment fractions as a percentage (%) of the total concentration of Mn at Wadi 100 (left) and Barqa el-Hetiye (right).

5.1.5 Iron

The total concentrations of iron in Wadi 100 sediments range from 3280 to 15,900 μg/g with a mean of 7900 ± 3330 μg/g (n = 24). Fe concentrations in the exchangeable fraction are low and range from 104 μg/g to 251 μg/g with a mean value of 157 ± 41 μg/g (n = 24). Reducible Fe concentrations at the Wadi 100 site range from 481 to 694 μg/g and have a mean of 603 ± 56 μg/g (n = 24). Iron concentrations are the lowest in the oxidizable fraction, ranging from 43 to 327 μg/g with a mean of 134 ± 74 μg/g (n = 24). Most of the Fe in the Wadi 100 sediments was extracted from the residual fraction. The concentrations of residual Fe range from 2280 to 14,900 μg/g with a mean of 7010 ± 3350 μg/g (n = 24). In Wadi 100 sediment, 88% of Fe is in the residual fraction, 8% is in the reducible fraction, and the exchangeable and oxidizable fraction each contain 2% of the total Fe (Figure 5.6).

The total Fe concentrations in Barqa el-Hetiye sediments range from 3760 μg/g to 10,500 μg/g and a mean of 6430 ± 1810 μg/g (n = 24). At the Barqa el-Hetiye site, 2% of Fe is available in the exchangeable fraction, 8% is reducible Fe, 1% is oxidizable Fe, and 89% is residual Fe (Figure 4.6). Exchangeable Fe concentrations range from 34 μg/g and 253 μg/g and have a mean of 124 ± 61 μg/g (n = 24). Fe concentrations in the reducible fraction 7.8% of the Fe_t range from 287 μg/g to 707 μg/g and have a mean concentration of 501 ± 105 μg/g (n = 24). Oxidizable Fe concentrations are lowest, ranging from 28 μg/g to 226 μg/g with a mean of 71 ± 54 μg/g (n = 24). Residual Fe concentrations range from 3110 to 9730 μg/g and have a mean concentration of 5740 ± 1790 μg/g (n = 24).

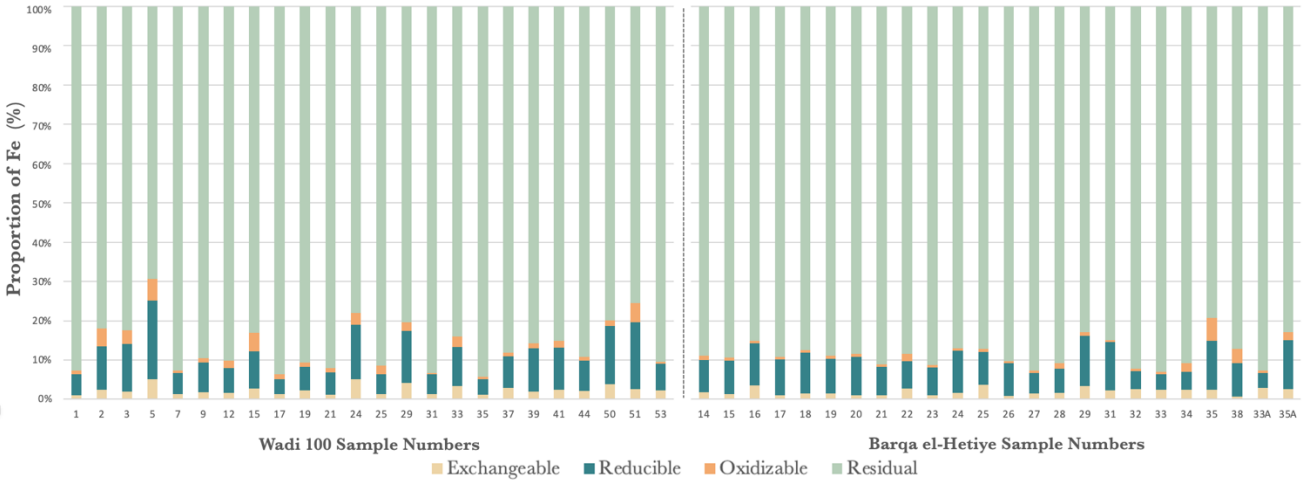

Figure 5.6: The distribution of Fe concentrations across all sediment fractions as a percentage (%) of the total concentration of Fe at Wadi 100 (left) and Barqa el-Hetiye (right).

5.1.6 Strontium

The total concentrations of Sr in the Wadi 100 sediments range from 155 to 426 μg/g and have a mean value of 260 ± 62 μg/g (*n* = 24). In Wadi 100 sediments, 85% of the total Sr is in the exchangeable fraction, 6% is in the reducible fraction, 1% is in the oxidizable fraction, and the residual fraction contains 8% (Figure 5.7). The average Sr concentration in the exchangeable fraction is 222 ± 56 μg/g (*n* = 24). Exchangeable Sr concentrations range from 133 μg/g to 391 μg/g. Concentrations of reducible Sr range from 5.9 to 36 μg/g and have a mean value of 16 ± 5.9 μg/g (*n* = 24). Oxidizable Sr concentrations range from 0.93 μg/g to 1.8 μg/g and have a mean of 1.5 ± 0.37 μg/g (*n* = 24). Sr concentrations in the residual fraction range from 8.4 μg/g to 56 μg/g and have a mean of 21 ± 12 μg/g (*n* = 23).

In Barqa el-Hetiye sediments, total Sr concentration range from 70 to 376 μg/g and have a mean of 158 ± 84 μg/g (*n* = 24). The Sr concentrations in the exchangeable fraction at Barqa el-Hetiye range from 46 μg/g to 319 μg/g and have a mean of 110 ± 74 μg/g (*n* = 24). Reducible Sr concentrations are low, ranging from 1.5 to 89 μg/g and have a mean of 8.9 ± 18 μg/g (*n* = 24). Sr concentrations in the oxidizable fractions are lower, ranging from 4.4 to 23 μg/g, with a mean of 7.9 ± 4.7 μg/g (*n* = 24). The concentrations of residual Sr range from a minimum of 17 μg/g to a maximum of 80μg/g and have a mean of 31 ± 13 μg/g (*n* = 24). The fractional distribution of Sr in Barqa el-Hetiye sediments (Figure 4.8) show that 70% of Sr is available in the exchangeable fraction, 6% is in the reducible fraction, 5% is in the oxidizable fraction, and 19% is locked in the residual fraction.

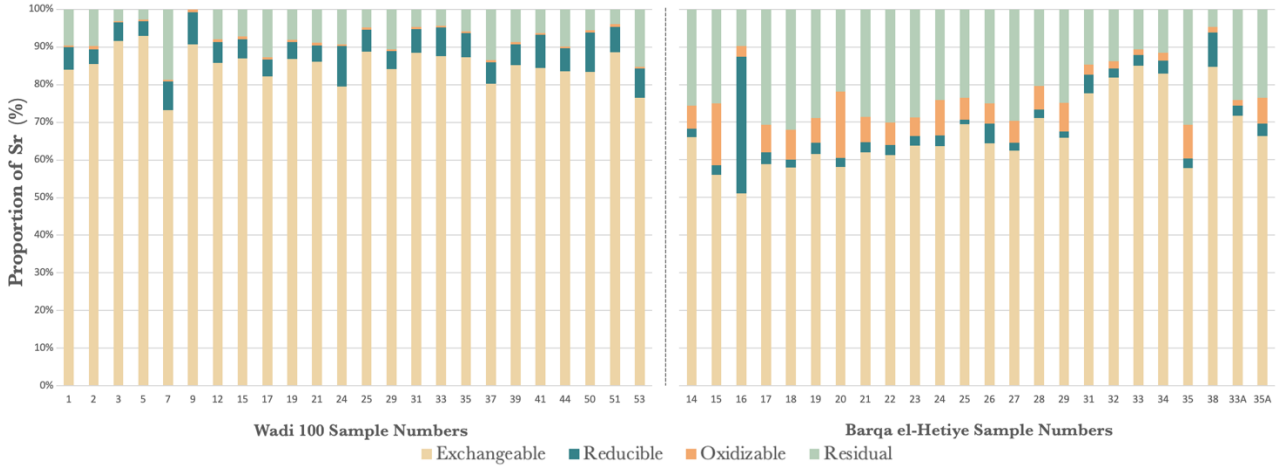

Figure 5.7: The distribution of Sr concentrations across all sediment fractions as a percentage (%) of the total concentration of Sr at Wadi 100 (left) and Barqa el-Hetiye (right).

5.1.7 Major Element Summary

The exchangeable fraction contains the highest proportion of Mg, Mn, and Sr at both sites (Figure 5.8). The reducible fraction has the highest proportion of P and the lowest proportion of Mg at both sites. The oxidizable fraction contains the lowest proportion of Al, P, Mn, Fe, and Sr at both sites. The residual fraction contains more than 50% of the total concentrations Al and Fe at both sites.

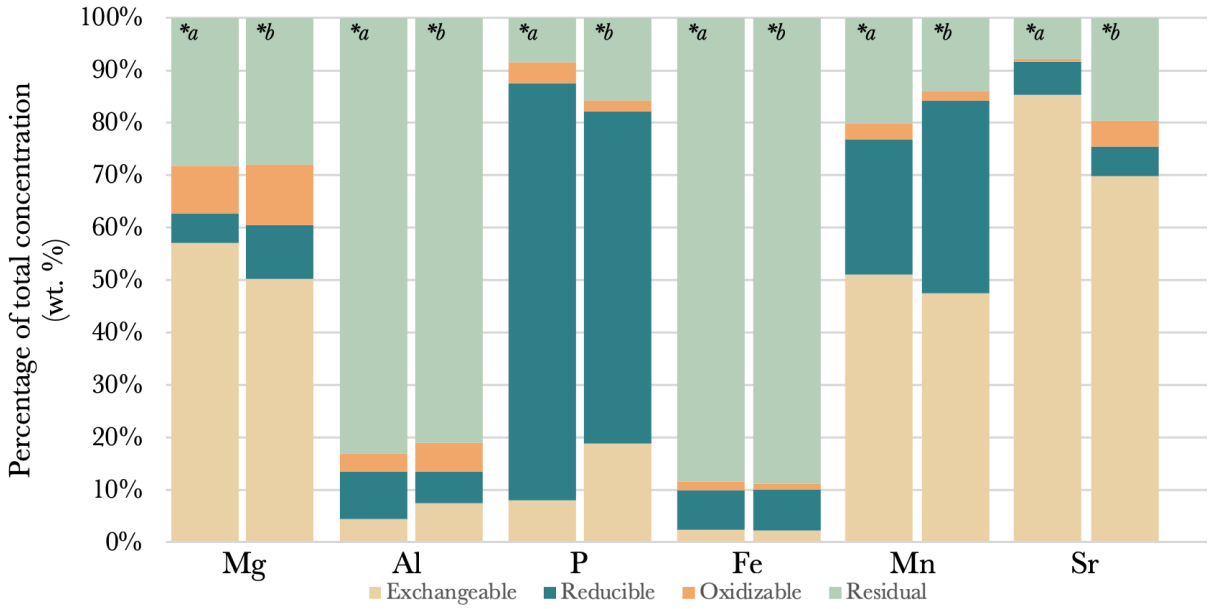

Figure 5.8: The distribution of average major element concentrations across all sediment fractions as a percentage (%) of the total element concentration at the Wadi 100 site (**a*) and the Barqa el-Hetiye site (**b*).

5.2 Trace Element Concentrations

The ranges in the total concentrations of Cu, Cr, Ni, Zn, Cd, and Pb at both the Wadi 100 and Barqa el-Hetiye sites are compared in Figure 5.9. The concentrations of each element in the exchangeable, reducible, oxidizable, and residual fractions are detailed below.

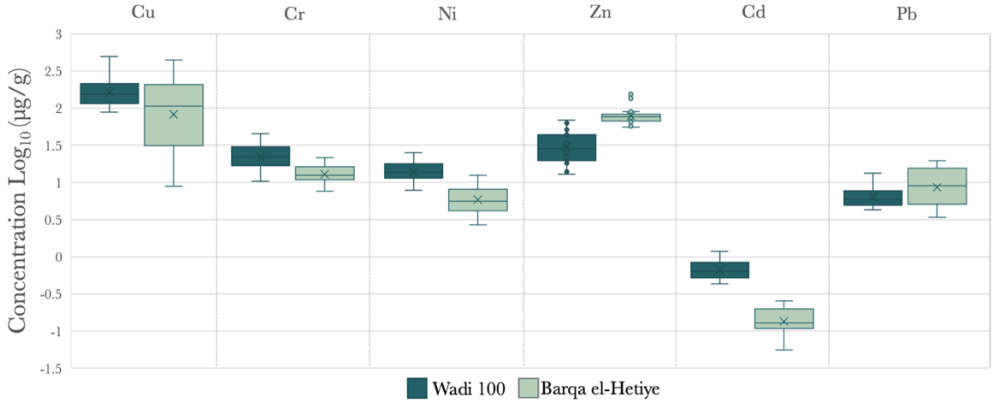

Figure 5.9: A box and whisker plot showing the range in the total concentrations of trace elements. Boxes extend to show the interquartile range of each element, horizontal lines mark the median, 'X' represents the mean. The whiskers extend to show the maximum and minimum values and the dots in line with the whiskers identify outliers.

5.2.1 Copper

The total Cu concentrations at the Wadi 100 site range from 76 to 417 μg/g, with a mean of 151 ± 76 μg/g (*n* = 24). Cu concentrations in the exchangeable fraction range from 2.3 to 87 μg/g and have a mean value of 18 ± 18 μg/g (*n* = 24). Reducible Cu ranges in concentration from 4.7 to 186 μg/g, with a mean value of 45 ± 35 μg/g (*n* = 23). Cu concentrations are slightly lower in the oxidizable fraction and range from 3.2 to 160 μg/g with a mean of 26 ± 31 μg/g (*n* = 24). Cu in the residual fraction has a minimum concentration of 13 μg/g and a maximum of 220 μg/g. The mean concentration of residual Cu at Wadi 100 is 64 ± 47 μg/g (*n* = 24). In the sediment samples at the Wadi 100 site, 12% of Cu was extracted with the exchangeable fraction, 28% was recovered from the reducible fraction, 17% was in the oxidizable fraction, and 43% remained in the residual fraction (Figure 5.10).

In the sediments collected from the Barqa el-Hetiye site, 27% of the Cu was available in the exchangeable fraction, 28% was in the reducible fraction, 12% was removed with the oxidizable fraction, and only 33% remained in the residual fraction. The total concentrations of Cu in the Barqa el-Hetiye samples range from 7.8 to 370 μg/g and have a mean of 125 ± 105 μg/g (*n* = 24). The Cu extracted with the exchangeable fraction had concentrations ranging from 0.37 to 148 μg/g with mean of 34 ± 33 μg/g (*n* = 24). Cu concentrations associated with the reducible fraction ranged from 0.87 to 113 μg/g, with a mean of 36 ± 33 μg/g (*n* = 24). Oxidizable Cu concentrations range from 0.52 to 47 μg/g and have a mean of 14 ± 13 μg/g (*n* = 24). Residual Cu concentrations range from 5.8 μg/g to 115 μg/g, with a mean of 41 ± 33 μg/g (*n* = 24).

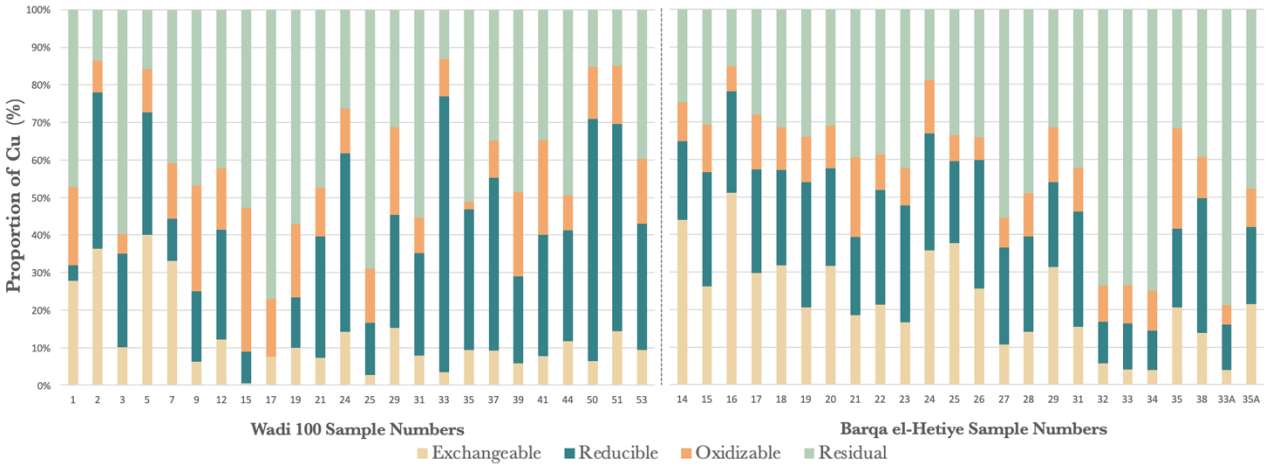

Figure 5.10: The distribution of Cu concentrations across all sediment fractions as a percentage (%) of the total concentration of Cu at Wadi 100 (left) and Barqa el-Hetiye (right).

5.2.2 Chromium

The total Cr concentrations in the sediments from the Wadi 100 site range from 5.9 to 42 μg/g and have a mean of 22 ± 8.0 μg/g (*n* = 24). Cr concentrations in the exchangeable fraction range from 1.4 to 2.8 μg/g and have a mean of 2.0 ± 0.32 μg/g (*n* = 24). Reducible Cr concentrations are lower, ranging from 1.2 to 2.1 μg/g, producing a mean value of 1.6 ± 0.22 μg/g (*n* = 24). Cr concentrations in the oxidizable fraction at Wadi 100 range from 2.0 to 4.2 μg/g and have a mean of 3.1 ± 0.64 μg/g (*n* = 24). Residual Cr has an average concentration of 16 ± 7.5 μg/g, with values ranging from 5.7 to 35 μg/g (*n* = 23). Cr in the residual fraction accounts for 70% of all Cr in Wadi 100 sediments, while only 9% is available in the exchangeable fraction, 7% is sequestered in the reducible fraction, and 14% is in the oxidizable fraction (Figure 5.11).

In Barqa el-Hetiye samples, 10% of the total Cr was extracted from the exchangeable fraction, 10% was recovered from the reducible fraction, 9% was bound in the oxidizable fraction, and 71% was removed from the residual fraction. The total concentrations of Cr range from 2.8 to 20 μg/g and have a mean of 12 ± 4.0 μg/g (*n* = 24). Exchangeable Cr concentrations range from 0.89 to 2.2 μg/g and produce a mean of 1.3 ± 0.29 μg/g (*n* = 24). Reducible Cr concentrations are higher, ranging from 0.90 to 3.1 μg/g and have a mean value of 1.2 ± 0.45 μg/g (*n* = 24). Cr concentrations in the oxidizable fraction at Wadi 100 range from 0.62 to 1.7 μg/g and have a mean of 1.1 ± 0.29 μg/g (*n* = 24). Residual Cr has an average concentration of 9.2 ± 3.3 μg/g, with values ranging from 4.6 to 16 μg/g (*n* = 23).

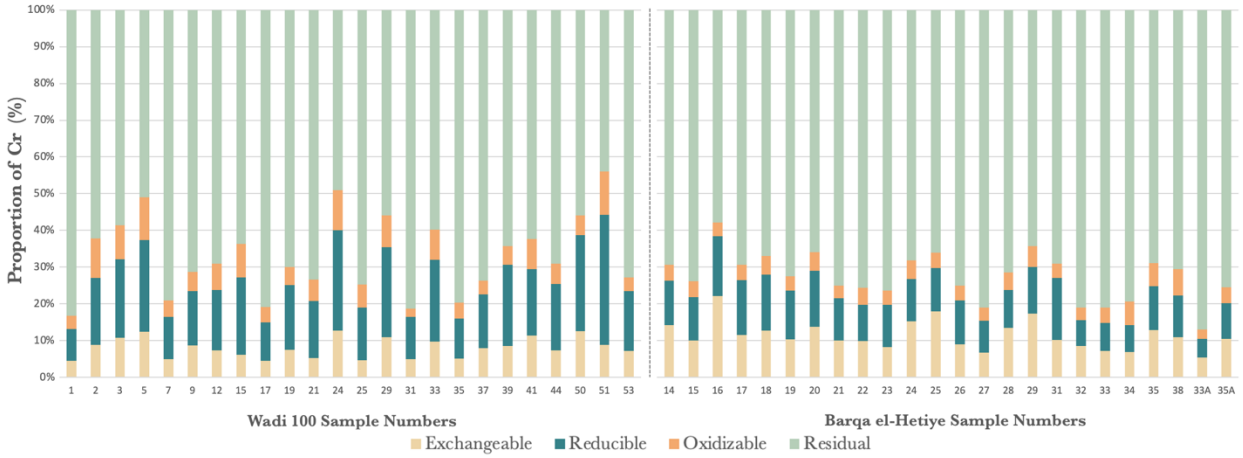

Figure 5.11: The distribution of Cr concentrations across all sediment fractions as a percentage (%) of the total concentration of Cr at Wadi 100 (left) and Barqa el-Hetiye (right).

5.2.3 Nickel

The total Ni concentrations in the samples from Wadi 100 range from 7.5 to 23 μg/g and have a mean value of 13 ± 3.8 μg/g (*n* = 24). Sequential extraction data show that 17% of all Ni is available in the exchangeable fraction, 13% is in the reducible fraction, 12% is in the oxidizable fraction, and 58% is locked in the residual fraction (Figure 5.12). The concentrations of exchangeable Ni range from 1.8 μg/g to 4.8 μg/g and have a mean of 2.3 ± 0.60 μg/g (*n* = 24). Reducible Ni concentrations range from 1.1 to 2.2 μg/g and produce a mean value of 1.7 ± 0.21 μg/g (*n* = 24). The Ni concentrations are lowest in the oxidizable fraction, ranging from 0.97 to 2.1 μg/g, with a mean concentration of 1.6 ± 0.31 μg/g (*n* = 24). Ni in the residual fraction has an average concentration of 7.8 ± 3.9 μg/g with values ranging from 2.1 to 18 μg/g (*n* = 24).

In Barqa el-Hetiye sediments, total Ni concentrations range from 2.6 to 12 μg/g and produce a mean concentration of 5.9 ± 2.4 μg/g (*n* = 24). Ni in the exchangeable fraction accounts for 7% of the total Ni in Barqa el-Hetiye sediments, the reducible fraction contains 16%, the oxidizable fraction has 9%, and 68% of the Ni is in the residual fraction at Barqa el-Hetiye. Only four samples had measurable concentration of Exchangeable Ni ranging from 1.4 to 3.1 μg/g and have a mean value of 2.3 ± 0.62 μg/g (*n* = 4). Ni concentrations in the reducible fraction range from 0.64 to 1.5 μg/g and have a mean value of 0.98 ± 0.25 μg/g (*n* = 24). Oxidizable Ni concentrations range from 0.34 to 0.87 μg/g, with a mean of 0.58 ± 0.18 μg/g (*n* = 21). Ni in the residual fraction has an average concentration of 4.0 ± 1.7 μg/g with values ranging from 1.60 to 7.3 μg/g (*n* = 24).

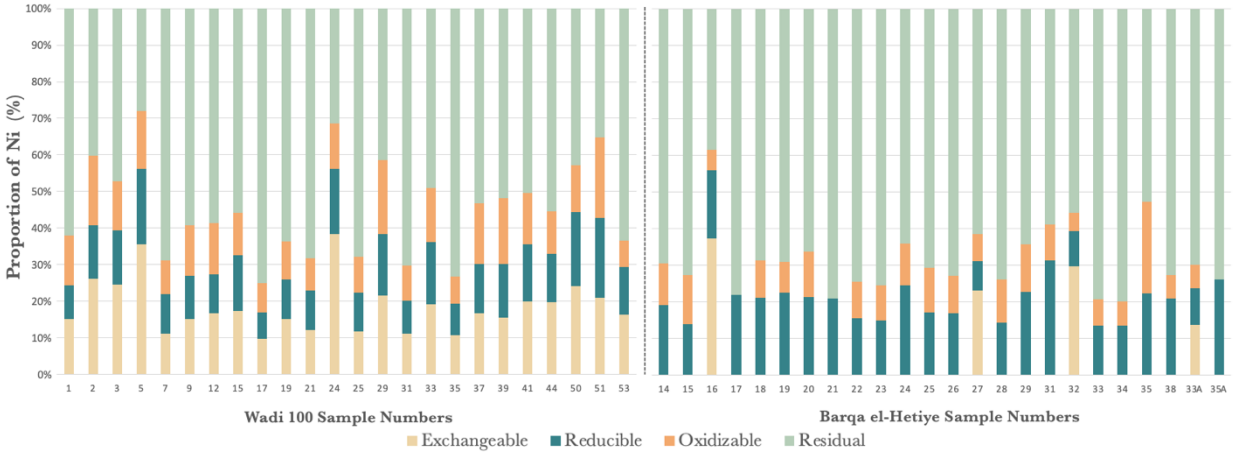

Figure 5.12: The distribution of Ni concentrations across all sediment fractions as a percentage (%) of the total concentration of Ni at Wadi 100 (left) and Barqa el-Hetiye (right).

5.2.4 Zinc

The total Zn concentrations in Wadi 100 sediments range from 11 to 59 μg/g and have a mean of 28 ± 13 μg/g (n = 24). The exchangeable fraction contains 13% of the total Zn in Wadi 100 sediments while the reducible fraction has 25%, the oxidizable fraction has 3%, and 65% is present as residual Zn (Figure 5.13). Exchangeable Zn concentrations range from 2.3 μg/g to 6.6 μg/g and have a mean value of 4.1 ± 1.2 μg/g (n = 21). Reducible Zn concentrations range from 2.9 to 16 μg/g, with a mean of 5.4 ± 3.2 μg/g (n = 24). Zn concentrations are lowest in the oxidizable fraction, ranging from 0.5 to 2.2 μg/g, producing a mean value of 1.2 ± 0.4 μg/g (n = 18). Residual Zn has the largest range in Zn concentrations from 7.0 μg/g to 47 μg/g and a mean of 21 ± 12 μg/g (n = 21).

Concentrations for total Zn in the Barqa el-Hetiye samples range from 48 to 131 μg/g, with a mean of 69 ± 19 μg/g (n = 24). Exchangeable Zn accounts for 13% of all Zn at the site, reducible Zn accounts for 5%, the oxidizable fraction holds 40%, and the residual fraction contains 42% of all Zn at Barqa el-Hetiye. The exchangeable fraction has a mean Zn concentration of 8.9 ± 14 μg/g (n = 24) and concentrations ranging from 2.2 μg/g to 56 μg/g. The reducible fraction at Wadi 100 has concentrations ranging from 1.1 to 11 μg/g and a mean value of 3.2 ± 2.4 μg/g (n = 24). Zn concentrations in the oxidizable fraction range from 15 to 40 μg/g with a mean of 27 ± 8.1 μg/g (n = 24). The residual fraction has Zn concentrations between 22 μg/g and 40 μg/g and a mean of 29 ± 4.1 μg/g (n = 24).

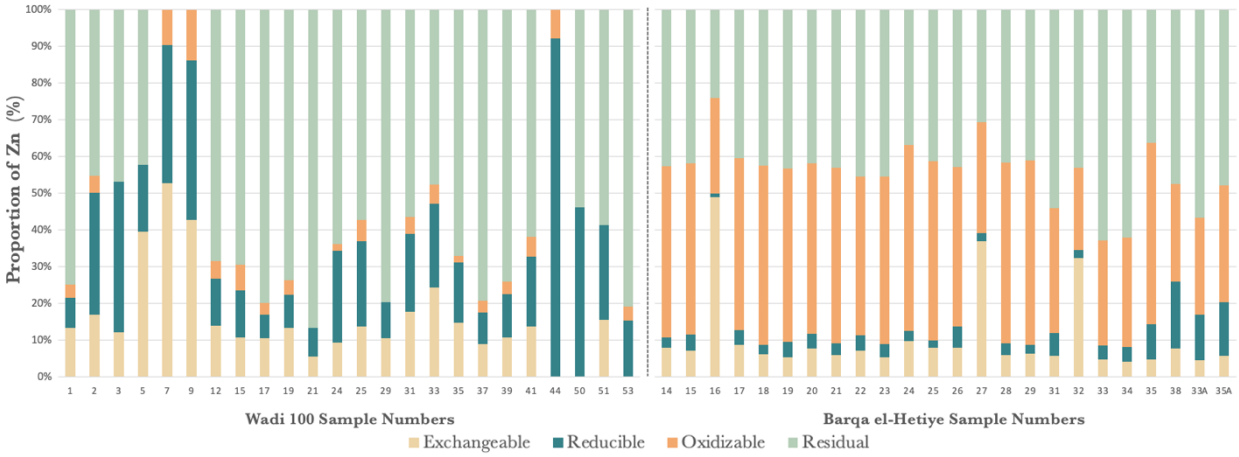

Figure 5.13: The distribution of Zn concentrations across all sediment fractions as a percentage (%) of the total concentration of Zn at Wadi 100 (left) and Barqa el-Hetiye (right).

5.2.5 Cadmium

Cadmium concentrations at the Wadi 100 site are only detectable in the exchangeable and reducible fractions, for this reason, the total concentration of Cd in the sediments sampled from the Wadi 100 site is evaluated as the sum of the exchangeable and reducible fractions. The total concentrations of Cd at the Wadi 100 site ranges from 0.05 to 0.73 μg/g and has a mean concentration of 0.43 ± 0.14 μg/g (n = 22). The mean concentration of Cd in the exchangeable fraction is 0.42 ± 0.11 μg/g (n = 21), with concentrations between 0.23 μg/g and 0.73 μg/g. The reducible fraction at the Wadi 100 site has Cd concentrations ranging from a minimum of 0.05 to a maximum of 0.12 μg/g and has a mean concentration of 0.10 ± 0.02 μg/g (n = 7). Cd in the exchangeable fraction makes up 92% of the total Cd while the residual fraction contains 8% of the total Cd at the Wadi 100 site (Figure 5.14).

The concentrations of Cd in the reducible, oxidizable, and residual fractions at the Barqa el-Hetiye site are all below the limit of detection of the instrument. Therefore, only the exchangeable fraction had measurable concentrations of Cd that were considered in the evaluation of total concentration of Cd in the sediments collected from the Barqa el-Hetiye site; 100% of the Cd extracted from Barqa el-Hetiye samples was extracted as exchangeable Cd. The total concentrations of Cd in the sediment samples collected from the Barqa el-Hetiye site range from a minimum of 0.05 to a maximum of 0.19 μg/g and these values produce a mean concentration of 0.11 ± 0.04 μg/g (n = 21).

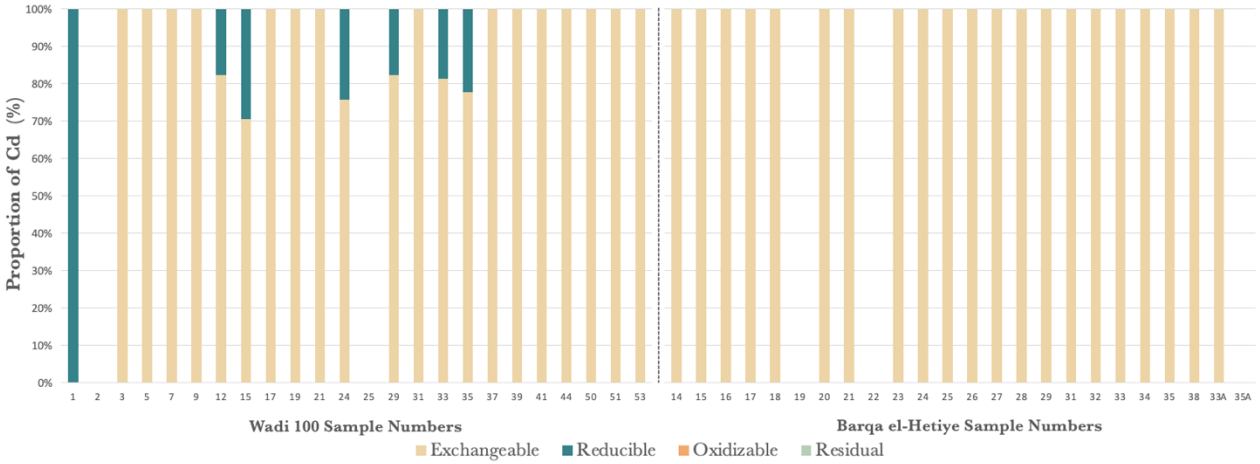

Figure 5.14: The distribution of Cd concentrations across all sediment fractions as a percentage (%) of the total concentration of Cd at Wadi 100 (left) and Barqa el-Hetiye (right). Samples without data indicate that the Cd concentration is <LOD in all sediment fraction.

5.2.6 Lead

The total Pb concentrations in the Wadi 100 samples range from 4.1 to 12 μg/g and have a mean of 6.5 ± 2.3 μg/g (n = 24). Only five samples yielded low, yet measurable concentrations of exchangeable Pb that range from 0.10 to 0.21 μg/g with a mean of 0.15 ± 0.03 μg/g (n = 24). Reducible Pb concentrations range from 0.96 to 2.3 μg/g and produce a mean of 1.5 ± 0.34 μg/g (n = 24). Pb concentrations are slightly lower in the oxidizable fraction and range from 0.47 to 2.2 μg/g with a mean of 1.1 ± 0.42 μg/g (n = 24). The residual fraction has a minimum Pb concentration of 3.8 μg/g and a maximum of 10 μg/g, with a mean value of 3.8 ± 2.2 μg/g (n = 24). The five samples with measurable Pb concentrations in the exchangeable fraction account for 2% of the total Pb at the Wadi 100 site, while reducible Pb accounts for 23%, oxidizable contains 17%, and 58% of Pb remains in the residual fraction (Figure 5.15).

Total Pb concentrations at the Barqa el-Hetiye site range from 3.2 to 18 μg/g, with a mean of 9.5 ± 4.9 μg/g (n = 24). The Pb in the exchangeable fraction has an average concentration of 0.52 ± 0.37 μg/g (n = 22) and concentrations ranging from 0.10 μg/g to 1.5 μg/g. Concentrations of reducible Pb range from 0.54 to 12 μg/g and have a mean of 4.1 ± 3.5 μg/g (n = 24). Pb concentrations in the oxidizable fraction range from 0.25 to 2.0 μg/g with a mean of 0.87 ± 0.51 μg/g (n = 24). Concentrations of residual Pb range from a minimum of 2.1 μg/g to a maximum of 6.01 μg/g and have a mean 4.0 ± 1.1 μg/g (n = 24). In Barqa el-Hetiye samples, 5% of Pb is available in the exchangeable fraction, 43% is in the reducible fraction, 9% is in the oxidizable fraction, and 43% is locked in the residual fraction.

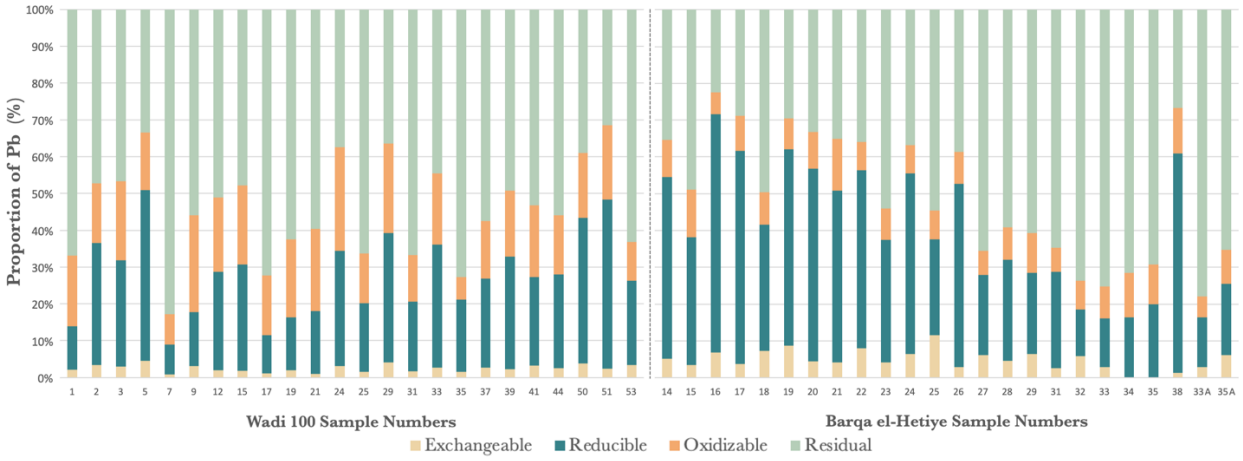

Figure 5.15: The distribution of Pb concentrations across all sediment fractions as a percentage (%) of the total concentration of Pb at Wadi 100 (left) and Barqa el-Hetiye (right).

5.2.7 Trace Element Summary

The exchangeable fraction contains the highest proportion of Cd at both sites and the lowest amount of Cu, Ni, and Pb in Wadi 100 sediments (Figure 5.16). The reducible fraction contains the highest amount of Pb and lowest amount of Cr in Barqa el-Hetiye sediments and the lowest amount of Zn in Wadi 100 sediments. The oxidizable fraction does not contain the highest proportion of any element, but accounts for the lowest proportions of Cu, Cr, and Ni in Barqa el-Hetiye sediments and Zn in Wadi 100 sediments. More than 50% of the total concentrations of Cr and Ni is in the residual fraction at both sites and Zn in the samples from Wadi 100. The residual fraction contains the largest proportion of Pb in sediments from the Wadi 100 site. Cd is the only element that does not have a measurable concentration in the residual fraction at both sites.

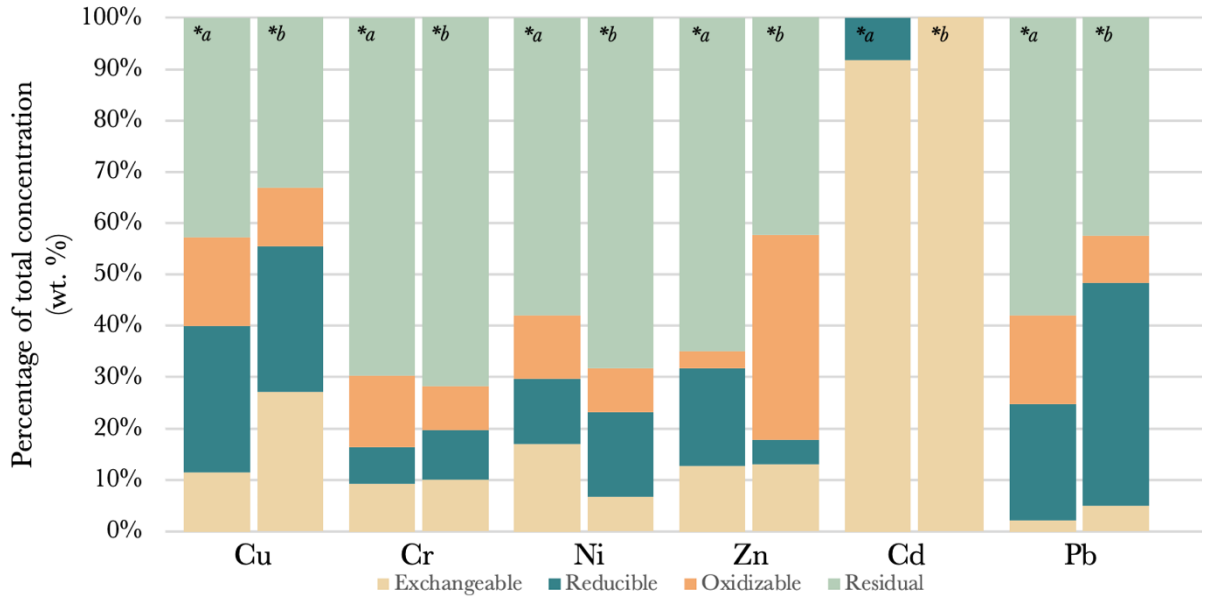

Figure 5.16: The average distribution of trace element concentrations across all sediment fractions as a percentage (%) of the total element concentration at the Wadi 100 site (**a*) and the Barqa el-Hetiye site (**b*).

5.3 Fractional Distribution Summary

5.3.1 Exchangeable Fraction Summary

In Wadi 100 sediments, 22% of all elements and 33% of heavy metals (Cr, Mn, Ni, Cu, Zn, Pb, Cd) were extracted in the exchangeable fraction. In Barqa el-Hetiye samples, 19% of all elements and 37% of metals (Cr, Mn, Ni, Cu, Zn, Pb, Cd) were extracted from the exchangeable fraction. The exchangeable fraction contains the highest proportion of Mg, Mn, Sr, and Cd at both sites, making these elements the most labile and easily accessible to biological organisms. The

concentrations of heavy metals in the exchangeable fraction at the Wadi 100 site (Mn >> Cu > Zn > Ni > Cr > Cd > Pb) varies from the Barqa el-Hetiye site (Mn >> Cu > Zn > Cr > Pb > Ni > Cd) with respect to Pb and Cd.

5.3.2 Reducible Fraction Summary

In Wadi 100 sediments, 11% of all elements and 25% of heavy metals (Cr, Mn, Ni, Cu, Zn, Pb, Cd) were recovered from the reducible fraction. In Barqa el-Hetiye samples, 8% of all elements and 36% of heavy metals (Cr, Mn, Ni, Cu, Zn, Pb, Cd) were extracted from the reducible fraction. The reducible fraction contains the second largest proportion of Zn in Wadi 100 sediments, Ni in Barqa el-Hetiye sediments, and Cu, Mn, and Pb in sediments from both sites. The order of the metal concentrations in the reducible fraction at the Wadi 100 site (Mn > Cu > Zn > Ni > Cr > Pb > Cd) varies from the Barqa el-Hetiye site (Mn > Cu > Pb > Zn > Cr > Ni) with respect to Pb.

5.3.3 Oxidizable Fraction Summary

In the sediments collected from the Wadi 100 and Barqa el-Hetiye sites, the oxidizable fractions contain 5% of all elements and less than 9% of the heavy metals (Cr, Mn, Ni, Cu, Zn, Pb, Cd) extracted from the sediment samples. The concentrations of oxidizable heavy metals in the sediment samples from Wadi 100 (Cu > Mn > Cr > Ni > Pb > Zn) varies from Barqa el-Hetiye (Zn > Cu > Mn > Cr > Pb > Ni) with respect to Zn and Ni.

5.3.4 Residual Fraction Summary

Over 60% of all elements extracted from Wadi 100 and Barqa el-Hetiye sediments were extracted from the residual fraction; 63% of all elements and 31% of heavy metals (Cr, Mn, Ni, Cu, Zn, Pb, Cd) in Wadi 100 sediments; 66% of all elements and 17% of heavy metals (Cr, Mn, Ni, Cu, Zn, Pb, Cd) in Barqa el-Hetiye samples. The concentrations of residual heavy metals in the Wadi 100 sediments (Cu > Mn > Zn > Cr > Ni > Pb) varies from the Barqa el-Hetiye samples (Mn > Cu > Zn > Cr > Ni ≈ Pb) with respect to Zn.

5.4 Statistical Analysis

5.4.1 Recovery Rates

The IAG reference standards used in the sequential analysis of the sediments in this study did not have reference concentrations for Mg, Al, P, Mn, Fe, and Ni. The recovery rates of Cr, Ni, Cu, Zn, Sr, Cd, and Pb were calculated using Equation 9 based on the reported concentrations of the SdAR-L2 IAG reference standard. The recovery rates for each element are as follow: Cr (105%), Ni (79%), Cu (82%), Zn (90%), Sr (94%), Cd (95%), and Pb (93%).

5.4.2 t-test Results

Unpaired t-tests were performed on total element concentrations and fractional element concentrations for Wadi 100 and Barqa el-Hetiye samples to identify which elements, if any, are statistically distinct between the two sites. Unpaired t-tests assuming unequal variance were performed on the fractional and total concentrations of elements with standard deviations that lie within a wide range of values between sites (i.e., Cu). Unpaired t-tests assuming equal variance were performed on elements with standard deviations that lie within a narrow range of values between sites (i.e., Ni). The significance value for these tests was set at .05; a p value < .05 rejects the null hypothesis and implies that there is a statistically significant difference in the concentration of the element in Wadi 100 samples and the concentration of the same element in Barqa el-Hetiye samples; a p value > .05 fails to reject the null hypothesis and indicates that there is no statistically significant difference in the concentrations of the element between sites.

The results of the t-tests (Table 5.4) indicate that there is no statistically significant difference in the total concentrations of Al (p = .750), Mn (p = .248), Fe (p = .066), and Cu (p = .337) at the Wadi 100 and Barqa el-Hetiye sites, thus, these values fail to reject the null hypothesis. The resulting p values for Mg (p < .001), P (p < .001), Sr (p < .001), Cr (p < .001), Ni (p < .001), Zn (p < .001), Cd (p < .001), and Pb (p = .010) are all below the significance value and therefore reject the null hypothesis, suggesting that these element concentrations are statistically different between sites.

The p values from the exchangeable fraction t-tests indicate that there is no statistically significant difference in the concentrations of P (p = .264), Mn (p = .394), Cu (p = .337), Zn (p = .072). The t-tests for the reducible fraction concentrations produced p values for Mg (p = .119), Mn (p = .120), Sr (p = .068), and Cu (p = .466) that fail to reject the null hypothesis. The p values

Table 5.4: A summary of *p* values for element concentrations in Wadi 100 and Barqa el-Hetiye samples. The results of unpaired t-tests assuming unequal variance for the element concentrations in each sediment fraction and the total element concentrations.

Major Elements						
Fraction	Mg	Al	P	Mn	Fe	Sr
Exchangeable	< .001	< .001	.264	.394	.035[a]	< .001
Reducible	.119	< .001	< .001	.120	< .001	.068[a]
Oxidizable	.051	< .001	< .001	.031[a]	.002[a]	< .001
Residual	.010	.925	.011	.551[a]	.110	.005[a]
Total	< .001	.750	< .001[a]	.248	.066	< .001[a]

Trace Elements						
Fraction	Cu	Cr	Ni	Zn	Cd	Pb
Exchangeable	.053[a]	< .001	< .001	.072	< .001	< .001
Reducible	.466[a]	.001[a]	< .001	.010[a]	.007	< .001
Oxidizable	.093[a]	< .001	< .001	< .001	–	.069[a]
Residual	.056[a]	< .001	< .001	< .001	–	.597[a]
Total	.337[a]	< .001[a]	< .001	< .001[a]	< .001[a]	.010[a]

[a] values are derived from an unpaired t-test assuming equal variance.
– indicates the element concentrations are < LOD at both sites; no data to compare.

for the concentrations of Mg ($p = .051$), Cu ($p = .093$), and Pb ($p = .069$) in the oxidizable fraction fail to reject the null hypothesis. The p values from the residual fraction t-tests indicate that the concentrations of Al ($p = .925$), Mn ($p = .551$), Fe ($p = .110$), Cu ($p = .056$), and Pb ($p = .597$) fail to reject the null hypothesis and have no statistically significant difference.

Elements with p values below the significance value in the exchangeable fraction include Mg ($p < .001$), Al ($p < .001$), Fe ($p = .035$), Sr ($p < .001$), Cr ($p < .001$), Ni ($p < .001$), Cd ($p < .001$), and Pb ($p < .001$).Elements with p values below the significance value in the residual fraction include Al ($p < .001$), P ($p < .001$), Fe ($p < .001$), Cr ($p < .001$), Ni ($p < .001$), Zn ($p = .010$), Cd ($p = .007$), and Pb ($p < .001$). Elements with p values below the significance value in the oxidizable fraction include Al ($p < .001$), P ($p < .001$), Mn ($p = .031$), Fe ($p < .001$), Sr ($p < .001$), Cr ($p < .001$), Ni ($p < .001$), Zn ($p < .001$), and Cd ($p < .001$). Elements with p values below the significance value in the residual fraction include Mg ($p < .010$), P ($p < .010$), Sr ($p = .005$), Cr ($p < .001$), Ni ($p < .001$), Zn ($p < .001$), and Cd ($p < .001$). These values are all below the significance value (0.05) and therefore reject the null hypothesis; suggesting that these concentrations are statistically different between the Wadi 100 and Barqa el-Hetiye sites.

6.0 Discussion

The Wadi 100 and Barqa el-Hetiye sites are both spatially and temporally related, situated in the same region and occupied by the same groups of people for thousands of years (Hauptmann 2007, Grattan 2007). Despite these similarities, different environmental and anthropogenic factors such as water availability and land use practices have shaped Wadi 100 and Barqa el-Hetiye into two distinct sites both in appearance and in composition. These differences are especially apparent when the fractional element distributions and total concentrations of major (Mg, P, Mn, Sr) and trace elements (Cu, Cd, Pb, Zn) are compared. The variability within and between these sites is compared below to identify the potential environmental or anthropogenic origins and the environmental risks associated with the element concentrations in Tables 5.2 and 5.3 above.

6.1 Total Element Concentrations

The Wadi 100 and Barqa el-Hetiye sites are situated 8 km apart in the sand-dominated desert environment of Faynan (Figure 3.5) and the sediments at these sites comprise a palimpsest of the regional lithologies (Rabb'a 1994, Hauptmann 2007). Given that both sites have sediments from similar lithologies the geochemical data collected from the Wadi 100 samples should be comparable to those of the Barqa el-Hetiye samples. Through the careful analysis of these seemingly similar sediments, stark variations in syn- and post-depositional land use are discernable on both the local and regional scale.

A comparison of the total element concentrations in the samples from the Wadi 100 and Barqa el-Hetiye sites reveals that many of the elements analyzed have comparable total concentrations (Figure 5.8 and Figure 5.16) (Table 5.2 and Table 5.3). The results of unpaired t-tests (Table 5.4) identified four elements (Al, Fe, Mn, Cu) for which the null hypothesis is retained and the differences in the concentrations of Al and Fe are not discussed further.

In the context of archaeological sites, high concentrations of Mg, P, Cr, Sr, Ni, Zn, and Cd in cultural sediments are often associated with known archaeological features (Table 4.1), while high concentrations of Mn, Cu, and Pb in the sediments of Faynan have been attributed to the historical mining and smelting of Cu and Mn ores since the Neolithic Period (c. 7000 years BP) (Pyatt et al. 2000, Grattan et al. 2016, Barker et al 2007, Hauptmann 2007). In other mining communities, the enrichment of metallurgical by-products and metals (e.g., Mn, Cu, Zn, Cd, Pb) have been documented in the sediments surrounding metallurgical sites in Japan (Xian 1987), the

U.S.A. (Kuo et al. 1983), Spain (Vega et al. 2006, Navarro et al. 2008), Mexico (Gómez-Álvarez et al. 2011), China (Li et al. 2014, Kang et al. 2017), Malaysia (Madzin et al. 2015), and in the Northern Wadi 'Araba Valley in Jordan (Ben-Yosef et al. 2016). Therefore, the sediment samples from Wadi 100 and Barqa el-Hetiye are expected to contain the local residua of ancient mining and smelting, i.e., Mn, Cu, and Pb, and high levels of Zn and Cd are also possible.

Assessing the anthropogenic contribution of an element in soil requires consideration of the sediment fractions that host them. Extraction schemes commonly cited in literature for metal speciation in sediments include the three-step sequential extraction scheme by the SM&T (Ure et al. 1993), the five-step sequential extraction scheme by Tessier et al. (1979), and modified combinations or variation of both (e.g., Xian 1987, Yarlagadda et el. 1995, Hseu et al. 2002, Sutherland and Tack 2003, Jain 2004, Jones et al. 2008, Zhang et al. 2014). Many authors have compared these methods to show how variations in reagent pH or type can target different fractions and how the optimal extraction scheme for one metal may not be effective for others (e.g., Mester et al. 1998, Davidson et al. 1998, Rauret et al. 1999, Ahnstrom and Parker 1999, Albores et al. 2000, Zhang et al. 2014). It is generally accepted that the total concentration of a metal is not an accurate indicator of environmental toxicity. The bioavailability and the relative eco-toxicity of metals in the environment is strongly dependent on the chemical forms of each element in the sediment (Ma and Rao 1997, Quevauviller et al. 1997, Vaněk et al. 2005). To assess the potential risk of a metal to the biogeochemical environment, the standard analysis of total metal content has been replaced with a sequential analysis, wherein trace metals in the labile and semi-labile sediment fractions were measured separately from those locked in the residual fraction.

6.2 Fractional Element Distribution

The concentration of each element was analyzed across four operationally defined fractions (exchangeable, reducible, oxidizable, and residual) to target specific pools of elements in the sediment (Table 4.2) (Figure 6.1). These four fractions have different sediment properties that affect the solubility, mobility, and potential environmental impact of each element (Quevauviller et al. 1997, Adriano 2001, Jones et al. 2008, Alloway 2013). Elements in the exchangeable fraction have the weakest bonds and are generally the most labile, posing the most immediate risk to the biogeochemical environment while elements in the residual fraction are considered non-labile and therefore pose the lowest risk to the biogeochemical environment (Adriano 2001, Jain 2004, Oliver

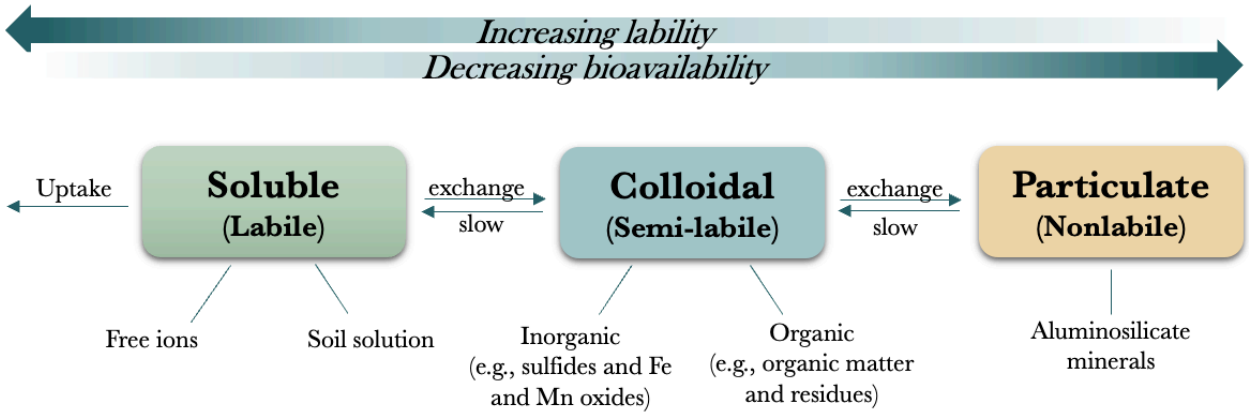

Figure 6.1: The general trend of element lability based on the operational form of the element in sediment. In the sequential extraction used in this thesis, the labile metal forms comprise the exchangeable fraction, the semi-labile metals comprise the reducible and oxidizable fractions, and the non-labile metals comprise the residual fraction. Transference of metals between labile and semi-labile phases can occur as a result of changes in soil pH. Transference of metals from the non-labile to semi-labile phases can only occur under extreme conditions that are rarely experienced in nature. Modified from Adriano (2001).

et al. 2005, Saeedi et al. 2012, Alloway 2013, Zhang et al. 2014). The results from each fraction and the importance of the results in understanding the distribution of metals in the sediment samples collected from both the Wadi 100 and Barqa el-Hetiye sites are described below progressing from most labile to least labile.

6.2.1 Exchangeable Fraction

Metals in the exchangeable fraction include soluble metals in the soil solution, weakly adsorbed metals, and metals bonded to carbonate phases that can be released by ion-exchange processes and changes in pH (Alloway 2013, Saeedi et al. 2012). In other studies, the soluble metals in the soil solution, the exchangeable metals held by loose electrostatic attractions, and metals bonded to carbonates have been extracted separately (e.g., Kuo et al. 1983, Gómez-Álvarez et al. 2011). The sum of the metals in the soil solution and exchangeable form rarely exceeds 10% of the total metal content in typical soils and is even lower in alkaline soils formed under an aridic moisture regime (Adriano 2001). Many of the reagents used to extract acid-exchangeable metals also liberate some metals bonded to carbonates (Tessier et al. 1979). Therefore, the metals in the soil solution, acid-exchangeable metals, and carbonate-bound metals in the sediment samples in this study were extracted together and comprise the exchangeable fraction.

6.2.2 Reducible Fraction

Metals bonded to or adsorbed on colloidal Fe/Mn-oxides (e.g., Mn oxides and amorphous Fe oxides) are easily reduced under anoxic conditions (Tessier et al. 1979, Jones et al. 2008).

Elements extracted in this sediment fraction comprise the reducible fraction. The transference of trace elements from the exchangeable fraction to the reducible fraction can occur naturally within a matter of days but may be accelerated when the trace element load increases (Han and Banin 1999, Zhang et al. 2014). For this reason, a high positive loading of metals in the reducible fraction is a common characteristic of contaminated sediments (Alloway 2013, Zhang et al. 2014).The transference of metals (e.g., Mn, Fe, Cr, Ni) from the exchangeable fraction to the reducible fraction has been associated with anthropogenically contaminated sediments in China (Zhang et al. 2014) and Spain (Gómez-Álvarez et al. 2011), noting that the large surface area and high cation exchange capability of Fe/Mn-oxides make them strong scavengers of trace metals in soils (Zhang et al. 2014).

6.2.3 Oxidizable Fraction

Metals bonded to organic matter (OM) and sulphides were extracted together and comprise the oxidizable fraction. Under oxidizing conditions, the decomposition of OM can release semi-labile metals into the soil solution (Tessier et al. 1979, Adriano 2001, Jones et al. 2008). Metals bonded to various forms of OM include living organisms, decaying or deceased remains, and organic coatings on mineral particles (Tessier et al. 1979, Zhang et al. 2014). H_2O_2 was used to oxidize OM and release organic gases and soluble trace metals prior to the extraction of metals associated with sulphides.

Though most of the ores exploited in Faynan comprise Cu/Mn oxide and Cu silicate minerals, sulphide minerals are present in the mineralized vein fillings of the Umm ʻIshrīn Sandstone (Figure 3.3), albeit at much lower concentrations (Hauptmann 2007), and in the igneous basement rocks that outcrop in the Wadi ʻAraba (Bender 1974, Rabb'a 1994). These sulphides can oxidize when exposed to the atmosphere or meteoric waters to form water soluble sulphates and carbonates which can become mobilized in water (Hauptmann 2007). The transference of metals from the oxidizable fraction to the soil solution in arid sediments is often attributed to an increase in sediment moisture regime (e.g., seasonal flooding, irrigation) (Gómez-Álvarez et al. 2011).

6.2.4 Residual Fraction

Metals in the residual fraction are fixed within the crystal lattices of primary and secondary mineral particles; primarily silicates, e.g., aluminosilicates (Tessier et al. 1979, Jones et al. 2008). Metals extracted from the residual fraction are the least labile are not bioavailable under normal

environmental conditions and can only be made available to plants and soil organisms through extensive weathering (Vaněk et al. 2005, Alloway 2013). Because these metals are fixed within the crystal structure of minerals, the residual fraction often reflects the background levels of metals in the regional geology (Alloway 2013). When a significant proportion (> 60%) of the total concentration of an element is locked in the residual fraction, the mobility of the element is considered low (Rauret et al. 1999).

6.3 Elements of Concern

6.3.1 High-risk Elements

Assessing the potential toxicity of a metal to the biogeochemical environment starts with determining the concentration of the metal in the exchangeable fraction. Elements with a majority (> 50%) of their total concentration in the exchangeable fraction are considered highly mobile and pose a high risk to biota, while elements with less than 10% of their total concentration in the exchangeable fraction are not considered to be highly mobile and therefore pose a low risk to the environment (Saeedi et al. 2012). Elements in the very high-risk category at both sites include Mg, Sr, and Cd and in the sediments collected from the Wadi 100 site Mn is also considered very high-risk (Table 5.1). The elements considered to be of low risk to the biogeochemical environment in the sediments from Wadi 100 include Al, P, Cr, Ni, Fe, and Pb and in the sediments from Barqa el-Hetiye include Al, Cr, Fe, Ni, Pb.

The concentrations of Al, Cr, Fe, and Ni in the exchangeable fractions and both sites are all below 10% and therefore pose a low risk to the biogeochemical environment. The total concentrations of Ni and Cr are well below the threshold concentrations given by the Canadian Soil Quality Guidelines (CSQG) of 50 and 64 μg/g for Ni and Cr, respectively, while Al and Fe are not acknowledged in the CSQG (Canadian Council of Ministers of the Environment 2007). For these reasons, the concentrations and fractional distribution of Al, Fe, Ni, and Cr and are not discussed further. While the Canadian Council of Ministers of the Environment (2007) do not have CSQG values for Mg, Sr, and P, the exchangeable concentrations of these elements are deemed very high risk and the associated environmental risks attributed to these elements are discussed below. The exchangeable concentrations of Mn and Cd are also deemed very high risk and the associated environmental risks of Mn and Cd are discussed in the following section (Section 6.3.2) with other heavy metals (Cu, Pb, Zn) associated with archaeometallurgy.

Magnesium

The calcareous sediments in Faynan are derived in part from the Numayrī Dolostone, Wadi As Sīr Limestone, and Na'ūr Limestone that outcrop in the Wadi 'Araba Escarpment (Bender 1963, Hauptmann et al. 1992, Rabb'a 1994). It is probable that the high concentration of Mg in the Wadi 100 and Barqa el-Hetiye sediments is in part the result of the natural weathering of these alkaline sedimentary rocks. The Numayrī Dolostone unit is *c*. 60 wt. % dolomite and is the primary source of the Cu-bearing ore that was processed in the region for thousands of years. A significant amount of the Mg extracted from the exchangeable fraction would originate from the dissolution of carbonates like dolomite, which can contain >13 wt. % Mg. Therefore, though it is possible that the processing of these ores introduced Mg to the environment, during the later stages of ore extraction (i.e., in the Roman Period) only small amounts of the dolostone host rock were removed and transported to ore processing sites (Hauptmann 2007), such that the processing of these ores would not have contributed high amounts of Mg to the sediments at these sites.

The fractional distribution of Mg in the sediments sampled from the Wadi 100 (i) and Barqa el-Hetiye (ii) sites generally follow the following order:

(i) exchangeable >> residual >> oxidizable > reducible
(ii) exchangeable > residual > oxidizable > reducible

The results of unpaired t-tests indicate that there are statistically significant differences between the concentration of exchangeable Mg in the Wadi 100 and Barqa el-Hetiye samples (Table 5.4). Very high levels of Mg, especially in the exchangeable fraction like those seen in the Wadi 100 samples (Table 5.2) can have deleterious effects on soil structure (Daliakopoulos et al. 2016, Qadir et al. 2018). At the time of sample collection (2019), Bedouin farmers were growing tomatoes in the sediments sampled at the Wadi 100 site. Irrigated crops take up water but are unable to take up high levels of Mg, especially when present as a salt ($MgCl_2$ or $MgSO_4$) (Qadir et al. 2018). The build-up of Mg salts can degrade soil structure and reduce soil permeability which inhibits plant growth if left untreated (Qadir et al. 2018).

The Bedouin farmers in the Faynan Valley use local groundwater to irrigate small fields of crops, namely tomatoes and melons (Hauptmann 2007). The concentration of Mg in Faynan groundwater ranges from 35 mg/L near the Wadi Ghuwayr and increases to 61 mg/L near the Fidān Spring (Wade et al. 2011) (Figure 4.1). Though these values are both below the recommended maximum concentration of Mg for irrigation waters (< 100 mg/L) given by the

European Health-Based standard (Ayers and Westcot 1985), long-term use can still cause the build-up of Mg salts and can be detrimental to soil structure (Ayers and Westcot 1985, Crook 2009).

Though the crops at the Wadi 100 site are grown in sediments (i.e., immature soils with no clearly defined soil structures), the continued cycle of irrigation, fertilization, and crop rotation can increase the quantity and quality of soil constituents such as OM, moisture, and air in these sediments. Over time, sediments with high Mg concentrations or irrigated using water with high Mg content are often reported to have low productivity (Ayers and Westcot 1985, Daliakopoulos et al. 2016, Oster et al. 2016). In addition to the high concentration of Mg in irrigation waters, soil amendments (e.g., poultry manures, nitrate fertilizers) contain appreciable amounts of Mg (Amiri and Fallahi 2009; Vandecasteele et al. 2014). Modern Bedouin farmers in Faynan are known to use soil amendments (J.P. Grattan, personal communication, 2022) that contribute to the high Mg concentrations in the Wadi 100 sediments.

Given the differences in the total concentrations of Mg at the Wadi 100 and Barqa el-Hetiye sites, the higher concentration of Mg in the Wadi 100 sediments may reflect differences in historical land use (i.e., higher quantities of ore-handling) or differences in modern land use (i.e., the use of groundwater for irrigation and the application of soil amendments). There is other evidence of a recent increase in the Mg levels in both irrigation waters and sediment from many irrigated areas in similar arid environments in countries in the Near and Middle East (Qadir et al. 2018). Soil studies from these other sites suggest that the primary concern in soils and sediments with high Mg concentrations is the gradual degradation of soil structure (Qadir et al. 2018), and that a high Mg to Ca ratio in irrigation waters is a diagnostic indicator for the adverse effects of Mg on soil structure (Oster et al. 2016).

In other studies, Mg was used to amend the up-take and distribution of heavy metals in corn (e.g., Fan et al. 2018) and immobilize metals in contaminated sediments (e.g., Yuan et al. 2018). Therefore, though the high concentration of exchangeable Mg is considered very high risk in the samples collected from the Wadi 100 and Barqa el-Hetiye sites, the imposed 'very high risk' categorization does not merit inherent concern because the uptake of Mg by plants can be restricted in soils with high Mg content (Qadir et al. 2018) and because high levels of Mg in plants may have the ability to immobilize heavy metals, or preferentially store them in the roots of the plants as opposed to the fruits (Yuan et al. 2018) for which the plants in the Faynan Valley are primarily cultivated.

Strontium

Strontium is a nonessential element and Sr compounds are generally of low toxicity (Adriano 2001). Sr can enter the biological environment through plants by substituting for Ca due in organic matter thereby depriving organisms of the essential nutrient Ca (Pathak and Gupta 2020). Soil Sr levels are considered normal when concentrations are less than 500 μg/g, while plants grown in soils with Sr levels above 600 μg/g may contain elevated Sr concentrations and lowered Ca concentrations (Chatterjee et al. 2020). Sr is primarily stored in the leaf tissues, the fruits, and the seeds of a plant and can replace Ca in the bodies of the organisms that consume these plants which can leads to Ca deficiency and a variety of associated medical issues (Pathak and Gupta 2020). Sr levels in the sediment samples from the Wadi 100 and Barqa el-Hetiye sites are within the normal range of Sr concentrations, suggesting that the biological risk of Sr in the environment is not significant.

The fractional distribution of Sr in the sediments sampled from the Wadi 100 (i) and Barqa el-Hetiye (ii) site generally follow the following order:

(i) exchangeable >> residual > reducible ≈ oxidizable
(ii) exchangeable > residual > reducible > oxidizable

The results of unpaired t-tests suggest that the Sr concentrations in the exchangeable, oxidizable, and residual fractions vary between the Wadi 100 and Barqa el-Hetiye sites. The sediments sampled from the Wadi 100 site have higher exchangeable and lower oxidizable and reducible Sr concentrations than the sediments sampled from the Barqa el-Hetiye site (Table 5.2).

In Faynan, Grattan et al. (2007) used Sr concentrations to identify the source of heavy metals across different stratigraphic layers; decreases in Cu and Pb concentrations accompanied by increases in Sr concentrations were interpreted as an indication of the movement of allochthonous carbonate sediment. This analysis helped distinguish uncontaminated stratigraphy from anthropogenically contaminated layers. In the samples analyzed in this thesis, there is no clear relationship between the concentration Sr and the concentrations of Cu or Pb in any fraction. This lack of a relationship suggests that the metals in the sediments at Wadi 100 and Barqa el-Hetiye reflect both the background levels and the reworking of metallurgical products by wind, runoff, and tilling, as described by Grattan et al. (2007). Alternatively, they could simply reflect the sampling strategy implemented in this study, wherein no specific stratigraphic layer was targeted, resulting in element concentrations from various stratigraphic layers.

Phosphorus

Phosphorous is a reactive nonmetal, the 11th most abundant element on the Earth's surface, and an integral component in agricultural soils with average global P concentrations ranging from 500 μg/g to 8000 μg/g (Mengel et al. 2001, Fink et al. 2016). Phosphorus, in the form of phosphate (PO_4^{3-}), is essential for plant growth and only available for root uptake when present in the soil solution; in many soils, the available P accounts for less than 10% of the total P (Fink et al. 2016).

The availability of phosphate to plants is typically determined by measuring the concentration of PO_4^{3-} in the soil solution (Mengel et al. 2001). The method of extraction implemented in this thesis was designed for the extraction of trace metals and is not considered an effective method for the analysis of essential nutrients such as P, N, Ca, or K in soil. Additionally, the available P in the soil solution of the sediment analyzed from the Wadi 100 and Barqa el-Hetiye sites was extracted with metals bonded to carbonates and exchangeable metals in the exchangeable fraction (Table 4.2), and therefore cannot be used to accurately determine the amount of P available for root uptake.

Though the phosphorous data from this study cannot be used to determine the amount of total P that is available to plants in the Wadi 100 and Barqa el-Hetiye sediments, the data can still provide information regarding the distribution of P at both sites. The fractional distribution of P in the sediments sampled from the Wadi 100 (i) and Barqa el-Hetiye (ii) site generally follow the following order:

(i) reducible >> residual > exchangeable > oxidizable
(ii) reducible > exchangeable > residual > oxidizable

Phosphorus is the only element analyzed in this thesis wherein the dominant form (i.e., >50 wt.%) of P was extracted from the reducible fraction (Table 5.1). When comparing the concentrations of P at these two sites, the total concentration of P is significantly higher in sediments from the Wadi 100 site than it is sediments from the Barqa el-Hetiye site (Table 5.1). A similar trend is seen in the reducible, oxidizable, and residual fractions wherein the concentration of P in these fractions in Wadi 100 samples are all higher than those measured in the Barqa el-Hetiye samples. Though the mean concentrations in the exchangeable fraction are comparable between sites (Table 5.4), the range in *p* values across each of the four fractions at the Wadi 100 site is much larger than the ranges in the Barqa el-Hetiye samples.

The history of anthropogenic activity at the Wadi 100 and Barqa el-Hetiye sites makes the interpretation of the P results more challenging, as elevated levels of P in sediment are an important geochemical indicator of human activity (Table 4.1) (Holliday and Gartner 2007, Oonk et al. 2009, Vranová et al. 2015, Bintliff and Degryse 2022, Weihrauch et al. 2022). Human activity can spike natural soil P levels (Bintliff and Degryse 2022) which can persist in the soil for millennia due to the high retention capacity for P in the soil matrix (Oonk et al. 2009, Weihrauch et al. 2022). In the field system surrounding the Wadi 100 site, the discovery of pottery shards containing manure and food waste suggest that the field systems were fertilized during the Roman Age occupation (Barker et al. 2007), a practice that is known to raise soil P above natural levels (Oonk et al. 2009).

More recently, the use of poultry manure-based nitrate fertilizers by the modern Bedouin farmers when growing tomato plants in the Wadi 100 fields has been observed (J.P. Grattan, personal communication, 2022). Poultry manure-based fertilizers commonly contain high levels of organic P in the form of phytate ($C_6H_{18}O_{24}P_6$), labile inorganic P in the form of struvite ($NH_4MgPO_4\ H_2O$) and anhydrous dicalcium phosphate (DCPA) ($CaHPO_4$), and as less labile inorganic P in the form of tricalcium phosphate (TCP) ($Ca_3(PO_4)_2$) and hydroxyapatite ($Ca_5(PO_4)_3(OH)$) (Vandecasteele et al. 2014, Komiyama and Toyoaki 2019). Many of the organic phosphates in poultry and litter-based fertilizers have a high affinity for polyvalent cations like Al(III) and Fe(III) and often form insoluble metal compounds that can become mobilized under reducing conditions (He et al. 2006, Vandecasteele et al. 2014). In a study analyzing the effects of soils amended with various manure-based fertilizers, soils amended with poultry manures had between 72 and 86% more P than the control soils (Vandecasteele et al. 2014). In the sediments sampled in this thesis, the total concentration of P removed from the Wadi 100 samples is 72% higher than the total concentration of P removed from the Barqa el-Hetiye samples. Thus, it is probable that a significant portion of the P recovered from the reducible fraction in Wadi 100 samples likely originates from the application of soil amendments.

In addition to the known anthropogenic sources of P in Faynan, there are economically viable phosphate deposits that have been continuously exploited in the sedimentary bedrock at the top of the escarpment for decades and the upper parts of the Numayrī Dolostone have significantly high enrichments of phosphorites with >22% P_2O_5 (Hauptmann 2007). Because the differences in total P concentration is significantly higher in Wadi 100 sediments and because this trend is not seen in any other element analyzed, the redistribution of P from local sources (i.e., katabatic winds

transporting P from the phosphate deposits at the top of the escarpment down into the wadis Faynan and 'Araba) is unlikely to be the source of excess P in Wadi 100 sediments. Additionally, during the removal of Cu ores from the Numayrī Dolostone, only very small amounts of the host rock containing phosphorites were removed (Hauptmann 2007), thus, it is also unlikely that the processing of these ores introduced a significant amount of P to the sediments at Wadi 100.

Though the natural occurrences of P have likely contributed to the local background P levels, the confirmed use of P-rich fertilizers is the most probable cause of the high P concentration in Wadi 100 sediment. The long-term use of poultry manure-based fertilizers on agricultural fields can lead to the accumulation of soil P which can transfer to water bodies through runoff or during periods of flooding and can cause eutrophication in surface waters if left untreated (Turner and Leytem 2004). In the Faynan Valley, where rainwater is minimal and flooding is infrequent, the extent and potential risk of the accumulation of P in surficial water bodies is not known.

6.3.2 Elements Associated with Metallurgy

Elevated concentrations of elements associated with metallurgical sites in the Faynan Valley and in the other mining communities mentioned earlier include Cu, Mn, Pb, Zn, and Cd. Of these metals, Cu, Pb, Zn, and Cd are considered potential environmental contaminants by the Canadian Council of Ministers of the Environment (2007). The threshold concentrations for Cd, Cu, Zn, and Pb as per CSQG are compared to the total concentrations of Cd, Cu, Zn, and Pb measured in the sediment samples collected from the Wadi 100 and Barqa el-Hetiye sites in Table 6.1 below.

Table 6.1: The minimum, maximum, and mean concentrations of Cd, Cu, Pb, and Zn in sediments from the Wadi 100 and Barqa el-Hetiye sites compared to CSQG values. The CSQG for the protection of environmental and human health (Canadian Council of Ministers of the Environment 2007) values are given as guidelines for government use and are not legal limits.

Metal	Wadi 100 (µg/g)			Barqa el-Hetiye (µg/g)			Canadian Soil Quality Guidelines[a] (µg/g)			
	Min	Mean	Max	Min	Mean	Max	Agricultural	Residential/ Parkland	Commercial	Industrial
Cd	0.05	0.43	0.73	0.05	0.11	0.19	1.4	10	22	22
Cu	76	151	417	7.8	125	370	63	63	91	91
Pb	4.1	6.5	12	3.2	9.5	18	70	140	260	600
Zn	11	28	59	48	69	131	200	200	360	360

[a] concentrations obtained from Canadian Council of Ministers of the Environment (2007).

Manganese

The average Mn content in the lithosphere is *c.* 1000 μg/g (Adriano 2001) and the Mn values in the bedrock in Faynan are comparatively higher: the Finān Granite in the Jabal Hamrat Fidān has *c.* 5000 μg/g Mn (Rabb'a 1994), the volcanic rocks in the Wadi Ghuwayr have up to 2000 μg/g Mn (Rabb'a 1994), and Numayrī Dolostone ores in the Wadi Dana can exceed 26 wt. % Mn (El-Hasan et al. 2001). This high Mn content is not reflected in the sediments in Faynan; the mean concentration of Mn in the sediments sampled from the Wadi 100 and Barqa el-Hetiye sites are low (Table 5.2) when compared to the Mn concentrations in comparable surficial sediments in arid environments with Mn concentrations ranging from 500 to 1000 μg/g (Adriano 2001).

The fractional distribution of Mn in the sediments sampled from the Wadi 100 (i) and Barqa el-Hetiye (ii) site generally followed the following order:

(i) exchangeable >> reducible > residual >> oxidizable
(ii) exchangeable > reducible >> residual >> oxidizable

The ranges in oxidizable and residual Mn concentration for the samples from the Wadi 100 and Barqa el-Hetiye sites are similar, while the exchangeable and reducible Mn concentrations vary considerably (Figure 5.5). Overall, the reported total concentrations of Mn are more variable in the sediment samples from the Barqa el-Hetiye site than in the samples from the Wadi 100 site (SD, Table 5.2). It is possible that this variation reflects the sampling strategy implemented at the Barqa el-Hetiye site where wind erosion exposed both EBA and Iron Age stratigraphy at ground level.

The samples from the Barqa el-Hetiye site were collected in a section that had no modern vegetation while the Wadi 100 samples were collected from agricultural plots. Under most conditions, Mn content will be highest in the surficial sediment and reach a minimum in the rhizosphere due to the uptake of Mn by roots (Adriano 2001). Though a larger proportion of the total Mn is available for plant uptake in the exchangeable fraction of Wadi 100 sediments (Table 5.1), the sum of exchangeable Mn extracted from Barqa el-Hetiye samples is 19% higher than the sum of exchangeable Mn extracted from Wadi 100 samples. One possible explanation for this difference of 19% in the sum of exchangeable Mn between sites is the uptake of Mn by the roots of the tomato plants cultivated at the Wadi 100 site.

At the time of sample collection in June of 2019, local Bedouin farmers were using the Wadi 100 site to grow tomato plants. In a study analyzing the mineral requirements of tomato plants, Sainju et al. (2003) found that Mn toxicity can appear when acid-exchangeable Mn is > 80 μg/g. While the mean concentration of exchangeable Mn in the samples from the Wadi 100 and Barqa el-Hetiye sites exceeds 80 μg/g (Table 5.2), a portion of the Mn in the exchangeable fraction could also originate from the dissolution of carbonate minerals (e.g., rhodochrosite ($MnCo_2$) or kutnahorite ($CaMn(CO_3)_2$ (Böttcher (2011)), though the occurrence of Mn carbonate minerals is rare, and no such minerals have been identified in Faynan. Therefore, the results for the exchangeable Mn concentrations in this study cannot be used to accurately determine the true risk of Mn toxicity to the tomato plants grown in Wadi 100 soils.

High soil pH can limit the uptake of Mn by plants by inhibiting the transfer of reducible Mn to exchangeable Mn (Katyal and Sharma 1991, Adriano 2001, Sainju et al. 2003). In the alkaline sediments at the Wadi 100 site, the concentration of reducible Mn is considerably lower and accounts for a much smaller percentage of the total Mn compared to the reducible Mn in Barqa el-Hetiye samples. High levels of P, like those measured in the Wadi 100 samples, can also reduce the toxicity of Mn in tomato plants which can occur naturally or by applying a water-soluble P fertilizer (El-Jaoual and Cox 1998, Sainju et al. 2003).

A considerable proportion of the total Mn in both the Wadi 100 and Barqa el-Hetiye sites is available in the exchangeable fraction in amounts classified as very high risk. Though the source of the exchangeable Mn in the Wadi 100 and Barqa el-Hetiye samples is not known, it is possible that a portion of the Mn extracted from the reducible fraction originates from Mn-oxide ores. In other soils with elevated Mn concentrations that were sampled near a copper smelter, the largest proportion of Mn was extracted from labile fractions (Kuo et al. 1983). This suggests that part of the Mn extracted from the exchangeable and reducible fractions could originate from nearby pyrometallurgical activity. Because the sampling strategy at the Barqa el-Hetiye site did not target a continuous stratigraphic layer, the large range in Mn concentrations could therefore reflect the Mn concentrations from more than one stratigraphic layer, wherein some samples were collected from a layer contaminated by smelting processes that occurred on the nearby ridge, and others were sampled from a layer of sediments that were deposited during a time with minimal or no smelting near the site.

Cadmium

The total concentrations of Cd in Wadi 100 and Barqa el-Hetiye sediments are within the normal range of values for Aridisols (0.07 to 0.70 ug/g) (Adriano 2001) and well below the CSQG threshold values (Table 6.1). Sediments derived from sedimentary rocks generally have higher concentrations of Cd (0.30 to 11 μg/g) than sediments derived from igneous (<0.10 to 0.30 μg/g) or metamorphic rocks (0.10 to 1.0 μg/g) (Adriano 2001). Under natural weathering conditions, Cd is commonly associated with primary minerals and when Cd concentrations reflect background levels the residual fraction often contains the largest proportion of total Cd (Alloway 2013).

Excess Cd in agricultural soils is often associated with phosphate fertilization, though the use of these fertilizers is now restricted in many countries due to the toxic effects of Cd and other additives (Yan et al. 2015, Capri 2021). In most cases, Cd added to soils remains labile in the exchangeable fraction and is largely unaffected by changes in moisture content (Han and Banin 1999) but may transfer to the reducible fraction if Cd loading continues (Alloway 2013). Anthropogenic Cd is generally immobile in most soils and will remain on the depositional surface with minimal downward movement, except in the case of agricultural soils where stratigraphy is disturbed by tilling (Adriano 2001).

The fractional distribution of Cd in the sediments sampled from the Wadi 100 (i) and Barqa el-Hetiye (ii) site generally followed the following order:

(i) exchangeable >> reducible >> (oxidizable and residual < LOD)
(ii) exchangeable >> (reducible, oxidizable, and residual < LOD)

The proportions of exchangeable Cd in the Wadi 100 and Barqa el-Hetiye sediments are comparable to the results of a similar study assessing the fractionation of heavy metals in agricultural soils in Ecuador, where Cd in the exchangeable fraction (85%) was the highest of all heavy metals in the study (Ochoa et al. 2020). Though a smaller proportion of the total Cd is available in the exchangeable fraction in Wadi 100 samples than in the Barqa el-Hetiye samples, the average concentration of exchangeable Cd is 3.8 times higher in Wadi 100 samples than it is in Barqa el-Hetiye samples (Table 5.3). This difference in the exchangeable Cd concentrations between sites is likely the result of a higher initial loading of Cd at the Wadi 100 site which induced the transference of exchangeable Cd to reducible Cd, explaining the presence of measurable concentrations of Cd in the reducible fraction in Wadi 100 samples and not in Barqa el-Hetiye samples.

Several studies discussed by Adriano (2001) concluded that Cd from metallurgical activities, such as the mining and smelting operations in Faynan, is more bioavailable than Cd from uncontaminated soils, even at similar concentrations. This is because when Cd is present at background concentrations it is usually present in the residual fraction, as is typical of metals associated with primary minerals (Alloway 2013). None of the sediment samples analyzed in this study had measurable concentrations of Cd in the residual fraction (Table 5.2).

High concentrations of Cd can inhibit the uptake of essential micronutrients in plants which can be detrimental to most plant species, while Cd concentrations of 5 μg/g can be lethal in most cases (Andersen and Küpper 2013). According to De Vries et al. (2007b), the critical concentration of Cd in sandy soils with low levels of OM and a high pH (pH >7), is 2.8 μg/g Cd, which is notably higher than anything measured in sediment sampled in this study. Cd is one of the most toxic metals that is present in the agricultural soils at the Wadi 100 site and because 100% of the Cd is associated with labile fractions the Cd is more easily accessible to the biological environment than metals associated with less labile fractions (Yusuf 2007, Ochoa et al. 2020). While the fractional distribution of Cd at the Wadi 100 site may be indicative of anthropogenic contamination, the true source of Cd in Faynan soils cannot be definitively identified due to limitations in this study.

Copper

Global Cu concentrations in soils typically range from 2 to 250 μg/g and have an average concentration of 30 μg/g (Adriano 2001, Alloway 2013). Arable soils typically have lower concentrations of Cu that range from 10 to 20 μg/g, while less fertile soils like Aridisols generally have higher Cu concentrations between 21 and 27 μg/g (Chen et al., 1991; Adriano 2001, Alloway 2013). Though well within the typical range of global Cu concentrations, the mean Cu concentrations measured in Wadi 100 and Barqa el-Hetiye samples (Table 5.2) are comparatively higher than the mean Cu values in Aridisols and the recommended limits set by the CSQG (Table 6.1). However, these average Cu concentrations are a measure of the total Cu content in soils and do not accurately identify the amount of phytoavailable Cu in these soils. The fractional distribution of Cu in the sediments sample from Wadi 100 (i) and Barqa el-Hetiye (ii) generally follow the following order:

(i) residual > reducible >> oxidizable > exchangeable
(ii) residual > reducible ≈ exchangeable > oxidizable

The distribution and mobility of Cu in sediments is strongly influenced by the presence and quantity of OM and Mn/Fe oxides (McBride 1981, Oliver et al. 2005, de Vries et al. 2007a, Alloway 2013). Copper has a strong affinity for OM and in typical arable soils, most of the semi-labile Cu that can be made bioavailable is bonded to OM in the oxidizable fraction (Adriano 2001, Cerqueira et al. 2011, Alloway 2013). Conversely, OM levels decline with increasing lime content, and carbonate-rich sediments in an arid environment like Faynan are characteristically low in OM (Katyal and Sharma 1991, Weil and Brady 2016). Therefore, the organically bound oxidizable Cu is expectedly low in both the Wadi 100 and Barqa el-Hetiye samples.

In addition to OM, Cu bonded to sulphides was also extracted in the oxidizable fraction. Though sulphides are commonly associated with mineral deposits and occur in other copper deposits in the Near East (e.g., massive sulphide deposits in Cyprus), the primary ores in Faynan are oxidic and silicate ores and only traces of sulphides occur (Hauptmann 2007). Though no evidence of smelting was found on the surface of the Wadi 100 site, Fe-rich slags with Cu sulphides have been found in other sections of the Wadi Faynan Field System (Hauptmann 2007).

The largest proportion of Cu in both the Wadi 100 and Barqa el-Hetiye sites was extracted as residual Cu (Table 5.1), which is the most stable form of Cu in sediment; transference of residual Cu to more labile fractions can only occur through weathering. The amount of Cu extracted from the Wadi 100 sediments is higher than the amount of Cu extracted from Barqa el-Hetiye sediments, which suggests that more of the Cu at the Wadi 100 site is associated with primary mineral phases and is less likely to be associated with anthropogenic contamination.

Concentrations of Cu in the sediments around Faynan vary considerably. The average Cu concentration in the highly contaminated sediments at Khirbet Faynan (WF1, Figure 3.5), are over 11,900 μg/g, Cu concentrations from a control site 2.5 km south of Khirbet Faynan are *c.* 920 μg/g, and Cu concentrations in sediments that predate the mining in Faynan are *c.* 32 μg/g (Pyatt et al. 2000). Cu concentrations in modern braid-plain (TWF, Figure 3.5) deposits near the Wadi 100 site range from 1 to 147 μg/g, averaging 46 μg/g (n = 17); in the Tell Loam Member near the banks of the Wadi Faynan range from 18 to 1170 μg/g, averaging 138 μg/g (n = 49); in an anthropogenic-fluvial facies found along the northern bank of the Wadi Faynan, Cu values range from 49 to 1460 μg/g, averaging 264 μg/g (n = 14); and in the marl sediments sampled near the Barqa el-Hetiye site, Cu concentrations range from 13 to 426 μg/g, averaging 77.4 μg/g (n = 28) (Grattan et al. 2016).

The total Cu concentrations measured in Wadi 100 and Barqa el-Hetiye samples are higher than other comparable soils and the reported CSQG values, but within the expected range for local background levels. More than one third of the total Cu extracted from Wadi 100 and Barqa el-Hetiye samples was extracted from the residual fraction which is not available to plants and organisms. Therefore, the average concentration of Cu that is readily available or that can be easily solubilized or mobilized in solution (i.e., exchangeable Cu, reducible Cu, and oxidizable Cu) is below 90 μg/g in both Wadi 100 and Barqa el-Hetiye samples, which is high, but within the maximum threshold values for industrial and commercial soils given by the CSQG (Table 6.1).

While the measured total concentrations of Cu in the Wadi 100 and Barqa el-Hetiye samples are higher than other arable soils, Aridisols, and the CSQG values, the fractional distributions of Cu in the sediments from both sites is more typical of unpolluted sediment than of highly polluted sediments. In highly polluted sediments, the exchangeable and reducible fractions typically contain a significant portion (> 70%) of total the Cu (e.g., Kou et al. 1983, Xian et al. 1987, Asami et al. 1995, Ma and Rao 1997, Han and Banin 1999, Yusuf 2007, Cerqueira et al. 2011). Therefore, the Cu concentrations measured in the Wadi 100 and Barqa el-Hetiye samples likely reflect background Cu concentrations and possibly the redistribution of Cu from more contaminated sites through aeolian and fluvial processes.

Lead

Lead is present in all soils, even if only in trace amounts with concentrations below 1.0 μg/g (Adriano 2001). The average concentration of Pb in global soils is between 10 and 25 μg/g, though Pb concentrations in surficial sediments sampled near urban and industrial areas can easily exceed 50 μg/g (Adriano 2001). Pb is often associated with crystalline oxides and iron hydroxides that limit the mobility of Pb in soils (Ruby et al. 1999, Alloway 2013). In sediments with a pH range of 5-9, the solubility of Pb is about 100 times lower than that of Cd (Adriano 2001). Because the mobility of Pb is so low, the concentration of Pb in the exchangeable fraction is typically higher in polluted soils than it is in unpolluted soils (Asami et al. 1995). In soils affected by mining, Pb is often present as the lead sulphide mineral galena (PbS) and incorporated in the matrix of pyrometallurgical wastes (i.e., slag) (Ruby et al. 1999).

The local background levels of Pb in Faynan were determined based on samples collected from the Lower Faynan Member (*c.* 15,800 ± 1300 BP) at the Wadi Faynan site (TWF, Figure 3.5)

north of the Wadi 100 site and range from <1.0 to 30 μg/g, with a mean of 10.7 μg/g (Grattan et al. 2016). Samples collected from modern deposits in the Wadi Faynan range from <1.0 to 17 μg/g and have a mean concentration of 8 μg/g (Grattan et al. 2016). The average Pb concentration in the highly contaminated sediments at Khirbet Faynan exceed 15,000 μg/g; from a control site 2.5 km south of Khirbet Faynan are *c.* 1560 μg/g; and in sediments that predate the mining in Faynan are *c.* 18 μg/g (Pyatt et al. 2000). Based on these known local background levels, the total concentrations of Pb measured in the Wadi 100 and the Barqa el-Hetiye sediments in this thesis (Table 5.2) fall comfortably within the lower bounds of the expected background levels, and well within the recommended CSQG values (Table 6.1).

Smelting processes in the EBA in Faynan were markedly inefficient (Hauptmann 2007), and inefficient smelting processes can increase the amount of PbS and lead (II) carbonate ($PbCO_3$) in soils (Ruby et al. 1999). During the EBA, the Barqa el-Hetiye site was used for smelting and ore-processing (Fritz et al. 1994) while no evidence of smelting has been uncovered at the occupational Wadi 100 site (Wright et al. 1998). Based on the known EBA land-use practices, the Barqa el-Hetiye sediments are expected to have higher concentrations of Pb than the Wadi 100 sediments.

Pb speciation in the sediments sampled from the Wadi 100 (i) and Barqa el-Hetiye (ii) site generally followed the following order:

(i) residual >> reducible > oxidizable >> exchangeable

(ii) reducible ≈ residual >> oxidizable > reducible

The fractional distribution of Pb in the sediments at the Wadi 100 differs from that of the Barqa el-Hetiye site with respect to exchangeable and reducible Pb concentrations (Table 5.1, Table 5.4). The concentrations of exchangeable and reducible Pb extracted from Barqa el-Hetiye sediment samples are more than 3 times higher than the concentrations of exchangeable and reducible Pb in the Wadi 100 sediment samples (Table 5.3). The fractional distribution of Pb in the samples from the Wadi 100 site differs from that of typical polluted sediments wherein the exchangeable and reducible fractions typically contain the highest proportion of total Pb, and the residual fraction typically contains the lowest proportion of total Pb (Yarlagadda et al. 1995). In other soils contaminated by mining, reducible Pb accounted for 73 to 85%, while residual Pb accounted for less than 20% of total Pb (Li et al. 2020), and in soils contaminated by smelting, Pb was most abundant in the reducible fraction (44 to 54 %), while Pb in the residual fraction (2.1 to 8.9 %) was low (Li et al. 2020).

Based on the expected fractional distribution of Pb at known heavily contaminated sites, the fractional distribution of Pb in the sediments collected from the Wadi 100 site is not indicative of anthropogenic metal contamination. While the distribution of Pb in the exchangeable and reducible fractions in the Barqa el-Hetiye sediments is more suggestive of highly contaminated sediments, the high proportion of residual Pb in Barqa el-Hetiye samples is not typical of highly contaminated sediments. A possible explanation for the dichotomy in the concentrations and fractional distribution of Pb in Barqa el-Hetiye samples is that more than one stratigraphic layer was sampled at the Barqa el-Hetiye site; wherein at least one layer reflects natural background Pb concentrations, and another represents elevated levels associated to metallurgical activity.

Zinc

The amount of water-soluble Zn in the soil solution and Zn adsorbed on the exchange sites of soil colloids is generally negligible in desert soils and soils with low OM (Adriano 2001). In alkaline and calcareous sediments like those in Faynan, the concentration of Zn in the carbonate fraction is typically high, reflecting the local background levels of Zn (Adriano 2001). In the sediments sampled from the Wadi 100 and Barqa el-Hetiye sites, water-soluble Zn, acid-exchangeable Zn, and carbonate-bound Zn were extracted together and comprise 13% of the total Zn at each site. While the concentrations of exchangeable Zn extracted from the Wadi 100 and Barqa el-Hetiye samples are statistically similar (Table 5.4), there are significant statistical differences in the reducible, oxidizable, residual, and total concentrations of Zn.

Many authors have reported dominant proportions of Zn associated with Fe/Mn oxides in the reducible fraction (Adriano 2001, Vaněk et al. 2005, Yusuf 2007, Alloway et al. 2013) and the residual fraction (Kuo et al. 1983, Xian 1987, Asami et al. 1995, Ma and Rao 1997, Sutherland and Tack 2003). The main factors that differentiate the sediments reported to have high positive loadings of reducible Zn and the sediments reported with dominant residual Zn are pollution source and water. In sediments contaminated with Zn from mining wastes, excess Zn is associated with more labile fractions (Vaněk et al. 2005), while the presence of water mobilizes soluble Zn and induces the transference of Zn between fractions (e.g., Zn mobility increases during episodes of flooding (Alloway 2013)). In the presence of meteoric water, Zn bonded to OM or sulphides can be oxidized and transferred to the soil solution where Zn it most labile. In uncontaminated soils, or soils sampled farther from smelters, Zn concentrations are highest in the residual fraction, reflecting more stable, background concentrations (Adriano 2001).

Zn speciation in the sediments sampled from the Wadi 100 (i) and Barqa el-Hetiye (ii) site generally follow the following order:

(i) residual >> reducible > oxidizable > exchangeable
(ii) residual ≈ oxidizable >> exchangeable > reducible

The dominant form of Zn in Wadi 100 sediments was extracted from the residual fraction (Table 5.1). The highest concentration of Zn in Barqa el-Hetiye samples was extracted from the residual fraction (42 wt.%) and a comparable concentration of Zn was extracted from the oxidizable fraction (40 wt.%). The mean concentration of oxidizable Zn in Barqa el-Hetiye sediments is more than 22 times higher than the mean concentration of oxidizable Zn in Wadi 100 sediments. Based on these findings, differences in the soil moisture between these sites (i.e., Wadi 100 soils are irrigated and more affected by seasonal flooding than the aeolian sediments at Barqa el-Hetiye) is the most probable cause of the significant difference ($p < .001$) in oxidizable Zn.

The total concentration of Zn in Wadi 100 samples is 60% lower than the total concentration of Zn measured in Barqa el-Hetiye samples. Considering that water is the dominant mobilizing agent for Zn, the lower Zn concentrations in the Wadi 100 samples may simply reflect a higher degree of seasonal flooding or irrigation practices. In the alkaline sediments in Faynan, the transference of mobile Zn into less labile fractions likely occurred within a matter of years following the initial deposition of Zn, as is typical of sediments with anthropogenic Zn contamination (Alloway 2013).

The background levels of Zn in the sediments in Faynan are not known. Appreciable amounts of Zn have been measured in the Numayrī Dolostone that hosts the dominant Cu ores that were exploited through antiquity (Barker et al 2007). The Zn derived from the Numayrī Dolostone would likely have originated as carbonate Zn (i.e., exchangeable Zn), but the origin of the oxidizable Zn is unknown.

7.0 Conclusions

When metals are first added to or deposited on soils by anthropogenic sources, most metals will adsorb to mineral surfaces and form relatively loose bonds with exchangeable cations, carbonates, and Fe/Mn oxides. Post-depositional changes in soil chemistry can enable the transference of metals between sediment fractions. Though the weakly developed soil horizons at the Wadi 100 and Barqa el-Hetiye sites suggest that soil forming processes have had a minimal effect in the presumed millennia since their initial deposition, it is still reasonable to assume that seasonal flooding and variations in land use have both physically and chemically altered the distribution of metals in these sediments.

Although the extent of the transference of metals is not known, the following conclusions can be made regarding the reported fractional distributions and concentrations of the elements discussed in Section 6:

- **Magnesium**: the higher concentration of exchangeable Mg in the Wadi 100 sediment likely reflects differences in modern land-use practices (i.e., irrigation, fertilization). The uptake of Mg can be restricted by plants and may also have immobilizing effects on noxious metals. Therefore, the high Mg levels are not of notable concern to the environment.
- **Strontium**: the high concentrations of exchangeable Sr in the sediments in this study are well within the optimal range of Sr values in arable soils, and therefore are not of concern.
- **Phosphorus**: the high concentration of P in the reducible fraction in the samples collected from the Wadi 100 site is likely resultant from the use of modern soil amendments by the Bedouin farmers. The high concentrations of P are within the acceptable range of P in arable soils, though with continued application of poultry manures the accumulation of soil P is expected to increase. This accumulation of soil P increases the risk of P transfer through seasonal flooding to surface water, which can lead to eutrophication if left untreated.
- **Manganese**: the elevated concentrations of Mn in only some of the Barqa el-Hetiye samples likely reflects the sampling strategy wherein more than one stratigraphic layer was likely sampled, including at least one anthropogenically contaminated layer and one uncontaminated layer. The comparatively lower exchangeable and reducible Mn concentrations in Wadi 100 samples could be explained by the uptake of Mn by the tomato plants grown in Wadi 100 soils or simply reflect the site's position, more distal from major ore-refining zones.

- **Cadmium**: all total concentrations of Cd measured in Wadi 100 and Barqa el-Hetiye samples are below the threshold values given by the CSQG. The total concentration of Cd measured in Wadi 100 samples is about 4 times higher than that measured in Barqa el-Hetiye samples. More than 90% of all Cd was extracted from the exchangeable fraction in samples from both sites. The use of soil amendments in Wadi 100 sediments likely contribute to a high positive loading of Cd in the exchangeable fraction necessitating the transfer of exchangeable Cd to the reducible fraction. The continued application of soil amendments will continue to increase the Cd concentration at Wadi 100 which will increase the risk of noxious Cd effects on the biogeochemical environment.
- **Copper**: the mean total concentrations of Cu in the Wadi 100 and Barqa el-Hetiye samples exceed the maximum threshold values given by the CSQG for agricultural, residential/parkland, commercial, and industrial soils. While the total concentrations of Cu in both Wadi 100 and Barqa el-Hetiye sediments are higher than typical sediments, the fractional distributions of Cu in the sediments from the Wadi 100 site is more typical of unpolluted sediment and reflect slightly elevated local background Cu concentrations. The fractional distribution of Cu in Barqa el-Hetiye samples is slightly more typical of anthropogenically polluted sediments and likely reflect the redistribution of Cu from nearby smelting through aeolian processes.
- **Lead**: the total concentrations of Pb do not exceed the threshold values given by the CSQG. The fractional distribution of Pb in the Wadi 100 samples is more typical of unpolluted sediment than highly contaminated sediments. There is a dichotomy in the fractional distribution of Pb in the Barqa el-Hetiye sediments (i.e., notably higher exchangeable and reducible Pb concentrations (typical of contaminated sediments), and a residual Pb concentration comparable to Wadi 100 samples (typical of uncontaminated sediments)) which suggests that more than one stratigraphic layer was sampled at this site.
- **Zinc**: the total concentration of Zn in the samples collected from the Wadi 100 and Barqa el-Hetiye sites are well within the threshold values given by the CSQG. The dominant form of Zn was extracted from the residual fractions at both sites, a characteristic trend for metals derived from natural sources and not of anthropogenic origin. The large difference in oxidizable Zn values between sites is likely due to differences in water management practices and seasonal variations in flooding.

Both the Wadi 100 and Barqa el-Hetiye sites were settled during the EBA and occupied intermittently into the Roman/Byzantine Period. Throughout this nearly 4000-year period of occupation, these sites served different land use purposes; Barqa el-Hetiye was used for smelting, Wadi 100 was used for agriculture. Following the collapse of the Roman empire both sites were effectively abandoned until the 20th century when the Modern Bedouin arrived and began to farm in the region, eventually expanding into the Wadi Faynan Field System at the Wadi 100 site.

Elevated exchangeable concentrations of Mg, P, and Cd in the sediments from the Wadi 100 site are evidence of modern anthropogenic activity (i.e., agriculture, irrigation, and addition of soil amendments) that have been transferred to the sediments and are discernable through sequential extraction. Unlike the Wadi 100 site, the sediments from the Barqa el-Hetiye site have not been impacted by modern anthropogenic activity but have instead experience gradual erosion and deflation due to strong aeolian forces. While both sites have statistically comparable concentrations of Cu, Mn, and Pb, a comparison of the fractional distributions of the metals between these sites shows that the origin of these metals differ and that the fractional distribution of Cu, Mn, and Pb at the Barqa el-Hetiye site is more suggestive of anthropogenic contamination than the fractional distribution of Cu, Mn, and Pb in the Wadi 100 samples. Because of this lack of modern anthropogenic input at the Barqa el-Hetiye site, the concentrations of Cu, Mn, and Pb most likely reflect slightly elevated background concentrations and the redistribution of these ore-related metals resultant from nearby smelting operations.

When interpreting land use in a region with a rich archaeometallurgical history like Faynan, the absence of metals can be just as informative as an abundance of metals. Where an abundance of metals may indicate high levels of contamination and proximity to pyrometallurgical sites, the absence, or lack of high concentrations of ore-related metals (namely Cu, Mn, and Pb at levels indicative of highly contaminated sediments) in the sediment samples collected from the Wadi 100 site (2 km from smelting) and Barqa el-Hetiye (200 m from smelting) site suggests that the large-scale regional pollution that is often associated with Faynan may not be as widespread as was once believed.

7.1 Future Work

The mobility of metals associated with archaeometallurgical activity in Faynan is dependent on soil properties. Variations in land-use, both historical and modern, can alter soil properties and thus the mobility and bioavailability of these metals. To better understand the implications and behaviour of metals in Faynan soils, future geochemical studies should employ a more detailed survey of the physical and chemical parameters of the sediments sampled, including an assessment of soil pH, carbonate content ($CaCO_3$), and organic matter content. To better understand the potential environmental consequences of the Wadi 100 soils amended with poultry manure-based fertilizers, a more complete understanding of the distribution and role of organic and inorganic P is required. Future work focusing on the mobility of trace elements in Faynan sediments should consider sampling sediments in the dry season and after a flooding event to assess the role of seasonal flooding on the mobility and fractional distribution of metals.

Future sampling strategies should be more intentional about the stratigraphic unit targeted during sample collection. By digging a trench, stratigraphic units can be correlated to ensure that only one cultural layer is sampled. The implementation of a trench would also allow for a more accurate analysis of soil horizons, soil structure, and may offer the potential of possible relative age-dating of stratigraphy as the sediments in Faynan are often full of archaeological artifacts.

The implementation of a sequential digestion is strongly recommended for future geochemical analyses. Future analyses could benefit from a 6-step sequential digestion wherein the soil solution, easily exchangeable, and carbonate-bound metals are extracted separately. In the arid soils of Faynan, understanding which metals and the concentrations of metals that can be mobilized in water is integral to understanding the potential environmental risks associated with metals. A 6-step extraction is recommended for future analysis, wherein deionized water, or Faynan groundwater, is first used to extract soluble metals in the soil solution, followed by the extraction of easily exchangeable metals with a 0.05 M solution of calcium chloride ($CaCl_2$) (Asami et al. 1995), before the dissolution of metals bound carbonate material using a 0.11 M solution of CH_3COOH.

Grain size and shape also play a very important role in metal mobility. Future sediment studies could be greatly improved by considering grain size distribution and variations between sites and across sites. The sediments collected from the Wadi 100 site were poorly sorted fluvial sediments while those collected from the Barqa el-Hetiye site were well sorted aeolian sediments.

All samples in this study were passed through a 2 mm sieve, but no further grain-size analysis was considered. A more detailed analysis of sediment grain size and sorting can offer future research insight on the frequency, magnitude, and direction of sediment transport and depositional processes at the (i) Wadi 100 and (ii) Barqa el-Hetiye sites:

(i) a more detailed analysis of the aeolian sediments in the dunes at the Barqa el-Hetiye site would offer insight on the trajectory and migration patterns of these dunes which would also further the regional understanding of dune mobility and thus the redistribution of metals across the aeolian landscape.

(ii) a more targeted sampling strategy across the Wadi Faynan, wherein a single stratigraphic layer is sampled at 100 m intervals starting 100 m east of the Khirbat Faynan site to the Fidān Spring in the west (Figure 4.1) would track the extent of metal redistribution from the Khirbat Faynan (WF1) site across the Wadi Faynan and help assess the mobility of these metals during flooding events.

Future environmental analysis in the Wadi Faynan region should analyze sediments, floral, and faunal samples from the same immediate area in order to correlate the metal concentrations in exchangeable sediment fraction, the metal concentrations in the floral species growing in that sediment, and the amount of metal that is then transferred from flora to fauna to establish a complete understanding of the mobility of these metals through the biological food chain in Faynan.

References

Adriano, D. 2001. Trace elements in terrestrial environments: biogeochemistry, bioavailability, and risks of metals, 2nd Edition. Springer New York.

Ahnstrom, Z.S., and Parker, D.R. 1999. Development and assessment of a sequential extraction procedure for the fractionation of soil cadmium. Soil Science Society of America Journal, **63**(6); 1650-1658.

Al-Bakri, J. 2008. Soils of Jordan. *In* Department of Land, Water, and Environment, University of Jordan. Amman, Jordan.

Albores, A., Cid, B., Gómez, E., and López, E. 2000. Comparison between sequential extraction procedures and single extractions for metal partitioning in sewage sludge samples. Analyst, **125**: 1353-1357.

Alloway, B. 2013. Heavy Metals in Soils: Trace Metals and Metalloids in Soils and their Bioavailability. Springer, Dordrecht.

Al-Qudah, B. 2001. Soils of Jordan. *In* Soil resources of Southern and Eastern Mediterranean countries. CIHEAM, **34**: 127-141.

Amiri, M.E., and Fallahi, E. 2009. Impact of Animal Manure on Soil Chemistry, Mineral Nutrients, Yield, and Fruit Quality in 'Golden Delicious' Apple. Journal of Plant Nutrition, **32**: 610-617.

Andersen, E., and Küpper, H. 2013. Cadmium toxicity in plants. *In* Cadmium: from toxicity to essentiality. Metal Ions in Life Sciences, **11**: 395-414.

Asami, T., Kubota, M., and Orikasa, K. 1995. Distribution of different fractions of cadmium, zinc, lead, and copper in unpolluted and polluted soils. Water, Air and Soil Pollution, **83**: 187-194.

Ayers, R., and Westcot, D. 1985. Water Quality for Agriculture: FAO Irrigation and Drainage. Food and Agriculture Organization of the United Nations, **29**(1): 174.

Barjous, M. 1992. Geology of the Ash Shawbak Area, Map Sheet NO. 3151 III. Amman, Jordan.

Barker, G.W., Creighton, O.H., Gilbertson, D.D., Hunt, O.C., Mattingly, D.J., McLaren, S.J., and Thomas, D.C., with an appendix by Morgan, G. 1997. The Wadi Faynan Project, Southern Jordan: a Preliminary Report on Geomorphology and Landscape Archaeology. *In* Levant, XXIX: 19-40.

Barker, G.W., Gilbertson, D.D., and Mattingly, D.J. 2007. Archaeology and Desertification: The Wadi Faynan Landscape Survey, Southern Jordan. Council for British Research in the Levant. Oxbow Books, Oxford.

Baruch, U., and Bottema, S., 1991. Palynological evidence for climatic changes in Levant ca. 17,000-9,000 B.P. *In* The Natufian Culture in the Levant. Archaeological Series 1. International Monographs in Prehistory, 11-20.

Beherec, M., Levy, T.E., Tirosh, O., Najjar, M., Knabb, K.A., and Ergel, Y. 2016. Iron Age Nomads and their relation to copper smelting in Faynan (Jordan): Trace metal and Pb and Sr isotopic measurements from the Wadi Fidan 40 cemetery. Journal of Archaeological Science.

Bender, F. 1963. Geology of the Arabian Peninsula. USGS Miscellaneous Geologic Investigations, Department of Mines, **560**: 1–34.

Bender, F. 1974. Geology of Jordan. Contributions to the Regional Geology of the Earth. *In* 7th edition. Gebrüder Borntraeger, Berlin.

Ben-Yosef, E., Gidding, A., Tauxe, L., Davidovich, U., Najjar, M., and Levy, T.E. 2016. Early Bronze Age copper production systems in the northern Arabah Valley: new insights from archaeomagnetic study of slag deposits in Jordan and Israel. Journal of Archaeological Science, **72**: 71-84.

Bintliff, J., and Degryse, P. 2022. A review of soil geochemistry in archaeology. Journal of Archaeological Science, **45**: 1-7.

Böttcher, M.E, (2011). Manganese (Sedimentary Carbonates and Sulfides). *In* Encyclopedia of Geobiology. *Edited by* Reitner, J., and Thiel, V. Encyclopedia of Earth Sciences Series. Springer, Dordrecht. pp. 541-542.

Canadian Council of Ministers of the Environment. 2007. Canadian soil quality guidelines for the protection of environmental and human health: Summary tables. *In* Canadian Environmental Quality Guidelines, 1999, update 7, Winnipeg.

Capri, E. 2021. Cadmium limits in phosphorous fertilizers. *In* Soil contamination. European Observatory on Sustainable Agriculture, Brussels. 12-17.

Cerqueira, B., Covelo, E.F., Andrade, M.L., and Vega, F. 2011. Retention and mobility of copper and lead in soils as influenced by soil horizon properties. Pedosphere. **21**(5): 603-614.

Chatterjee, S., Mitra, A., Walther, C., and Gupta, D.K. 2020. Plant response under strontium and phytoremediation. *In* Strontium Contamination in the Environment. The Handbook of Environmental Chemistry, **88**: 85-97.

Chen, J., Wei, F., Zheng, C., Wu, Y., and Adriano, D. C. 1991. Background concentrations of elements in soils of China. Water, Air, and Soil Pollution, **57**: 699-712.

Crook, D. 2009. Hydrology of the combination irrigation system in the Wadi Faynan, Jordan. Journal of Archaeological Science, **36**(10): 2427-2436.

Daliakopoulos, I.N., Tsanis, I.K., Koutroulis, A., Kourgialas, N.N., Varouchakis, A., Karatzas, G.P., and Ritsema, C.J. 2016. The threat of soil salinity: A European scale review. Science of the Total Environment, **573**: 727-739.

Davidson, C.M., Duncan, A.L., Littlejohn, D., Ure, A.M., and Garden, L.M. 1998. A critical evaluation of the three-stage BCR sequential extraction procedure to assess the potential mobility and toxicity of heavy metals in industrially-contaminated land. Analytica Chimica Acta, **363**(1): 45-55.

De Vries, W., Lofts, S., Tipping, E., Meili, M., Groenenberg, J., and Schütze, G. 2007a. Impact of soil properties on critical concentrations of cadmium, lead, copper, zinc, and mercury in soil and soil solution in view of ecotoxicological effects. Reviews of Environmental Contamination and Toxicology, **191**: 47-90.

De Vries, W., Römkens, P., and Schütze, G. 2007b. Critical concentrations of cadmium, lead, and mercury in soil and soil solution in view of ecotoxicological effects. Reviews of Environmental Contamination and Toxicology, **191**: 91-130.

El-Hasan, T.M., Al-Malabeh, A., Kajiwara, Y., and Komuro, K. 2001. Petrology, Mineralogy and Genesis of Wadi Dana Cambrian Manganese Deposit, Central Wadi Araba Region, Jordan. Qatar University Science Journal, **21**: 101-117.

El-Jaoual, T., and Cox, D.A. 1998. Manganese toxicity in plants. Journal of Plant Nutrition, **21**(2): 353-386.

Engel, T., and Frey, W. 1996. Fuel Resources for Copper Smelting in Antiquity in Selected Woodlands in the Edom Highlands to the Wadi Arabah/Jordan. Flora, **191**: 29-39.

Esri. 2020. UCSD Levantine Archaeology Laboratory [basemap]. The Kingdom of Copper Story Map. Available from https://arcg.is/XLG9u [cited April 13 2021].

Fan, Y., Li, Y., Li, H., and Cheng, F. 2018. Evaluating heavy metal accumulation and potential risks in soil-plant systems applied with magnesium slag-based fertilizer. Chemosphere, **197**: 382-388.

Fink, J.R., Inda, A.V., Tiecher, T., and Barrón, V. 2016. Iron oxides and inorganic matter on soil phosphorus availability. Ciência e Agrotecnologia, **40**: 369-379.

Förster, H.-J, Förster, A., Oberhänsli, R., and Stromeyer, D. 2010. Lithospheric composition and thermal structure of the Arabian Shield in Jordan. Tectonophysics, **481**: 29-37.

Freiwan, M., and Kadioğlu, M. 2008. Climate variability in Jordan. International Journal of Climatology, **28**(1): 69–89.

Fritz, V. 1994. Vorbericht über die Grabungen in Barqā el-Hetīye im Gebiet von Fēnān, Wādī el-'Araba (Jordanien) 1990. Zeitschrift des Deutschen Palästina-Vereins, **110**: 125-150.

Grattan, J.P., Huxley, S., Karaki, L.A., Tolund, H., Gilbertson, D.D., Pyatt, F.B., and Al-Saad, Z. 2002. 'Death… more desirable than life'? The human skeletal record and toxicological implications of ancient copper mining and smelting in Wadi Faynan, southwestern Jordan. Toxicology and Industrial Health, **18**: 297–307.

Grattan, J.P., Condron, A., Taylor, S., Abu Karaki, L., Pyatt, F.B., Gilbertson, D.D., and Al-Saad, Z. 2003a. A Legacy of Empires? An Exploration of the Environmental and Medical Consequences of Metal Production in Wadi Faynan, Jordan. *In* Geology and Health: Closing the Gap. Oxford University Press, 99-105.

Grattan, J.P., Huxley, S.N, and Pyatt, F.B. 2003b. Modern Bedouin exposures to copper contamination: an imperial legacy? Ecotoxicology and Environmental Safety, **55**(1): 108-115.

Grattan, J.P., Gillmore, G.K., Gilbertson, D.D., Pyatt, F.B., Hunt, C.O., McLaren, S.J., Phillips, P.S., and Denman, A. 2004. Radon and 'King Solomon's Miners': Faynan Orefield, Jordanian Desert. Science of the Total Environment, **319**(1-3): 99–113.

Grattan, J.P., Abu Karaki, L., Hine, D., Toland, H., Gilbertson, D.D., Al-Saad, Z., and Pyatt, F. B. 2005. Analyses of patterns of copper and lead mineralization in human skeletons excavated from an ancient mining and smelting centre in the Jordanian desert: A reconnaissance study. Mineralogical Magazine, **69**(5): 653–666.

Grattan, J.P., Gilbertson, D.D., and Hunt, C.O. 2007. The local and global dimensions of metalliferous pollution derived from a reconstruction of an eight thousand year record of copper smelting and mining at a desert-mountain frontier in southern Jordan. Journal of Archaeological Science, **34**(1): 83–110.

Grattan, J.P., Gilbertson, D.D., and Kent, M. 2013. Sedimentary metal-pollution signatures adjacent to the ancient centre of copper metallurgy at Khirbet Faynan in the desert of southern Jordan. Journal of Archaeological Science, **40**(11): 3834–3853.

Grattan, J.P., Gilbertson, D.D., Waller, J.H., Adams, R.B. 2014. The geoarchaeology of "waste heaps" from the ancient mining and beneficiation of copper-rich ores in the Wadi Khalid in southern Jordan. Journal of Archaeological Science, **46**: 428-433.

Grattan, J.P., Adams, R.B., Friedman, H., Gilbertson, D.D., Haylock, K.I., Hunt, C.O., and Kent, M. 2016. The first polluted river? Repeated copper contamination of fluvial sediments associated with Late Neolithic human activity in southern Jordan. Science of the Total Environment, **573**(15): 247-257.

Gómez-Álvarez, A., Valenzuela-García, J.L., Meza-Figueroa, D., de la O-Villanueva, M., Ramírez-Hernández, J., Almendariz-Tapia, J., and Pérez-Segura, E. 2011. Impact of mining activities on sediments in a semi-arid environment: Sonora, Mexico. Applied Geochemistry, **26**(12): 2101-2112.

Haberland, Ch., Maercklin, N., Kesten, D., Ryberg, T., Janssen, Ch., Agnon, A., Weber, M., Schulze, A., Qabbani, I., and El-Kelani, R. 2007. Shallow architecture of the Wadi Araba fault (Dead Sea Transform) from high-resolution seismic investigations. Tectonophysics, **432**(1-4): 37–50.

Han, F.X., and Banin, A. 1999. Long-term transformation and redistribution of potentially toxic heavy metals in arid-zone soils: II. Incubation at the field capacity moisture content. Water, Air, and Soil Pollution, **114**(3-4): 221-250.

Hauptmann, A., Bergemann, F., Heitkemper, E., Pernicka, E., and Schmitt-Strecker, S. 1992. Early Copper Produced at Feinan, Wadi Araba, Jordan: The Composition of Ores and Copper. Archaeomaterials, **6**(1): 1-33.

Hauptmann, A. 2007. The Archaeo-metallurgy of Copper: Evidence from Faynan, Jordan. Springer, Berlin, Heidelberg.

He, Z., Dao, T.H., and Honeycutt, C.W. 2006. Insoluble Fe-associated inorganic and organic phosphates in animal manure and soil. Soil Science, **171**(2): 117-126.

Holliday, V.T., and Gartner, W.G. 2007. Methods of soil P analysis in archaeology. Journal of Archaeological Sciences, **34**(2): 301-333.

Hseu, Z.Y., Chen, Z.S., Tsai, C.C., Tsui, C.C., Cheng, S.F., Liu, C.L., and Lin, H.T. 2002. Digestion Methods for Total Heavy Metals in Sediments and Soils. Water, Air, and Soil Pollution, **141**: 189–205.

Hunt, C.O., Elrishi, H.A., Gilbertson, D.D., Grattan, J.P., Mclaren, S.J., Pyatt, F.B., Rushworth, G., and Barker, G.W. 2004. Early-Holocene environments in the Wadi Faynan, Jordan. The Holocene, **14**(6): 921-930.

Hunt, C.O, Gilbertson, D.D., and El-Rishi, H.A. 2007. An 8000-year history of landscape, climate, and copper exploitation in the Middle East: the Wadi Faynan and the Wadi Dana National Reserve in southern Jordan. Journal of Archaeological Science, **34**(8): 1306-1338.

IAG. 2020. Reference Material Data Sheet for the selective extraction by aqua regia of SdAR-L2 Blended sediment, SdAR-M2 Metal-rich sediment, SdAR-H1 Metalliferous sediment. International Association of Geoanalysts. Available from https://www.iageo.com/sdar-reference-materials/ [cited 20 March 2021].

Issar, A.S., 1998. Climatic change and history during the Holocene in the Eastern Mediterranean Region. *In* Water, Environment and Society in Times of Climatic Change. Kluwer Academic Publishers, Dordrecht, 31: 113-128.

Jain, C.K. 2004. Metal fractionation study on bed sediments of River Yamuna, India. Water Research, **38**(3): 569-578.

Jones, R.P., Hassan, S.M., and Rodgers Jr, J.H. 2008. Influence of contact duration of sediment-associated copper fractionation and bioavailability. Ecotoxicology and Environmental Safety. **71**(1): 104-116.

Kang, X., Song, J., Yuan, H., Duan, L., Li, X., Li, N., Liang, X., and Qu, B. 2017. Speciation of heavy metals in different grain sizes of Jiaozhou Bay sediments: Bioavailability, ecological risk assessment and source analysis on a centennial timescale. Ecotoxicology and Environmental Safety, **143**: 296–306.

Katyal, J.C., and Sharma, B.D. 1991. DPTA-extractable and total Zn, Cu, Mn, and Fe in Indian soils and their association with some soil properties. Geoderma, **49**(1-2): 165-179.

Knabb, K.A., Erel, Y., Tirosh, O., Rittenour, T., Laparidou, S., Najjar, M., Levy, T.E. 2016. Environmental impacts of ancient copper mining and metallurgy: multi-proxy investigation of human-landscape dynamics in the Faynan valley, southern Jordan. Journal of Archaeological Science. **74**: 85-101.

Komiyama, T., and Toyoaki, I. 2019. The characteristics of phosphorus in animal manure composts. Soil Science and Plant Nutrition, **65**(3): 281-288.

Kuo, S., Heilman, P.E., and Baker, A.S. 1983. Distribution and forms of copper, zinc, cadmium, iron, and manganese in soils near a copper smelter. Soil Science, **135**(2): 101-109.

Levy, T.E., Adams, R.B., and Shafiq, R. 1999. The Jabal Hamrat Fidan Project: Excavations at the Wadi Fidan 40 Cemetery, Jordan (1997). Levant, **31**(1): 293–308.

Levy, T.E., Ben-Yosef, E., and Najjar, M. 2012. New perspectives on Iron Age copper production and society in the Faynan region, Jordan. *In* Eastern Mediterranean metallurgy and metalwork in the 2nd millennium BC. Oxbow Books, Oxford.

Li, Z., Ma, Z., van der Kuijp, T.J., Yuan, Z., and Huang, L. 2014. A review of soil heavy metal pollution from mines in China: Pollution and Health risk assessment. Science of the Total Environment, **468-469**: 843-853.

Li, S., Li, M., Sun, H., Li, H., and Ma, L. 2020. Lead bioavailability in different fractions of mining- and smelting-contaminated soils based on a sequential extraction and mouse kidney model. Environmental Pollution, **262**: 1-6.

Ma, L.Q., and Rao, G.N. 1997. Chemical Fractionation of Cadmium, Copper, Nickel, and Zinc in Contaminated Soils. *In* Heavy Metals in the Environment. Journal of Environmental Quality, **26**: 259-264.

Madzin, Z., Shai-in, M.F., and Kusin, F.M. 2015. Comparing Heavy Metal Mobility in Active and Abandoned Mining Sites in Bestary Jaya, Selangor. Procedia Environmental Sciences, **30**: 232-237.

McBride, M.B. 1981. Forms and Distribution of Copper in Solid and Solution Phases of Soil. *In* Copper in Soils and Plants. *Edited by* J.F. Loneragan, A.D. Robson, and R.D. Graham. Academic Press Australia, Perth.

McLaren, S.J., Gilbertson, D.D., Grattan, J.P., Hunt, C.O., Duller, G.A.T., Barker, G.A. 2004. Quaternary palaeogeomorphologic evolution of the Wadi Faynan area, southern Jordan. Palaeogeography, Palaeoclimatoloy, Palaeoecology; **205**(1-2), 131-154.

Mengel, K., Kirkby, E.A., Kosegarten, H., and Appel, T. 2001. Phosphorus. *In* Principles of Plant Nutrition. 5th edition. *Edited by* Mengel, K., Kirkby, E.A., Kosegarten, H., and Appel, T. Kluwer Academic Publishers, Springer, Dordrecht. pp. 481-511.

Mester, Z., Cremisini, C., Ghiara, E., Morabito, R. 1998. Comparison of two sequential extraction procedures for metal fractionation in sediment samples. Analytica Chimica Acta, **359**(1): 133-142.

Navarro, M.C., Pérez-Sirvent, C., Martínez-Sánchez, M.J., Vidal, J., Tovar, P.J., and Bech, J. 2008. Abandoned mine sites as a source of contamination by heavy metals: A case study in a semi-arid zone. Journal of Geochemical Exploration, **96**(2-3): 183-193.

Niemi, T.M., Zhang, H., Atallah, M., and Harrison, J.B.J. 2001. Late Pleistocene and Holocene slip rate of the Northern Wadi Araba fault, Dead Sea Transform, Jordan. Journal of Seismology, **5**: 449–474.

Oliver, I.W., Hass, A., Merrington, G., Fine, P., and McLaughlin, M.J. 2005. Copper Availability in Seven Israeli Soils Incubated with and without Biosolids. Journal of Environmental Quality, **34**: 508-513.

Oonk, S., Slomp, C.P., and Huisman, D.J. 2009. Geochemistry as an Aid in Archaeological Prospection and Site Interpretation: Current Issues and Research Directions. Archaeological Prospection, **16**: 35-51.

Oster, J.D., Sposito, G., and Smith, C.J. 2016. Accounting for potassium and magnesium in irrigation water quality assessment. California Agriculture, **70**(2): 71-76.

Palmer, C. 2007. The Wadi Faynan today; landscape, environment, people. *In* Archaeology and Desertification: The Wadi Faynan Landscape Survey, southern Jordan. *Edited by:* Barker, G., Gilbertson, D., and Mattingly, D. Oxbow: Council for British Research in the Levant and Oxbow Books, Oxford. pp. 25-57.

Pathak, P., and Gupta, D. 2020. Strontium Contamination in the Environment. The Handbook of Environmental Chemistry, **88**: 43-64.

Perry, M.A., Coleman, D.S., Dettman, D.L., and Halim al-Shiyab, A. 2009. An isotopic perspective on the transport of Byzantine mining camp laborers into southwestern Jordan. American Journal of Physical Anthropology, **140**: 429-441.

Perry, M.A., Coleman, D.S., Dettmen, D.L., Grattan, J.P., Halim al-Shiyab, A. 2011. Condemned to metallum? The origin and role of 4th - 6th centruy A.D. Phaeno mining campresidents using multiple chemical techniques. Journal of Archaeological Science, **38**: 558-569.

Pyatt, F.B., Barker, G.W., Birch, P., Gilbertson, D.D., Grattan, J.P., and Mattingly, D.J. 1999. King Solomon's Miners - Starvation and Bioaccumulation? An Environmental Archaeologial Investigation in Southern Jordan. Ecotoxicology and Environmental Safety, **43**(3): 305-308.

Pyatt, F.B., Gilmore, G., Grattan, J.P., Hunt, C.O., and McLaren, S. 2000. An Imperial Legacy? An Exploration of the Environmental Impact of Ancient Metal Mining and Smelting in Southern Jordan. Journal of Archaeological Science, **27**(9): 771-778.

Pyatt, F.B., Amos, D., Grattan, J.P, Pyatt, A.J, and Terrell-Nield, C.E. 2002. Invertebrates of ancient heavy metal spoil and smelting tip sites in sourthern Jordan: Their distribution and use as bioindicators of metalliferous pollution derived from ancient sources. Journal of Arid Environments, **52**(1): 53-62.

Pyatt, F.B., Pyatt, A.J., Walker, C., Sheen, T., and Grattan, J.P. 2005. The heavy metal content of skeletons from an ancient metalliferous polluted area in southern Jordan with particular reference to bioaccumulation and human health. Ecotoxicology and Environmental Safety, **60**(3): 295-300.

Qadir, M., Schubert, S., Oster, J.D., Sposito, G., Minhas, P.S., Cheraghi, S.A.M., Murtaza, G., Mirzabaev, A., Saqib, M. 2018. High-magnesium waters and soils: Emerging environmental and food security constraints. Science of The Total Environment, **642**: 1108-1117.

Quevauviller, Ph., Rauret, G., López-Sánchez, J.-F., Rubio, R., Ure, A., and Muntau, H. 1997. Certification of trace metal extractable contents in a sediment reference material (CRM 601) following a three-step sequential extraction procedure. Science of the Total Environment, **205**(2-3): 223-234.

Rabb'a, I. 1994. Geology of the Al Qurayqira Area (Jabal Hamra Faddan); Map Sheet NO. 3051 II. Geology/Directorate/NRA, Amman. Bulletin **28**: 58.

Rauret, G., López-Sánchez, J.F., Sahuquillo, A., Rubio, R., Davidson, C., Ure, A., and Quevauviller, Ph. 1999. Improvement of the BCR three step sequential extraction procedure prior to the certification of new sediment and soil reference materials. Journal of Environmental Monitoring, **1**: 57-61.

Roberts, N., Stevenson, T., David, B., Cheddadi, R., and Brewster, S., 2004. Holocene climate, environment and cultural change in the circum-Mediterranean region. *In* Past Climate Variability Through Europe and Africa. *Edited by* Battarbee, R.W., Gasse, F., and Stickley, C.E. Kluwer, Dordrecht, Netherlands; pp. 343-362.

Ruby, M.V., Schoof, R., Brattin, W., Goldade, M., Post, G., Harnois M., Mosby, D.E., Casteel, S.W., Berti, W., Carpenter, M., Edwards, D., Cragin, D., and Chappell, W. 1999. Advances in Evaluating the Oral Bioavailability of Inorganics in Soil for Use in Human Health Risk Assessment. Environmental Sciences & Technology, **33**(21): 3697-3705.

Saeedi, M., Li, L.Y., Karbassi, A.R., and Zanjani, A.J. 2012. Sorbed metals fractionation and risk assessment of release in river sediment and particulate matter. Environmental Monitoring and Assessment, **185**: 1737-1754.

Sainju, U.M., Dris, R., and Singh, B. 2003. Mineral nutrition of tomato. Food, Agriculture & Environment, **1**(2): 176-183.

Sawkins, F.J. 1984. Metal Deposits in Relation to Plate Tectonics. *In* Minerals and rocks, **17**. *Edited by* P.J. Wyllie, A. El Goresy, W. von Engelhardt, and T. Hahn. Springer-Verlag, Berlin. pp. 177-212.

Smith, G.H.S., Nicholas, A.P., and Ferguson, R.I. 1997. Measuring and defining bimodal sediments: Problems and implications. Water Resources Research, **33**(5): 1179–1185.

Sutherland, R.A., and Tack, F.M.G. 2003. Fractionation of Cu, Pb and Zn in certified reference soils SRM 2710 and SRM 2711 using the optimized BCR sequential extraction procedure. Advances in Environmental Research, **8**(1): 37–50.

Szefer, P., Szefer, K., Glasby, G.P., Pempkowiak, and J., Kaliszan, R. 1996. Heavy metal pollution in surficial sediments from the Southern Baltic sea off Poland. Journal of Environmental Science and Health. Part A: Environmental Science and Engineering and Toxicology. **31**: 2723-2754.

ten Brink, U.S., Rybakov, M., Al-Zoubi, A.S., Hassouneh, M., Frieslander, U., Batayneh, A.T., Goldschmidt, V., Daoud, M.N., Rotstein, Y., and Hall, J.K. 1999. Anatomy of the Dead Sea transform: Does it reflect continuous changes in plate motion? Geology, **27**(10): 887–890.

Tessier, A., Campbell, P.G.C., and Bisson, M. 1979. Sequential extraction procedure for the speciation of particulate trace metals. Analytical Chemistry, **51**(7): 844-85.

Turner, B.L., and Leytem, A.B. 2004. Phosphorus Compounds in Sequential Extracts of Animal Manures: Chemical Speciation and a Novel Fractionation Procedure. Environmental Science and Technology, **38**(22): 6101-6108.

Ugolini, F.C., Hillier, S., Certini, G., and Wilson, M.J. 2008. The contribution of aeolian material to an Aridisol from southern Jordan as revealed by mineralogical analysis. Journal of Arid Envrionments; **72**(8): 1431-1447.

Ure, A.M., Quevauviller, Ph., Mantau, H., and Griepink, B. 1993. Speciation of Heavy Metals in Soils and Sediments: An Account of the Improvement and Harmonization of Extraction Techniques Undertaken Under the Auspices of the BCR of the Commission of the European Communities. International Journal of Environmental Analytical Chemistry, **51**(1-4): 135-151.

Vandecasteele, B., Reubens, B., Willekens, K., and De Neve, S. 2014. Composting for Increasing the Fertilizer Value of Chicken Manure: Effects of Feedstock on P Availability. Waste Biomass Valor, **5**: 491-503.

Vaněk, A., Borůvka, B., Drábek, O., Mihaljevič, M., and Komárek, M. 2005. Mobility of lead, zinc and cadmium in alluvial soils heavily polluted by smelting industry. Plant, Soil and Environment, **51**(7): 316-321.

Vega, F.A., Covelo, E.F., and Andrade, M.L. 2006. Competitive sorption and desorption of heavy metals in mine soils: Influence of mine soil characteristics. Journal of Colloid and Interface Science, **298**(2): 582-592.

Vranová, V., Marfo, T.D., and Rejšek, K. 2015. Soil scientific research methods used in archaeology – promising soil biochemistry: A mini review. ACTA Universitatis Agriculturae et Silviculturae Mendelianae Brunensis, **63**(155): 1417-1427.

Wade, A., Holmes, P., El Bastawesy, M., Smith, S., Black, E., and Mithen, S. 2011. The hydrology of the Wadi Faynan. *In* Water, Life and Civilization: Climate, Environment and Society in the Jordan Valley. *Edited by* Mithen, S., and Black, E. Cambridge University Press. 157-174.

Wdowinski, S., and Zilberman, E. 1997. Systematic analysis of the large-scale topography and structure across the Dead Sea Rift. Tectonophysics, **16**(3): 409-424.

Weihrauch, C., Söder, U., Stoddart, S. 2022. The Identification of Archaeologically Interesting Depths from Vertical Soil Phosphorus Prospections in Geoarchaeology. Geoderma, **418**: 1-17.

Weil, R.R., and Brady, N.C. 2019. Elements of the Nature and Properties of Soils, 4th edition. Pearson, New York, NY.

Weston, A. 2019a. Geospatial Map of the Barqa el-Hetiye Sampling Site in Faynan, Jordan.

Weston, A. 2019b. Geospatial Map of the Wadi 100 Sampling Site in Faynan, Jordan.

Wright, K., Najjar, M., Last, J., Moloney, N., Flender, M., Gower, J., Jackson, N., Kennedy, A., and Shafiq, R. 1998. The Wadi Faynan Fourth and Third Millennia Project, 1997: Report on the first season of test excavations at Wadi Faynan 100. Levant, **30**(1): 33-60.

Xian, X. 1987. Chemical partitioning of cadmium, zinc, lead, and copper in soils near smelter. Journal of Environmental Science and Health. Part A: Environmental Science and Engineering, **22**(6): 527-541.

Yan, Y., Zhou, Y.Q., Liang, C.H. 2015. Evaluation of Phosphate Fertilizers for the Immobilization of Cd in Contaminated Soils. PLoS ONE, **10**(4): e0124022.

Yan, K., Dong, Z., Wijayawardena, M.A.A., Liu, Y., Naidu, R., and Semple, K. 2017. Measurement of soil lead bioavailability and influence of soil types and properties: A review. Chemosphere, **184**: 27-42.

Yarlagadda, P.S., Matsumoto, M.R., VanBenschoten, J.E., and Kathuria, A. 1995. Characteristics of Heavy Metals in Contaminated Soils. Journal of Environmental Engineering, **121**(4): 276-286.

Yuan, X., Xiong, T., Wang, H., Wu, Z., Jiang, L., Zeng, G., and Li, Y. 2018. Immobilization of heavy metals in two contaminated soils using a modified magnesium silicate stabilizer. Environmental Science and Pollution Research, **25**: 32562-32571.

Yusuf, K. A. 2007. Sequential Extraction of Lead, Copper, Cadmium and Zinc in Soils near Ojota Waste Site. Journal of Agronomy, **6**(2): 331-337.

Zhang, C., Yu, Z., Zeng, G.M., Jiang, M., Yang, Z., Cui, F., Zhu, M., Shen, L., and Hu, L. 2014. Effects of sediment geochemical properties on heavy metal bioavailability. Environment International, **73**: 270–281.

Zhong, A., Kraemer, L., and Evans, D. 2013. Influence of contact time and sediment composition on the bioavailability of Cd in sediments. Envrionmental Pollution, **173**: 11-16.

Appendix A

Table A1: All sequential extraction concentrations from Wadi 100 samples.

Sample number	Sediment Fraction	Mg (µg/g)	Al (µg/g)	P (µg/g)	Cr (µg/g)	Mn (µg/g)	Fe (µg/g)	Ni (µg/g)	Cu (µg/g)	Zn (µg/g)	Sr (µg/g)	Cd (µg/g)	Pb (µg/g)
1	Exchangeable	5680	262	86.3	2.08	176	104	2.37	31.2	4.68	297	< LOD	0.17
	Reducible	391	879	574	1.48	37.2	567	1.43	4.68	2.86	21.2	0.05	0.96
	Oxidizable	805	272	29.9	3.36	12.9	89.9	2.12	23.4	1.26	1.46	< LOD	1.56
	Residual	2430	12400	62.8	18.4	77.9	9650	9.66	53.1	26.2	33.5	< LOD	5.44
	Total	9310	13800	753	25.3	304	10400	15.6	112	35.0	353	0.05	8.13
2	Exchangeable	3570	462	36.6	1.71	122	117	2.03	40.9	3.40	133	< LOD	0.18
	Reducible	266	685	457	1.24	78.2	512	1.12	46.6	6.72	5.89	< LOD	1.84
	Oxidizable	618	464	26.2	2.82	8.08	214	1.48	9.50	0.91	1.46	< LOD	0.90
	Residual	914	4140	< LOD	6.15	35.4	3840	3.11	15.3	9.13	15.0	< LOD	2.61
	Total	5370	5750	520	11.9	244	4680	7.73	112	20.2	155	0	5.54
3	Exchangeable	5870	209	59.4	2.15	270	107	2.80	12.7	3.56	391	0.73	0.14
	Reducible	469	1060	914	2.15	65.1	648	1.67	31.1	12.0	20.9	< LOD	1.36
	Oxidizable	722	487	40.8	3.20	7.78	188	1.53	6.58	< LOD	1.28	< LOD	1.01
	Residual	1710	5530	< LOD	10.0	37.5	4420	5.38	74.7	13.7	13.0	< LOD	2.20
	Total	8770	7290	1010	17.5	380	5360	11.4	125	29.2	426	0.73	4.71
5	Exchangeable	5880	416	110	2.45	189	166	2.65	34.0	6.57	288	0.56	0.19
	Reducible	496	1010	1090	1.40	58.5	659	1.54	27.6	3.05	12.0	< LOD	1.93
	Oxidizable	887	324	41.8	2.04	8.05	181	1.17	9.8	< LOD	1.09	< LOD	0.65
	Residual	564	2930	< LOD	< LOD	18.7	2280	2.09	13.4	7.04	8.35	< LOD	1.39
	Total	7830	4680	1240	5.89	274	3290	7.45	84.7	16.7	309	0.56	4.15
7	Exchangeable	3740	368	503	1.36	102	136	1.88	87.5	6.50	218	0.30	0.11
	Reducible	553	820	878	1.63	62.2	566	1.80	29.4	4.62	23.1	< LOD	1.00
	Oxidizable	868	247	97.9	2.64	10.4	63.7	1.55	39.1	1.20	1.08	< LOD	1.04
	Residual	3200	11500	183	23.7	76.6	9720	11.6	108	< LOD	55.7	< LOD	10.3
	Total	8360	12900	1660	29.3	251	10500	16.8	264	12.3	298	0.30	12.5
9	Exchangeable	5350	319	149	1.91	165	126	2.17	11.4	4.89	230	0.54	0.21
	Reducible	575	743	912	1.39	92.9	542	1.69	34.1	4.95	21.4	< LOD	0.97
	Oxidizable	772	245	81.4	3.41	9.26	79.7	1.97	51.3	1.59	1.87	< LOD	1.75
	Residual	2180	7810	138	17.6	49.2	6360	8.50	85.0	< LOD	< LOD	< LOD	3.71
	Total	8880	9110	1280	24.3	317	7110	14.3	182	11.4	254	0.54	6.63
12	Exchangeable	5010	284	83.3	1.61	163	128	2.31	25.7	4.10	209	0.46	0.12
	Reducible	419	741	885	1.32	63.8	481	1.44	62.1	3.77	13.7	0.10	1.76
	Oxidizable	974	507	65.7	3.59	11.6	151	1.93	34.8	1.39	1.75	< LOD	1.33
	Residual	2080	8280	97.1	15.3	54.6	6960	8.05	89.4	20.1	19.2	< LOD	3.36
	Total	8480	9810	1130	21.8	293	7720	13.7	212	29.3	244	0.56	6.56
15	Exchangeable	4130	502	51.9	1.73	83.1	185	2.02	2.29	3.48	233	0.24	0.11
	Reducible	440	908	901	1.63	87.2	653	1.77	34.8	4.12	13.7	0.10	1.73
	Oxidizable	870	271	59.6	2.29	7.93	327	1.34	160	2.24	1.88	< LOD	1.30
	Residual	2200	6440	101	12.4	50.7	5720	6.50	220	22.5	19.2	< LOD	2.87
	Total	7640	8120	1110	18.1	229	6890	12	417	32.4	268	0.34	6.00
17	Exchangeable	4760	443	78.0	2.30	104	217	2.28	13.7	6.25	243	0.34	0.13
	Reducible	407	853	823	1.45	64.3	584	1.70	< LOD	3.82	13.3	< LOD	1.22
	Oxidizable	710	371	73.9	3.28	7.96	213	1.87	27.9	1.79	1.97	< LOD	1.92
	Residual	5360	16800	323	34.5	119	14900	17.6	140	47.4	37.4	< LOD	8.56
	Total	11200	18500	1300	41.5	295	15900	23.5	181	59.3	296	0.34	11.8
19	Exchangeable	4740	485	90.0	2.77	118	221	2.51	13.2	5.07	233	0.49	0.15
	Reducible	398	841	770	1.33	64.2	609	1.81	17.9	3.47	12.1	< LOD	1.11
	Oxidizable	828	307	41.9	3.31	6.87	112	1.75	26.0	1.54	1.48	< LOD	1.62
	Residual	3320	9190	214	20.8	75.8	9050	10.6	76.2	28.1	21.6	< LOD	4.80
	Total	9290	10800	1120	28.2	265	9990	16.7	133	38.2	268	0.49	7.68
21	Exchangeable	5110	327	89.8	1.96	115	132	2.04	9.13	2.94	292	0.38	0.10
	Reducible	474	949	949	1.65	94.0	647	1.84	40.6	4.22	14.8	< LOD	1.72
	Oxidizable	760	308	67.9	2.52	9.04	131	1.52	16.2	< LOD	2.52	< LOD	2.25
	Residual	3710	11000	214	22.1	90.9	10600	11.6	59.5	47.1	29.9	< LOD	6.00
	Total	10100	12600	1320	28.2	309	11500	17.0	126	54.3	339	0.38	10
24	Exchangeable	5080	525	57.3	2.49	139	231	4.80	11.6	3.77	269	0.33	0.13
	Reducible	589	1100	1130	2.05	66.2	672	2.23	38.7	10.2	36.4	0.11	1.29
	Oxidizable	866	442	66.4	4.18	7.62	151	1.55	9.64	0.79	1.61	< LOD	1.16
	Residual	1830	4090	44.4	8.22	30.9	3800	3.92	21.4	26.1	31.2	< LOD	1.54
	Total	8370	6160	1300	16.9	243	4850	12.5	81.3	40.8	338	0.44	4.12

Appendix A

Table A1: All sequential extraction concentrations from Wadi 100 samples.

Sample number	Sediment Fraction	Mg (µg/g)	Al (µg/g)	P (µg/g)	Cr (µg/g)	Mn (µg/g)	Fe (µg/g)	Ni (µg/g)	Cu (µg/g)	Zn (µg/g)	Sr (µg/g)	Cd (µg/g)	Pb (µg/g)
25	Exchangeable	3870	481	46.2	1.88	98	151	1.86	2.90	2.26	182	< LOD	0.11
	Reducible	423	842	852	1.39	75.0	587	1.65	15.2	3.87	11.9	< LOD	1.32
	Oxidizable	792	308	38.2	3.96	8.39	272	1.55	15.8	0.96	1.29	< LOD	0.96
	Residual	4550	11700	158	23.3	84.5	10700	10.7	75.6	9.49	9.62	< LOD	4.69
	Total	9640	13300	1100	30.5	266	11700	15.8	110	16.6	205	0	7.07
29	Exchangeable	5620	389	64.5	2.11	169	190	2.11	11.5	4.01	216	0.44	0.17
	Reducible	404	856	842	1.48	63.5	607	1.64	22.9	3.74	12.2	0.09	1.43
	Oxidizable	748	271	37.8	3.76	8.07	98.0	1.97	17.8	< LOD	1.33	< LOD	1.00
	Residual	1560	4530	39.5	8.16	27.7	3660	4.05	23.8	30.3	27.0	< LOD	1.49
	Total	8330	6050	984	15.5	269	4550	9.77	76.0	38.0	257	0.53	4.10
31	Exchangeable	4420	349	51.2	1.85	129	149	1.97	13.8	3.37	189	0.38	0.12
	Reducible	472	832	940	1.62	73.3	576	1.61	47.6	4.04	13.3	< LOD	1.38
	Oxidizable	748	237	40.6	3.34	5.69	43.4	1.71	16.7	0.88	1.29	< LOD	0.92
	Residual	3960	12600	149	24.3	81.2	10600	12.5	96.6	10.8	9.88	< LOD	4.87
	Total	9600	14000	1180	31.1	289	11400	17.8	175	19.1	214	0.38	7.29
33	Exchangeable	6370	389	34.6	2.14	168	224	2.16	8.73	5.28	205	0.46	0.15
	Reducible	591	935	1120	1.65	65.6	643	1.90	186	5.02	17.9	0.11	1.89
	Oxidizable	787	228	< LOD	3.84	9.32	181	1.67	24.9	1.11	1.21	< LOD	1.09
	Residual	1980	6310	88.8	11.3	45.2	5500	5.50	33.1	10.4	10.0	< LOD	2.52
	Total	9730	8760	1240	18.9	288	6550	11.2	253	21.8	234	0.57	5.65
35	Exchangeable	5270	330	87.4	1.75	141	152	2.00	15.8	3.62	221	0.42	0.12
	Reducible	524	823	1010	1.39	64.3	543	1.61	64.0	4.01	16.2	0.12	1.51
	Oxidizable	792	331	38.9	2.65	8.43	88.5	1.37	3.15	0.48	0.97	< LOD	0.47
	Residual	4680	14500	114	26.1	94.1	12900	13.6	87.2	16.5	14.7	< LOD	5.64
	Total	11300	16000	1250	31.9	308	13700	18.6	170	24.6	253	0.54	7.75
37	Exchangeable	5230	426	59.5	2.07	148	207	2.13	8.94	3.99	195	0.42	0.15
	Reducible	472	807	776	1.45	63.7	573	1.73	45.2	3.76	13.6	< LOD	1.31
	Oxidizable	380	740	21.8	4.03	5.06	66.7	2.12	9.65	1.43	1.72	< LOD	0.86
	Residual	1920	7890	71.2	13.1	45.9	6280	6.82	34.0	35.3	32.5	< LOD	3.12
	Total	8000	9860	928	20.7	262	7130	12.8	97.8	44.5	243	0.42	5.43
39	Exchangeable	4290	355	83.2	1.65	125	125	1.76	5.02	3.25	173	0.35	0.12
	Reducible	349	947	857	1.50	74.0	694	1.66	20.2	3.62	11.2	< LOD	1.59
	Oxidizable	671	401	29.1	3.57	7.56	80.1	2.03	19.5	1.08	1.49	< LOD	0.94
	Residual	1490	6240	70.3	11.5	40.6	5440	5.89	42.2	22.7	17.4	< LOD	2.57
	Total	6800	7940	1040	18.3	248	6340	11.3	87.0	30.6	203	0.35	5.23
41	Exchangeable	4100	473	97.2	1.90	146	122	2.12	8.20	3.41	196	0.43	0.15
	Reducible	593	768	922	1.43	93.8	555	1.68	34.2	4.68	20.4	< LOD	1.07
	Oxidizable	806	217	60.7	2.39	9.79	87.9	1.48	26.7	1.32	1.05	< LOD	0.87
	Residual	1460	5880	82.1	10.0	35.2	4370	5.37	36.7	15.3	14.3	< LOD	2.38
	Total	6960	7340	1160	15.7	285	5140	10.7	106	24.7	231	0.43	4.47
44	Exchangeable	5280	412	30.9	2.20	141	158	2.85	16.8	< LOD	220	0.46	0.15
	Reducible	467	991	983	1.92	70.7	579	1.90	42.1	15.9	16.1	< LOD	1.44
	Oxidizable	761	394	51.6	2.75	8.25	73.3	1.68	13.4	1.35	1.51	< LOD	0.91
	Residual	2100	8100	97.9	16.0	51.6	6650	8.01	70.6	< LOD	25.7	< LOD	3.18
	Total	8610	9900	1160	22.9	272	7460	14.4	143	17.2	263	0.46	5.67
50	Exchangeable	4380	505	71.5	2.27	141	174	2.31	8.43	< LOD	154	0.36	0.18
	Reducible	524	981	1020	1.69	66.2	675	1.92	85.0	9.33	19.4	< LOD	1.81
	Oxidizable	432	163	24.7	2.18	5.52	68.0	1.21	18.4	< LOD	1.18	< LOD	0.81
	Residual	1150	4550	40.7	7.73	27.2	3640	4.07	20.0	10.9	10.0	< LOD	1.78
	Total	6490	6200	1160	13.9	240	5460	9.51	132	20.2	185	0.36	4.58
51	Exchangeable	4690	286	47.6	1.67	127	105	1.82	13.0	2.49	204	0.37	0.12
	Reducible	491	1040	1320	1.59	87.3	661	1.90	50.0	4.12	15.5	< LOD	2.26
	Oxidizable	870	522	46.6	3.61	9.95	196	1.92	14.1	< LOD	1.62	< LOD	0.99
	Residual	721	3250	< LOD	5.74	22.3	2950	3.07	13.5	9.39	8.97	< LOD	1.55
	Total	6770	5100	1410	12.6	246	3910	8.71	90.6	16.0	230	0.37	4.93
53	Exchangeable	3360	612	63.9	2.05	98.4	137	2.17	13.9	< LOD	138	0.32	0.21
	Reducible	499	930	1030	1.56	91.4	633	1.71	50.5	4.21	14.0	< LOD	1.43
	Oxidizable	971	133	41.2	2.40	7.52	49.5	0.97	25.8	0.99	0.92	< LOD	0.65
	Residual	2550	9580	47.0	16.4	65.0	8390	8.40	59.5	22.2	27.2	< LOD	3.94
	Total	7380	11300	1180	22.4	262	9210	13.2	150	27.4	180	0.32	6.23

Appendix B

Table A2: All sequential extraction concentrations from Barqa el-Hetiye samples.

Sample number	Sediment Fraction	Mg (µg/g)	Al (µg/g)	P (µg/g)	Cr (µg/g)	Mn (µg/g)	Fe (µg/g)	Ni (µg/g)	Cu (µg/g)	Zn (µg/g)	Sr (µg/g)	Cd (µg/g)	Pb (µg/g)
14	Exchangeable	2250	630	66.2	1.07	218	93.5	< LOD	75.3	5.01	72.4	0.10	0.56
	Reducible	460	605	158	0.97	50.8	432	0.86	36.0	1.70	2.41	< LOD	5.41
	Oxidizable	517	469	< LOD	0.86	5.36	57.7	0.52	17.7	29.5	6.81	< LOD	1.11
	Residual	1050	6980	46.3	6.70	34.1	4700	3.15	42.7	27.0	28.0	< LOD	3.87
	Total	4280	8680	270	9.60	308	5280	4.53	172	63.2	110	0.10	11.0
15	Exchangeable	2240	541	86.0	0.99	91.3	92.9	< LOD	97.1	5.08	78.5	0.09	0.31
	Reducible	710	1050	334	1.04	45.6	600	0.87	113	3.16	3.58	< LOD	3.13
	Oxidizable	815	1220	21.7	1.72	8.21	54.8	0.83	46.8	33.2	23.1	< LOD	1.17
	Residual	1620	9910	60.2	10.4	50.0	6240	4.57	114	29.9	35.1	< LOD	4.41
	Total	5390	12700	502	14.2	195	6990	6.28	370	71.3	140	0.09	9.01
16	Exchangeable	3410	1500	80.1	2.24	689	205	3.06	148	56.5	126	0.19	1.26
	Reducible	1050	1020	334	3.11	400	630	1.53	77.7	1.13	89.4	< LOD	11.8
	Oxidizable	406	400	< LOD	0.77	7.81	38.5	0.46	19.4	30.2	6.91	< LOD	1.10
	Residual	974	6140	39.7	7.05	53.0	4980	3.17	43.9	27.8	24.0	< LOD	4.10
	Total	5840	9060	453	13.2	1150	5850	8.21	289	116	246	0.19	18.3
17	Exchangeable	1720	675	29.8	1.04	199	57.5	< LOD	73.6	5.79	54.9	0.07	0.58
	Reducible	288	634	214	1.04	189	538	0.86	68.2	2.62	2.88	< LOD	9.01
	Oxidizable	388	416	< LOD	0.79	7.49	31.7	< LOD	36.1	30.8	6.88	< LOD	1.47
	Residual	1020	6840	42.5	7.36	52.7	5190	3.08	69.3	26.8	28.6	< LOD	4.49
	Total	3420	8570	286	10.2	449	5820	3.94	247	66.0	93.2	0.07	15.5
18	Exchangeable	1590	843	16.1	1.16	89.1	75.4	< LOD	29.1	3.80	49.3	0.09	0.48
	Reducible	221	587	161	1.01	35.9	520	0.79	23.2	1.60	1.84	< LOD	2.28
	Oxidizable	307	437	< LOD	0.73	4.08	30.8	0.39	10.4	30.2	6.69	< LOD	0.58
	Residual	751	5760	42.3	6.40	34.0	4350	2.60	28.8	26.4	27.3	< LOD	3.30
	Total	2870	7630	219	9.30	163	4980	3.78	91.5	61.9	85.1	0.09	6.64
19	Exchangeable	2130	657	56.1	0.97	86.3	95.9	< LOD	48.2	3.52	66.7	< LOD	1.52
	Reducible	405	700	254	1.07	213	541	1.18	78.3	2.77	3.19	< LOD	9.40
	Oxidizable	449	445	< LOD	0.86	8.50	52.1	0.44	28.3	31.1	7.14	< LOD	1.46
	Residual	1230	7390	56.8	8.85	58.8	5490	3.65	79.6	28.5	31.3	< LOD	5.20
	Total	4210	9190	367	11.8	366	6180	5.27	234	65.9	108	0	17.6
20	Exchangeable	2050	776	33.5	1.12	184	62.3	< LOD	52.4	5.27	73.1	0.12	0.62
	Reducible	389	671	205	1.07	119	576	1.04	43.1	2.75	3.02	< LOD	7.25
	Oxidizable	586	1120	16.1	1.18	7.03	38.0	0.60	18.7	31.6	22.1	< LOD	1.39
	Residual	1140	6540	51.0	7.29	48.0	5200	3.22	51.4	28.6	27.6	< LOD	4.62
	Total	4170	9110	306	10.7	358	5880	4.86	166	68.1	126	0.12	13.9
21	Exchangeable	1890	644	33.8	1.00	110	64.8	< LOD	29.5	3.80	62.4	0.10	0.52
	Reducible	378	542	125	0.91	146	457	0.94	33.0	2.04	2.70	< LOD	5.95
	Oxidizable	531	490	< LOD	1.12	6.88	37.4	< LOD	33.9	30.7	6.82	< LOD	1.79
	Residual	1230	7990	45.9	8.20	48.0	5740	3.56	62.9	27.6	28.8	< LOD	4.47
	Total	4030	9670	205	11.2	311	6300	4.50	159	64.1	101	0.10	12.7
22	Exchangeable	2600	873	75.1	1.34	116	214	< LOD	37.7	5.03	73.0	< LOD	1.18
	Reducible	647	829	238	1.16	102	558	1.02	54.1	3.01	3.14	< LOD	7.22
	Oxidizable	654	636	16.2	1.23	8.46	142	0.65	16.7	30.7	7.19	< LOD	1.15
	Residual	1720	10500	66.6	11.0	61.9	6990	4.89	68.4	32.3	35.8	< LOD	5.36
	Total	5620	12800	396	14.7	289	7900	6.55	177	71.0	119	0	14.9
23	Exchangeable	3090	705	28.0	1.27	125	87.4	< LOD	28.1	3.86	96.4	0.10	0.46
	Reducible	650	890	251	1.23	97.1	636	1.13	53.0	2.55	3.71	< LOD	3.71
	Oxidizable	722	568	17.6	1.15	7.40	60.4	0.74	16.8	32.8	7.37	< LOD	0.94
	Residual	2060	12500	90.5	13.4	64.9	8170	5.80	72.1	32.8	43.5	< LOD	6.01
	Total	6520	14700	387	17.0	294	8950	7.67	170	72.0	151	0.10	11.1
24	Exchangeable	1690	781	< LOD	1.20	430	75.7	< LOD	28.8	6.39	50.2	0.10	0.67
	Reducible	230	437	175	0.99	270	510	0.75	25.3	1.94	2.27	< LOD	5.17
	Oxidizable	256	449	< LOD	0.62	5.27	36.2	0.35	11.5	33.6	7.44	< LOD	0.82
	Residual	560	4180	26.3	4.37	35.3	4130	1.97	15.1	24.6	19.1	< LOD	3.87
	Total	2740	5850	201	7.18	741	4750	3.07	80.7	66.6	79.0	0.10	10.5
25	Exchangeable	2420	1340	< LOD	1.78	106	206	< LOD	34.2	5.38	87.0	0.11	0.69
	Reducible	248	533	114	1.03	26.7	468	0.81	20.0	1.32	1.49	< LOD	1.56
	Oxidizable	362	491	< LOD	0.85	5.42	42.3	0.58	6.28	33.3	7.35	< LOD	0.47
	Residual	1070	7040	43.2	7.60	36.8	4870	3.39	30.5	28.1	29.4	< LOD	3.26
	Total	4100	9400	157	11.3	175	5590	4.79	90.9	68.1	125	0.11	5.97

Appendix B

Table A2: All sequential extraction concentrations from Barqa el-Hetiye samples.

Sample number	Sediment Fraction	Mg (µg/g)	Al (µg/g)	P (µg/g)	Cr (µg/g)	Mn (µg/g)	Fe (µg/g)	Ni (µg/g)	Cu (µg/g)	Zn (µg/g)	Sr (µg/g)	Cd (µg/g)	Pb (µg/g)
26	Exchangeable	2710	730	33.8	1.33	492	80.4	< LOD	42.3	6.1	94.0	0.16	0.41
	Reducible	645	860	319	1.27	506	707	1.43	56.3	4.53	7.61	< LOD	7.27
	Oxidizable	737	542	22.5	1.20	15.0	39.2	0.87	10.1	33.8	7.86	< LOD	1.25
	Residual	1880	11000	93.3	13.8	93.4	7750	6.23	56.2	33.2	36.6	< LOD	5.64
	Total	5970	13100	469	17.6	1106	8580	8.54	165	77.5	146	0.16	14.6
27	Exchangeable	2910	1110	64.6	1.56	67.7	159	2.70	8.17	48.4	95.9	0.11	0.52
	Reducible	825	852	193	1.17	31.8	553	0.95	19.8	2.73	3.18	< LOD	1.86
	Oxidizable	851	590	10.5	1.37	7.10	63.1	0.87	6.17	39.7	8.90	< LOD	0.55
	Residual	2850	15000	86.9	16.0	77.0	9730	7.24	42.6	40.0	45.5	< LOD	5.58
	Total	7440	17600	355	20.1	184	10500	11.8	76.8	131	153	0.11	8.50
28	Exchangeable	2510	660	69.7	1.24	117	121	< LOD	9.48	4.53	99.8	0.12	0.33
	Reducible	580	601	233	1.11	49.4	475	1.02	17.1	2.51	3.15	< LOD	1.97
	Oxidizable	692	666	14.9	1.34	7.57	103	0.85	7.84	38.2	8.72	< LOD	0.64
	Residual	1840	9870	64.3	11.0	57.1	6920	5.30	33.0	32.2	28.6	< LOD	4.25
	Total	5620	11800	382	14.7	231	7620	7.17	67.5	77.5	140	0.12	7.18
29	Exchangeable	1790	590	34.6	1.15	57.6	126	< LOD	12.2	3.46	59.7	0.06	0.24
	Reducible	211	370	141	0.98	19.7	483	0.64	8.83	1.35	1.53	< LOD	0.83
	Oxidizable	298	420	< LOD	0.83	2.29	31.6	0.37	5.69	28.1	6.92	< LOD	0.41
	Residual	668	3840	25.6	4.93	25.7	3120	1.83	12.3	22.9	22.5	< LOD	2.29
	Total	2970	5220	201	7.88	105	3760	2.85	39.1	55.8	90.6	0.06	3.77
31	Exchangeable	2660	391	86.8	1.08	42.9	115	< LOD	3.30	2.75	126	0.08	0.10
	Reducible	1040	715	215	1.89	26.0	631	1.52	6.54	2.95	7.97	< LOD	1.01
	Oxidizable	642	288	< LOD	0.82	3.21	28.2	0.47	2.48	16.2	4.49	< LOD	0.25
	Residual	1170	5690	34.7	6.84	32.6	4350	2.86	9.02	25.7	23.8	< LOD	2.51
	Total	5510	7080	336	10.6	105	5120	4.85	21.3	47.6	162	0.08	3.88
32	Exchangeable	3910	738	57.3	1.39	53.6	163	2.23	0.44	21.9	176	0.13	0.25
	Reducible	740	381	126	0.90	17.2	287	0.73	0.87	1.47	5.23	< LOD	0.54
	Oxidizable	753	271	< LOD	1.06	3.31	39.6	0.38	0.76	15.1	4.38	< LOD	0.34
	Residual	1950	8130	41.4	9.32	49.9	5730	4.20	5.78	29.1	29.5	< LOD	3.17
	Total	7350	9520	225	12.7	124	6220	7.54	7.84	67.5	215	0.13	4.30
33	Exchangeable	4850	342	79.6	1.29	72.9	213	< LOD	0.37	2.56	248	0.18	0.14
	Reducible	895	453	223	1.14	25.9	342	1.03	1.10	2.03	7.99	< LOD	0.66
	Oxidizable	942	342	12.5	1.32	4.66	61.5	0.55	0.93	15.3	4.51	< LOD	0.43
	Residual	2660	9810	58.6	13.0	75.2	8130	6.08	6.65	33.7	31.0	< LOD	3.74
	Total	9350	10900	374	16.7	179	8750	7.65	9.05	53.6	291	0.18	4.97
34	Exchangeable	4470	351	113	1.22	66.3	192	< LOD	0.38	2.22	207	0.16	0.00
	Reducible	965	494	219	1.11	21.7	342	0.96	1.01	2.08	8.68	< LOD	0.80
	Oxidizable	987	548	11.9	1.56	4.68	165	0.48	1.03	15.9	5.21	< LOD	0.59
	Residual	3160	9510	55.1	11.3	61.7	6920	5.72	7.23	33.1	28.7	< LOD	3.48
	Total	9580	10900	400	15.2	154	7620	7.15	9.65	53.3	250	0.16	4.87
35	Exchangeable	1830	751	19.5	1.18	41.4	93.2	< LOD	5.70	2.86	46.3	0.05	0.00
	Reducible	210	490	108	1.14	13.3	492	0.69	5.79	6.02	2.08	< LOD	0.70
	Oxidizable	708	682	< LOD	1.40	4.94	226	0.77	7.40	30.6	7.15	< LOD	0.38
	Residual	562	4350	29.3	4.56	19.8	3110	1.62	8.80	22.5	24.6	< LOD	2.43
	Total	3310	6270	156	8.28	79.4	3920	3.07	27.7	62.0	80.1	0.05	3.51
38	Exchangeable	5180	283	305	0.89	612	34.3	< LOD	40.4	4.58	319	0.10	0.20
	Reducible	1210	601	276	1.12	819	439	1.10	105	11.0	34.6	< LOD	9.65
	Oxidizable	1250	613	18.0	0.90	16.1	189	0.34	32.5	15.9	5.36	< LOD	1.98
	Residual	2460	6240	40.5	7.51	73.9	4520	3.84	115	28.5	17.8	< LOD	4.32
	Total	10100	7740	639	10.4	1522	5180	5.28	293	60.0	376	0.10	16.1
33A	Exchangeable	5150	403	84.4	1.40	74.0	253	1.43	0.39	2.63	238	0.19	0.17
	Reducible	623	547	248	1.33	24.5	336	1.04	1.20	7.11	9.23	< LOD	0.79
	Oxidizable	1190	394	< LOD	1.23	6.35	63.6	0.67	0.52	15.1	4.62	< LOD	0.34
	Residual	3100	13100	75.4	14.7	77.2	8190	7.27	7.88	32.6	80.2	< LOD	4.58
	Total	10100	14400	408	18.6	182	8840	10.4	10.0	57.4	332	0.19	5.87
35A	Exchangeable	1850	785	< LOD	1.24	41.1	100	< LOD	5.88	2.84	46.7	< LOD	0.20
	Reducible	190	470	101	1.12	13.0	475	0.68	5.61	7.15	2.31	< LOD	0.62
	Oxidizable	374	398	< LOD	0.82	3.01	76.1	< LOD	2.79	15.7	4.80	< LOD	0.30
	Residual	865	4720	20.6	4.75	20.7	3170	1.91	13.1	23.6	16.6	< LOD	2.11
	Total	3280	6370	122	7.93	77.7	3820	2.59	27.3	49.3	70.3	0	3.23

Appendix C

Supplemental element statistics for both Wadi 100 and Barqa el-Hetiye samples

Table A3: A statistical overview of the mean total element concentrations in Wadi 100 sediment samples. Total concentrations were calculated using Equation 9.

Descriptive Stats	Mg (µg/g)	Al (µg/g)	P (µg/g)	Cr (µg/g)	Mn (µg/g)	Fe (µg/g)	Ni (µg/g)	Cu (µg/g)	Zn (µg/g)	Sr (µg/g)	Cd (µg/g)	Pb (µg/g)
Mean (µg/g)	8460	9770	1150	22.0	277	7900	13.4	151	28.3	260	0.43	6.51
Standard Error	295	748	45.0	1.57	6.74	680	0.78	15.6	2.59	12.7	0.03	0.47
Median	8420	9460	1160	21.2	270	7120	13.0	129	26.1	253	0.42	5.84
Standard Deviation	1440	3660	220	7.68	33.0	3330	3.84	76.4	12.7	62.0	0.14	2.28
Sample Variance	2082420	13415961	48605	59.1	1090	11086953	14.7	5840	160	3840	0.02	5.19
Range	5930	13830	640	31.8	151	12620	16.0	341	47.9	271	0.68	8.39
Maximum	11300	18500	1160	41.5	380	15900	23.5	417	59.3	426	0.73	12.5
Minimum	5370	4670	520	9.76	229	3280	7.45	76.0	11.4	155	0.05	4.10
Sum	203000	234000	27500	527	6640	190000	322	3620	680	6250	9.45	156
Count (*n*)	24	24	24	24	24	24	24	24	24	24	22	24
Confidence Level (95.0%)	577	1465	88.2	3.07	13.2	1332	1.53	30.6	5.07	24.8	0.06	0.91
Upper Confidence Int.	9040	11231	1236	25.0	290	9236	15.0	181	33.4	285	0.49	7.42
Lower Confidence Int.	7885	8301	1059	18.9	263	6571	11.9	120	23.3	235	0.37	5.60

Table A4: A statistical overview of the mean total element concentrations in Barqa el-Hetiye sediment samples. Total concentrations were calculated using Equation 9.

Descriptive Stats	Mg (µg/g)	Al (µg/g)	P (µg/g)	Cr (µg/g)	Mn (µg/g)	Fe (µg/g)	Ni (µg/g)	Cu (µg/g)	Zn (µg/g)	Sr (µg/g)	Cd (µg/g)	Pb (µg/g)
Mean (µg/g)	5570	10100	326	12.5	369	6430	5.93	125	68.6	158	0.11	9.50
Standard Error	478	642	25.7	0.75	77.2	370	0.49	21.5	3.82	17.1	0.01	1.01
Median	5450	9460	346	11.5	213	6030	5.28	91.2	65.9	133	0.10	8.76
Standard Deviation	2340	3150	126	3.66	378	1810	2.40	105	18.7	83.9	0.04	4.94
Sample Variance	5482037	9906074	15904	13.4	143188	3291061	5.75	11046	351	7037	0.002	24.4
Range	7360	12300	517	13.0	1440	6740	9.17	362	83.2	306	0.14	15.0
Maximum	10100	17500	639	20.1	1520	10500	11.8	370	131	376	0.19	18.3
Minimum	2740	5220	122	7.18	77.7	3760	2.59	7.84	47.6	70	0.05	3.23
Sum	134000	242000	7820	301	8850	154000	142	3001	1650	3790	2.41	228
Count (*n*)	24	24	24	24	24	24	24	24	24	24	21	24
Confidence Level (95.0%)	937	1260	50.5	1.46	151	726	0.96	42.0	7.49	33.6	0.02	1.98
Upper Confidence Int.	6510	11300	376	14.0	520	7160	6.89	167	76.1	192	0.13	11.5
Lower Confidence Int.	4640	8820	275	11.1	217	5710	4.97	83.0	61.1	124	0.10	7.52

Appendix C

Supplemental element statistics for both Wadi 100 and Barqa el-Hetiye samples

Table A5: A summary of the fractional distribution of each element for the Wadi 100 sediment samples. The fractional sum of each element is the total amount of each element (in μg/g) that was extracted from all samples (n = 24).

Summary of Fractional Distributions	Mg (μg/g)	Al (μg/g)	P (μg/g)	Cr (μg/g)	Mn (μg/g)	Fe (μg/g)	Ni (μg/g)	Cu (μg/g)	Zn (μg/g)	Sr (μg/g)	Cd (μg/g)	Pb (μg/g)
Exchangeable mean	4820	400	88.9	2.00	141	157	2.30	17.5	4.14	222	0.42	0.15
Exchangeable Sum	116000	9610	2130	49.2	3380	3760	55.1	420	86.9	5330	8.78	3.49
% of Total	57%	4%	8%	9%	51%	2%	17%	12%	13%	85%	92%	2%
Reducible Average	470	889	914	1.56	71.8	603	1.71	44.8	5.42	16.3	0.10	1.47
Reducible Sum	11300	21300	21900	37.8	1720	14500	41.0	1030	130	390	0.78	35.3
% of Total	6%	9%	80%	7%	26%	8%	13%	28%	19%	6%	8%	23%
Oxidizable Average	768	341	48.9	3.13	8.38	134	1.65	25.8	1.24	1.46	< LOD	1.12
Oxidizable Sum	18400	8190	1130	73.5	201	3210	39.5	620	22.3	35.0		26.9
% of Total	9%	4%	4%	14%	3%	2%	12%	17%	3%	1%	0%	17%
Residual Average	2400	8140	117	15.3	55.8	7010	7.77	64.5	21.0	21.4	< LOD	3.77
Residual Sum	57600	195000	2340	367	1340	168000	187	1550	441	491		90.5
% of Total	28%	83%	9%	70%	20%	88%	58%	43%	65%	8%	0%	58%
Total Average	8460	9770	1150	22.0	277	7900	13.4	151	28.3	260	0.43	6.51
Total Sum	203000	234000	27500	527	6640	190000	322	3620	680	6250	9.56	156

Table A6: A summary of the fractional distribution of each element for the Barqa el-Hetiye sediment samples. The fractional sum of each element is the total amount of each element (in μg/g) that was extracted from all samples (n = 24).

Summary of Fractional Distributions	Mg (μg/g)	Al (μg/g)	P (μg/g)	Cr (μg/g)	Mn (μg/g)	Fe (μg/g)	Ni (μg/g)	Cu (μg/g)	Zn (μg/g)	Sr (μg/g)	Cd (μg/g)	Pb (μg/g)
Exchangeable mean	2790	712	69.2	1.26	174	124	2.36	33.8	8.92	110	0.11	0.52
Exchangeable Sum	66900	17100	1450	30.2	4180	2980	9.42	811	214	2650	2.41	11.4
% of Total	50%	7%	19%	10%	47%	2%	7%	27%	13%	70%	100%	5%
Reducible Average	575	622	207	1.20	136	501	0.98	35.6	3.23	8.88	0	4.11
Reducible Sum	13800	14300	4970	28.9	3260	12000	23.6	854	77.5	213	0	98.6
% of Total	10%	6%	64%	10%	37%	8%	17%	28%	5%	6%	0%	43%
Oxidizable Average	642	537	16.2	1.07	6.67	71.1	0.58	14.2	27.4	7.86	0	0.87
Oxidizable Sum	15400	12900	162	25.7	160	1710	12.2	341	657	189	0	20.9
% of Total	12%	5%	2%	9%	2%	1%	9%	11%	40%	5%	0%	9%
Residual Average	1570	8040	51.5	9.02	51.7	5740	4.05	41.5	29.1	31.0	0	4.04
Residual Sum	37600	193000	1240	216	1240	138000	97.2	996	697	744	0	97.1
% of Total	28%	81%	16%	72%	14%	89%	68%	33%	42%	20%	0%	43%
Total Average	5570	10100	326	12.5	369	6430	5.93	125	68.6	158	0.11	9.50
Total Sum	133700	237300	7820	301	8850	154690	142	3001	1646	3790	2.41	228